The Fibro-Inflammatory Hypothesis: TGFβ2 – TLR4 Signaling Crosstalk in the Glaucomatous Optic Nerve Head

by

Emma K. Geiduschek

A dissertation submitted in partial fulfillment of

the requirements for the degree of

Doctor of Philosophy

(Neuroscience)

at the

UNIVERSITY OF WISCONSIN-MADISON

2024

Date of final oral examination: April 10th, 2024

The dissertation is approved by the following members of the Final Examination Committee:

Colleen M. McDowell, Assistant Professor, Department of Ophthalmology and Visual Sciences
Robert W. Nickells, Professor, Department of Ophthalmology and Visual Sciences
Gillian McLellan, Professor, Department of Surgical Sciences
Mrinalini Hoon, Assistant Professor, Department of Ophthalmology and Visual Sciences
Michael E. Cahill, Assistant Professor, Comparative Biosciences

Acknowledgements

I would like to dedicate this thesis and my work to my grandparents. My Grandpa Ron, who taught me to always reach out to help others with compassion and grace. My Papa Peter, an unofficial-official extra committee member, who's love of science, discovery, and exploration fueled my own passion for research while teaching me to ask the hard questions. To my Grandma Janet and Grandma Joyce, my role models for family women working in STEM. Grandma Janet, one of my best friends and confidants growing up, and Grandma Joyce, my second unofficial-official extra committee member, both of whom inspired me to reach for the stars within my STEM and life goals.

I would first and foremost like to thank Dr. Colleen McDowell. As someone who took a chance on a lab transfer student, she is the type of mentor and teacher I hope to one day be able to emulate. Thank you for your support, encouragement, and infinite patience as you guided me to be a better student, scientist, and mentor.

To my thesis committee: Dr. Gillian McLellan, Dr. Rob Nickells, Dr. Mrinalini Hoon, and Dr. Michael Cahill, thank you for your wisdom, encouragement, and support. I am grateful for your knowledge as I ventured into a new field in neuroscience, I would not have been able to reach my academic goals without you all.

To my lab, thank you for always making my workday entertaining even when I was exhausted, for your calmness and consistency when I was running around like a chicken with my head cut off, and for always being my soundboard about all my research projects. Philip Myzk, thank you for your mentorship, friendship, and endless time exploring the maze that is MSC. Kelsey Mathers, thank you for the gift of constant conversation. Your support, stories, water breaks, and commiserations brightened my day every day.

To my wonderful family. These years of late-night phone calls, conversations about specifics of my experiments, listening to my inane anxieties and hopeful opportunities, you all have been integral in this entire graduate school experience. I would not have been able to complete this without your love, support, and constant reassurances that just maybe I'm smart enough.

To my COVID pod: Dr. Katy Bjornson, (soon-to-be-Dr.) Mike Seibert, and Dr. Grace George. I will forever be grateful for our weekly Saturday meals, the hours you all spent teaching me euchre, and all your support through my own personal hurdles I experienced during the "unprecedented times" of a year that was 2020. My highlights of graduate school will always include "micycle," Thanksgiving volleyball, the trials and tribulations of 610, Katy's inability to drink water without spilling on herself, discovering dungeons and dragons with Mike, and every lesson on tarot cards and proper seasoning of my food from Grace. I am so grateful I got to experience this with all of you.

A special thank you to Julianna Giacomini. You were my first graduate student mentor when I was just a baby undergraduate student. You passion for science, discovery, and encouragement initiated my drive to go for a PhD. Thank you for being an amazing science mentor and friend over the years. And big thank you for introducing me to Matt. I feel the positive impact of being your friend every day, especially at the culmination of my graduate school career.

To Andrew Knutson, thank you for being one of my first best friends in graduate school. I will always remember every day we had to spend hours isolating microglia, your excitement when I (finally) got a western blot to (kind of) work, and every video game experience with Sock. Your ability to distract me from my own anxieties and worries with humor is a special

skill, and I am so grateful that you were able to act as my science mentor and nerdy friend throughout my PhD career.

To my Wisconsin friends still here or moved away: Akshay Kohli, Rachel Puralewski, Kendra Hanslik, Jason and Danielle Anderson, and Amanda Vanderplow. Thank you for every card game night that always ended up with us catching up for the first two hours, for birthday parties, trampoline time, introducing me to a plethora of board games, and your general support and encouragement. Without you all I doubt I would have any semblance of work/life balance.

And finally, I want to thank my wonderful fiancé Matt. You have been my rock and my best friend through thick and thin these last six years. You've listened to my thesis at least 20 times, you've celebrated all my data discoveries, and comforted me when I didn't think I could make it through. Thank you for Frank, the emotional support sturgeon, for being the 2nd option for Ginger to sit on, for introducing me to video games, and for always being by my side. I am so excited to be the family of Dr. and Dr. Klinka.

Table of Contents

Abstract

Glaucoma is currently the leading cause of irreversible blindness. Many patients receiving glaucoma treatments are still exhibiting progressive vision loss, indicating a crucial need for a better understanding of the molecular and cellular mechanisms behind disease progression to generate more effective treatments. Significant fibrosis and immune responses have been reported in the glaucomatous optic nerve head (ONH) in humans and model systems. Specifically, TGFβ2-induced fibrosis generates damage associated molecular patterns (DAMPs) that can subsequently activate toll-like receptor 4 and initiate an immune system response. TLR4 activation through MyD88 and NFκB signaling inhibits the transcription of the TGFβ2 negative regulator BAMBI, resulting in a vicious feed-forward fibrotic and immune system cycle during disease progression. Recently published work from our lab investigates the mechanisms involved in signaling crosstalk between TGFβ2 and TLR4 to induce fibrotic and immune system responses in human ONH cells and the ONH of a novel mouse model of glaucoma. We found that TLR4 signaling is necessary and sufficient to induce TGFβ2-induced fibrosis in an autocrine and paracrine manner in human ONH LC cells and astrocytes. Additionally, we identify time-specific DAMP and interferon (IFN) signaling variations, highlighting novel mechanisms for pharmaceutical interventions.

Chapter 1: The Fibro-Inflammatory Response in the Glaucomatous Optic Nerve Head

Adapted from: **Emma K. Geiduschek** and Colleen M. McDowell. The Fibro-Inflammatory Response in the Glaucomatous Optic Nerve Head. *Int J Mol Sci* 2023;24.

Abstract

Glaucoma is a progressive disease and the leading cause of irreversible blindness. The limited therapeutics available are only able to manage the common risk factor of glaucoma, elevated intraocular pressure (IOP), indicating a great need for understanding the cellular mechanisms behind optic nerve head (ONH) damage during disease progression. Here we review the known inflammatory and fibrotic changes occurring in the ONH. In addition, we describe a novel mechanism of toll-like receptor 4 (TLR4) and transforming growth factor beta-2 (TGFβ2) signaling crosstalk in the cells of the ONH that contribute to glaucomatous damage. Understanding molecular signaling within and between the cells of the ONH can help identify new drug targets and therapeutics.

Introduction

Glaucoma is currently a leading cause of irreversible blindness, estimated to effect 75 million individuals worldwide and proposed to increase to over 100 million by the year 2040.[1, 2] The glaucomas are a heterogenous group of optic neuropathies characterized by the loss of retinal ganglion cells (RGCs) and subsequent optic nerve head damage (ONH) and changes, resulting in a progressive loss of vision in distinctive and well-studied patterns.[3-5] In this review, we are focusing on the most common form of glaucoma, primary open-angle glaucoma (POAG). Risk factors include age, race, and sex, though much of the attention is focused on the role of intraocular pressure (IOP) and IOP management due to the high correlation between increased IOP and decreasing vision scores.[6, 7] Elevated IOP has been implicated as the most prominent risk factor for the development and progression of glaucoma, and it has been shown by multiple groups across different populations that lowering IOP through medication or surgery can delay glaucoma progression.[7-9] IOP homeostasis is disrupted when the production of aqueous humor

(AH) is not balanced by the rate of AH drainage through the outflow pathways in the iridocorneal angle of the eye. Most of the AH outflow is through the trabecular meshwork (TM) and Schlemm's canal, where extracellular matrix (ECM) proteins form a fluid-flow pathway for the AH.[10] In glaucoma, increased resistance through the outflow pathways in the TM, particularly in the juxtacanalicular connective tissue (JCT) region and at the inner wall of Schlemm's canal, results in increases in IOP.[11] Unfortunately, even with well-managed IOP through pharmaceuticals or surgery, many patients still exhibit progressive vision loss.[12] Exploring the molecular and cellular mechanisms behind glaucoma progression at the ONH will help address the crucial need for more effective treatments.

Glaucoma is defined by the loss of retinal ganglion cells (RGCs), the thinning of the retinal nerve fiber layer, and the cupping and remodeling of the ONH resulting in a gradual loss of vision.[13, 14] Multiple insults, including chronic mechanical stress due to high IOP, hypoxia microenvironments, and loss of neurotrophic factors and nutrient transport, all contribute to the loss of the RGCs.[15, 16] The exiting RGC axons is most vulnerable at the ONH due to the 90° turn the axons make, and the majority of the damage occurs at the layer of the lamina cribrosa (LC), a mesh-like connective tissue structure of pores through which the RGC axons travel to the eye.[13, 17] The LC region of the ONH acts as both a physical support to these exiting RGC axons, as well as the scaffolding for support cells to deliver nutrients and survey the microenvironment for potential cites of damage. The biomechanics of the LC region are highly implicated in glaucoma pathology, including balancing forces between IOP and intracranial pressure, the stiffness and elasticity of the LC region, and tissue-specific biomechanical responses.[18] These biomechanical

changes directly interfere with the interaction between the LC scaffolding and ECM proteins, the RGC axons, and the supporting cells in the ONH.

There are three major supporting cell types in the LC region: Iba1 positive microglial cells, glial fibrillary acidic protein (GFAP) positive ONH astrocytes, and α-smooth muscle actin (αSMA) positive LC cells. Microglia, the resident macrophages of the immune system, are regularly spaced along the walls of the blood vessels, within the glial columns, and in the LC region in the ONH to optimize their ability to survey their microenvironment.[19-21] The astrocytes are located both along the longitudinal LC beams and in a transverse orientation across multiple beams.[22] Finally, LC cells are located within the LC beams, within or between the cribriform plates.[22] All three of these cell types have been implicated in glaucomatous pathophysiology as described below.

In homeostatic environments, microglia efficiently clear dead cells and cellular debris.[23] This "resting" state is a highly active process of constantly surveying the microenvironment.[20] Upon activation during disease states or with damage to the CNS, microglia undergo morphological changes from ramified surveyors to an ameboid shape,[24-26] and rapidly respond and migrate to the site of damage within minutes.[21, 27] This migration is ATP-dependent, where ATP activates the P2Y12 receptor on the microglia.[28] Microgliosis is known to be associated with many CNS diseases including Parkinson's disease, Alzheimer's, and glaucoma.[20] Increased numbers of reactivated microglia are seen in the glaucomatous human ONH compared to age-matched controls.[19, 29] In mouse models of glaucoma, there is an increased number of microglia and increased activation of microglia prior to RGC death and axonal damage.[30-32] In addition, the

severity of early microglial activation correlates with the severity of RGC and ON axon pathology.[32] Genes that are expressed in activated microglia are significantly increased in mouse and rat models of glaucoma, such as: major histocompatibility complex–II (MHC-II), highly involved in the adaptive immune response; complement 1 complex components, involved in the innate immune response; P2Y12, the receptor responsible for initiating microglial migration to sites of damage; and TLR4, also involved in the innate immune response.[33-35] Minocycline, an inhibitor of microglial activation, has been previously used to explore the role of microglia in glaucoma progression. Minocycline treatment has been shown to enhance the survival of RGCs and rescue RGC nutrient transport.[36-38] Driving the immune response in human and mouse models of glaucoma, microglia sit as a key mediator for the progressive pathophysiology in the disease.

Astrocytes are the most common glial cell in the mammalian ONH,[22] providing cellular support by facilitating nutrient transport and distribution throughout the ONH as well as secreting ECM proteins to provide physical structure support.[22, 39] Human ONH astrocytes have region-dependent molecular heterogeneity.[40] There are three subtypes of astrocytes in the ONH: type 1A, type 1B, and type 2. Type 1A are in the unmyelinated LC and prelaminar regions of the ONH and express GFAP but are negative for neural cell adhesion molecule (NCAM). Type 1B are also in the LC and prelaminar regions, but express both GFAP and NCAM. Type 2 astrocytes are in the myelinated post-laminar region of the ONH.[41] In early glaucoma, ONH astrocytes are hypothesized to be protective. It is known that astrocytes can redistribute nutrients from healthy to stressed microenvironments after IOP increases, and the knock-out of astrocyte reactivity genes early in a disease model results in more RGC death.[39, 42, 43] In later glaucoma disease

states, astrocytes transition to a neurotoxic phenotype, a process called astrogliosis. This reactive phenotype transition is hypothesized to be initiated by activated microglia and is microglia dependent, where mice without functioning microglia do not exhibit a reactive astrocyte phenotype after insult.[44, 45] Reactive astrocytes in the LC region take on an activated physical phenotype, showing rounded bodies with a loss of cell processes.[44-46] Reactivated astrocytes in the glaucomatous ONH secrete higher levels of ECM proteins prominent in the LC region,[47] and interfere with the exiting RGC anterograde transport of nutrients.[39] During glaucoma progression, increased IOP is known to result in a loss of nutrient transport and astrogliosis, implicating astrocytes as a major contributor to RGC axon damage and eventual progressive vision loss.

The main function of the LC cells is to secret ECM proteins such as collagens, elastin, and fibronectin, to maintain the structural laminar beams that physically support the exiting RGC axons.[48] LC cells are highly responsive to chemical and mechanical stimuli, altering their gene expression levels when exposed to transforming growth factors (TGFs), known to be involved in ocular wound healing and glaucoma pathophysiology, or under mechanical strain.[49-53] Previous studies have shown that LC cells collected from patients with POAG have upregulated ECM protein expression,[54] and undergo fibrosis and mechanical failure compared to age-matched controls.[55] Glaucoma-like stimuli (TGFβ exposure, mechanical stress, hypoxia) have all generated increases in ECM proteins in LC cells,[50, 51, 56, 57] and increased immunostaining for enzymes controlling the breakdown of collagen and fibronectin that have been shown in the LC region of the ONH.[29, 49, 58] These data implicate a critical role for LC cells in glaucoma by contributing to the increased fibrosis and remodeling of the ONH.

All three supporting cell types in the ONH have been implicated in perpetuating glaucomatous damage (Table 1). However, the cell–cell signaling between these cell types and the RGC axons is not fully understood.

Fibrosis in the Glaucomatous ONH

The drastic changes to the ECM and increased fibrosis in the glaucomatous ONH and LC region have been extensively reviewed.[14, 49, 59, 60] Fibrosis is defined as the excessive production and accumulation of ECM proteins, inducing structural and functional abnormalities in the affected tissue.[61] Elevated IOP causes significant strain and stress on the ONH region, resulting in posterior migration of the LC and eventual cupping of the ONH.[22] This mechanical strain induces increased fibrosis, specifically the deposition and dysregulation of ECM proteins elastin, tenascin, collagens I, IV, V, XI, proteoglycan, and fibronectin.[22, 54-56, 62-65] ECM deposition and dysregulation induces a plethora of physical changes, including elastosis, increased fibrosis, the thickening of the connective tissue around the ON fibers impairing nutrient transport, and disorganization of the regular collagen structure.[22, 55, 62] This ECM remodeling adversely affects the capacity of the LC to support the exiting RGC axons, predisposing them to the axonal compression and disruption of nutrient transport.[39] While it is established that elevated IOP leads to stress and strain on the ONH, the pathogenic molecular mechanisms responsible for the structural changes are not well understood.

One predominant hypothesis indicates TGFβ2-induced ECM production as a major player in instigating and exacerbating the increased ECM buildup and dysregulation in glaucoma.[66] The

molecular signaling pathway of TGFβ2-induced ECM synthesis has been well studied. TGFβ2 binding induces a heterotetrameric complex between two type I receptors and two type II receptors to initiate the canonical Smad signaling pathway.[67] The Smad signaling pathway results in the phosphorylation of Smad2/3, which colocalizes with Co-Smad4 in the nucleus of both human ONH astrocytes and LC cells.[68, 69] The downregulation of Smad signaling is induced by the increased expression of SMAD7, which recruits Smad6 to inhibit the phosphorylation of SMAD2/3 by directly interacting with the TGFβ receptors intracellularly.[70-72] The Smad7 inhibition of TGFβ2-signaling is amplified by BMP and activin membrane-bound inhibitor (BAMBI). BAMBI cooperates with inhibitory Smad7 to prevent Smad3 phosphorylation.[73] BAMBI also acts as a pseudoreceptor by replacing one of the TGFβ-receptors in the receptor complex, preventing the phosphorylation of Smad2/3.[73] This highly regulated TGFβ2 signaling pathway has been well studied in LC cells and tissues as well as in the ONH astrocytes.

TGFβ2 is the predominant isoform in the eye, and is found in in the trabecular meshwork (TM), aqueous humor, vitreous humor, neural retina, retinal pigment epithelium, and the ONH.[66] In the TM, TM cells are known to secret TGFβ2, and express TGFβ receptors and significantly increase ECM production in the presence of TGFβ2, indicating that the predominant outflow pathway for AH is under the influence of TGFβ signaling.[74] TGFβ2 levels are minor to non-existent in the healthy ONH,[75] but have been shown to be increased 70–100-fold in the glaucomatous ONH compared to healthy age-matched controls, with staining primarily occurring in astrocytes (Table 1).[75] The *in vitro* TGFβ2 treatment of primary human ONH astrocytes and LC cells induces the increased ECM deposition of elastin, collagen-IV, and fibronectin (FN) via canonical Smad signaling (Table 1).[56, 66, 69, 75-77] TGFβ2 is also present in activated microglia in

the retinal nerve fiber layer, prelaminar, LC, and post-laminar regions in human glaucomatous ONHs.[29] Taken together, TGFβ2 signaling has the ability to interact with and influence both the front and back of the eye in glaucoma disease progression.

Inflammation in Glaucoma

Notably, a physiological level of inflammation is beneficial and necessary to fight infection, maintain tissue homeostasis, and recruit immune cells to clear sites of tissue damage.[78] However, when tissue is exposed to severe or prolonged levels of stress, inflammation plays a neurotoxic and deleterious role. It has been postulated that a prolonged exposure to mechanical stress and strain from elevated IOP, the subsequent loss of nutrients, and resulting hypoxic microenvironments, can transition the innate immune system in the ONH from protective to neurotoxic.[79]

The role of innate immune activation and induced pathophysiology during glaucoma disease progression has been extensively reviewed,[16, 78, 80] with ONH astrocytes,[81] microglia,[82, 83] and LC cells implicated in initiating and responding to increased immune activation.[84] The ONH is an immune-privileged tissue, thus the defense systems consist of glial cells and the complement system.[78] These glial cells are the microglia and astrocytes, both found to be profoundly responsive to stress in the glaucomatous ONH. In a resting state, microglia survey their microenvironment and release neurotrophic factors to maintain RGC health.[85] Increased microglial activation is associated with human glaucoma,[19, 29] as well as in animal models of glaucoma.[83, 86] As discussed earlier, early microglial activation predicates RGC damage and correlates with RGC degeneration severity,[32, 83] and induces a neurotoxic phenotype in

astrocytes,[44] which subsequently secrete pro-inflammatory and pro-fibrotic signals. These signals activate the innate immune signaling pathway by binding to toll-like receptors (TLRs). The constant glial-inflammatory response has recently been recognized as a crucial mechanism of the gradual neurodegeneration of the exiting RGCs.[78, 87] Here, we will be focusing on the role of toll-like receptor 4 (TLR4) in the glaucomatous ONH.

The TLR family consists of 10 members (TLR1-10) in humans and 12 members (TLR1-9, TLR11-13) in mice.[88] The role of TLRs in glaucoma, age-related macular degeneration, and other retinal diseases has been extensively reviewed.[88-90] In this review we will be focusing on the role of TLR4 signaling in the glaucomatous ONH. TLR4 was first identified as the receptor for lipopolysaccharide, which is found on almost all Gram-negative bacteria and acts as an innate immunity signal.[91, 92] Recent evidence has implicated TLR4 signaling in augmenting fibrosis and the production and regulation of ECM proteins in fibrotic diseases.[31, 74, 93-96] Importantly, *Tlr4* gene polymorphisms are associated with primary open angle glaucoma in multiple patient populations,[97-99] and TLR4 pathway-related genes are differentially expressed in the retina and ONH of glaucomatous patients versus healthy patients.[34, 100] TLR4 activation through the Myd88 signaling pathway increases the production of nuclear factor κ B (NFκB), which translocates to the nucleus to act as a transcription factor, initiating the production of pro-inflammatory signals as well as pro-fibrotic signals. Some of these inflammatory and fibrotic products can act as endogenous ligands for TLR4, known as damage-associated molecular patterns (DAMPs). TLR4 can then be again activated by these endogenous DAMPs, creating a positive feedback loop, leading to a progressive fibroinflammatory response.[101]

DAMPs serve as key signals for tissue injury or damage. DAMPs are generated in situ in response to injury, oxidative stress, cell damage, or ECM remodeling.[102] Heat shock protein 60 was the first discovered endogenous DAMP, shown to induce cytokine synthesis through TLR4 activation.[103] Since then, dozens of endogenous DAMPs have been discovered, including different peptides, fatty acids, proteoglycans, and nucleic acids. The role of DAMPs and their involvement in immune system activation has been extensively reviewed by Piccinini and Midwood;[102] here, I will be discussing DAMPs and their involvement in primary open angle glaucomatous pathology. Interestingly, TLR4 can be activated by endogenous DAMPs that are known ECM molecules, including biglycan, tenascin-C, and the fibronectin EDA isoform (FN+EDA).[102] Along with TLR4 expression differentiation,[34, 100] DAMPs such as tenascin-C and FN+EDA have also been identified as differentially expressed in the ONH and retina in glaucoma.[34, 56, 64]

Biglycan is a proteoglycan that primarily supports tissue when exposed to compressional forces,[104] such as the force on the ONH. Biglycan, like fibronectin, can be upregulated by TGFβ stimulation in renal cell cultures and is involved in the pathophysiology of several renal fibrosis disorders.[105] Similarly, biglycan has also been shown to be upregulated in cultured LC cells after mechanical stress.[51] Biglycan is released from the ECM in stressed tissues, interacting with ECM proteins COLI, II, III, IV, and elastin.[106] Crucially, biglycan is a potent pro-inflammatory signal that is known to activate TLR4.[107] Biglycan knock-out mice live longer after LPS-induced sepsis than wild-type controls and produce significantly lower levels of pro-inflammatory cytokines.[107] Although biglycan is known to be expressed in the LC region of the ONH, and altered by mechanical strain in LC cell cultures, it remains to be determined if expression levels differ

between healthy and glaucomatous ONH in patients.[108] Additional studies are needed to fully understand the role of this important DAMP in TLR4-activation in the ONH.

Tenascin-C is a large glycoprotein expressed in neural and non-neural tissues,[108] and is known to be expressed in the LC region of the ONH.[108] Importantly, tenascin-C levels are prominent in the LC region of the ONH in elderly donor eyes, implicating increased levels with age, a potent risk factor for glaucoma development.[108] In addition, tenascin-C has been shown to be a TLR4 activator, and maintains pro-inflammatory signaling in other immune-dependent diseases.[109] Tenascin-C protein expression is significantly increased in human and porcine TM cells exposed to high IOP using perfusion organ cultures.[110] In autoimmune glaucoma mouse models, increased levels of tenascin-C are found in both the retina and ONH.[111] In a rat model of glaucoma, tenascin-C mRNA was significantly increased in the ONH with early ON damage, and remained significantly elevated throughout the glaucoma progression compared to controls.[35] Similarly, the knock-out of tenascin-C lowered levels of reactive astrocytes in the ONH and reactive microglia in the mouse retina,[112] highlighting the importance of this DAMP in disease progression. Functionally, tenascin-C is known to regulate TGFβ signaling during wound healing,[113] an important pathway involved in the changes to the ONH and LC in glaucoma, as we discussed above. Importantly, tenascin-C protein expression is increased in the glaucomatous LC region of the ONH compared to healthy, age-matched controls,[64] suggesting this DAMP may be intimately involved in the development of glaucomatous damage.

Finally, FN is a component of the ECM in the ONH, helping to form the intricate mesh-like layer of the LC region along with other ECM proteins.[56] FN is composed of either cellular FN

(cFN) or plasma FN (pFN).[114] cFN, found in the pericellular matrix, can contain various splice variant combinations of the extra domain—A (EDA), extra domain—B (EDB), or Type III homologies.[114] Conversely, pFN, secreted by hepatocytes directly into blood circulation, does not contain the EDA or EDB domains.[114] The FN+EDA isoform is a known DAMP that binds and activates TLR4.[56, 74, 115] During embryonic development, the FN+EDA isoform is abundant, lowering to minimal levels in adult tissues except during tissue injury, repair, or disease states, where expression is again upregulated.[116-120] FN+EDA is increased in other fibrotic and immune diseases such as atherosclerosis, psoriasis, scleroderma, and rheumatoid arthritis, and in human glaucomatous TM tissue compared to healthy controls.[74, 121-124] FN+EDA amplifies the TGFβ2-dependent ECM response in primary TM cells and can induce ocular hypertension in mouse models.[74, 96, 125] Importantly, we recently reported that FN+EDA is elevated in the LC region of the human glaucomatous ONH compared to healthy controls and amplifies the TGFβ2-dependent response in primary human LC cell cultures.[56] These data implicate FN+EDA as an important DAMP involved in modulating the glaucomatous ONH.

Here, we have described the role of ECM DAMPs in both immune system activation and glaucoma pathophysiology. Increased levels of DAMPs, induced by increased TGFβ2 levels, activate TLR4 and exacerbate these signaling pathways in the ONH. This leads us to a fibro-inflammatory hypothesis of TGFβ2 and TLR4 signaling crosstalk between the key ONH supporting cell types leading to glaucomatous damage.

Fibro-Inflammatory TGFβ2-TLR4 Signaling

Autocrine and paracrine signaling within and between astrocytes, microglia, and LC cells was first proposed over 20 years ago.[126, 127] Crosstalk between both TGFβ2 and TLR4 signaling pathways, within and between ONH cells, depends on the ability of the supporting astrocytes, microglia, and LC cells to secrete TGFβ2 and DAMPs, as well as express TLR4 and TGFβ2 receptors. Human ONH astrocytes, microglia, and LC cells all express TLR4,[45, 50, 128] and all produce TGFβ2 and express TGFβ-receptors.[29, 50, 69, 100, 129] This implies that each cell type can respond to increased TGFβ2, increase DAMP production, and respond in both an autocrine and paracrine manner. Here we will outline how the TGFβ2 and TLR4 signaling pathways can communicate with each other to regulate ECM and DAMP production within the ONH.

As we have referenced above, early microglial activation precedes RGC damage and death,[31, 32] increasing TLR4 expression and cytokine release (Figure 1, #1) [34, 35]. These activated microglia, and the increased pro-inflammatory signals, are able to cause the activation of astrocytes in ONH via IL-1α, TNFα, and C1q expression (Figure 1, #2).[44] These circulating molecules from microglia are necessary and sufficient to induce astrocyte activation and subsequent RGC damage after an initial axon insult [44]. However, RGC damage requires the presence of activated astrocytes also releasing pro-inflammatory cytokines to induce retinal injury and RGC degeneration (Figure 1, #3).[130] It has been shown that the TLR4-dependent production of pro-inflammatory cytokines is increased in POAG tears,[131] AH,[132] and in the ONH astrocytes in glaucoma models, indicating astrocyte paracrine and autocrine inflammatory signaling is increased across multiple tissues during glaucoma progression, making astrocyte activation a key instigator of ONH RGC damage.[35, 44, 130]

ONH astrocytes produce the DAMP tenascin-C,[133-135] a prominent activator of TLR4 that is significantly upregulated in human ONH glaucomatous astrocytes (Figure 1, #4).[64, 109, 133-135] In primary rat and mouse microglial cell cultures, the DAMP tenascin-C significantly increases IL-6 and TNFα expression levels through TLR4 activation (Figure 1, #2), potentially activating astrocytes through continued paracrine signaling.[136, 137] As mentioned previously, the knock-out of tenascin-C was able to inhibit both microgliosis and astrogliosis in a mouse model of glaucoma,[112] indicating its ability to act upon both of these cell types through TLR4 signaling. Thus, it is likely that activated microglia and activated astrocytes are able to interact via the paracrine signaling of proinflammatory cytokines and DAMPs. It has also been shown that ONH LC cells also express TLR4,[50] enabling the potential for proinflammatory and DAMP paracrine signaling between all three supporting cell types (Figure 1, #5). Primary ONH LC cells, when stimulated with either TGFβ2 or the DAMP FN+EDA, significantly increase ECM production in a TLR4-dependent manner, indicating autocrine signaling within the monoculture (Figure 1, #6).[56] Thus, it is likely that similar autocrine signaling is happening within microglia (Figure 1, #7) and astrocyte populations (Figure 1, #8), as well as paracrine signaling between all three population subtypes within the glaucomatous ONH (Figure 1, #9, 10, 11).

In addition, autocrine and paracrine signaling by neurotrophins (NTs) has been implicated in glaucoma disease progression, especially through the loss of such nutrient and growth factor transport through the damaged LC region of the ONH.[39, 138-140] NTs are a family of nerve-growth factors including nerve growth factor (NGF), brain-derived growth factor (BDNF), glial-derived neurotrophic factor (GDNF), neurotrophin 3 (NT-3), and neurotrophin 4/5 (NT-4/5).[138] NTs bind

to protein tyrosine kinase (Trk) receptors and are highly involved in the peripheral,[138] and central nervous immune responses.[141] In the healthy ONH, LC cells and astrocytes produce moderate levels of NTs, and microglia produce negligible levels.[126, 142] After acute insults, BDNF is able to exert a neuroprotective phenotype where BDNF injections significantly delay microglial activation post-ON sectioning,[143] LC cells and astrocytes increase NT secretions after acute ischemia,[127] mimicking the hypoxic microenvironments in the ONH during glaucoma, and activated microglia are known to initially release NGF, NT-4/5, and GDNF.[144] These findings implicate NTs as early responses in protecting the damaged RGCs; however, current hypotheses predict that the constant deprivation of NTs due to the reduced axonal transport greatly contributes to glaucoma disease progression.[140] The local synthesis and retrograde transport of BDNF is significantly reduced after excitotoxic stimuli, leading to retinal degeneration,[145] and chronic high IOP induces the loss of BDNF in RGC cell bodies.[146] Importantly, LC cells, astrocytes, and microglia are all able to secrete BDNF and express TrkB, the receptor for BDNF.[126, 127, 147, 148] Not only does this implicate potential autocrine and paracrine signaling between these cell types, but BDNF signaling is thought to slow microglial activation by inhibiting TLR4 downstream signaling, indicating another potential way for NTs to interact between cell types (Figure 1, #12).[147] The loss of this TLR4 inhibition could be perpetrating the autocrine (Figure 1, #13, 14, 15) and paracrine (Figure 1, #16, 17, 18) feed-forward cycle of TLR4-DAMP activation in all supporting cell types as glaucomatous damage progresses.

Hypothesized signaling crosstalk between microglia, astrocytes, and LC cells in the glaucomatous ONH are represented by the dashed lines in Figure 1 and represent current

knowledge gaps in the literature. Further research into this intricate crosstalk is necessary to better understand the glaucomatous pathophysiology.

In the previous sections, we have outlined the hypothesized immune system and NT autocrine and paracrine signaling within and between microglia, astrocytes, and LC cells in the glaucomatous ONH. Both the immune system and NT signaling have direct interactions with TGFβ2 signaling, a predominant contributor to increased ECM deposition in the glaucomatous ONH.[56, 74, 149] We have previously shown that TGFβ2-dependent ECM production is TLR4-dependent both in primary human TM cells and ONH LC cells.[56, 74] TGFβ2 or DAMP exposure from cFN, containing the FN+EDA DAMP, induced significant increases in total FN, collagen-I, and laminin in primary human TM cells, but caused the concurrent blockage of TLR4 signaling by the selective TLR4 inhibitor TAK-242, returning these ECM protein levels back to baseline.[74] A similar phenotype was found in primary human ONH LC cells, where TGFβ2 exposure significantly increased FN, FN+EDA, and collagen-I protein expression, but the concurrent blockage of TLR4 signaling rescued this phenotype back to control levels (Chapter 1: Figure 1).[56] These results implicate that TLR4 signaling is necessary for the TGFβ2-induced ECM production seen in two key structures involved in glaucoma pathophysiology.

The mechanism of TGFβ2 and TLR4 signaling crosstalk has previously been studied in other tissues and disease states through the TGFβ pseudoreceptor BMP and activin membrane-bound inhibitor (BAMBI). It is known that TLR4 activation downregulates BAMBI protein expression in a MyD88-dependent manner via NFκB signaling.[93, 94, 150, 151] In addition, the inhibition of NFκB signaling prevents the downregulation of *Bambi* mRNA after TLR4 activation.[94] When present,

BAMBI inhibits TGFβ2 signaling by preventing Smad2/3 phosphorylation, amplifying the Smad7 inhibition of TGFβ2 and acting as a pseudoreceptor, sequestering and inhibiting TGFβR activation and thus Smad3 phosphorylation.[73] We previously reported that the knockdown of *Bambi* in mice induces ocular hypertension and increases ECM production in the TM.[152] In addition, previous studies have implicated a role of BAMBI in other fibrotic diseases,[94] and we know astrocytes, microglia, and LC cells can express BAMBI.[129, 153] Thus, it seems likely that BAMBI is also an important mediator of TLR4-TGFβ2 signaling crosstalk in the ONH. Each cell can respond to the remodeling of the glaucomatous ONH via the DAMP-dependent activation of TLR4, inducing a pro-fibroinflammatory response. Future studies are needed to fully elucidate the molecular mechanisms of TLR4-TGFβ2 signaling crosstalk in the ONH and the role of each supporting cell type in propagating this response.

Conclusions

Extensive research has indicated the critical role of both TLR4-immune signaling and TGFβ-induced fibrosis in the glaucomatous ONH in furthering RGC loss. Here, we propose a novel mechanism of TLR4-TGFβ2 signaling crosstalk within and between the supporting cells of the ONH. Elucidating the molecular mechanisms behind this crosstalk in the ONH can hopefully produce more therapeutic targets in treating glaucoma.

Author Contributions

E.K.G. and C.M.M. wrote and edited the manuscript. All authors have read and agreed to the published version of the manuscript.

Funding

This work was funded by the National Institute of Health R01EY026529 (CMM). This work was also supported by an Unrestricted Grant from Research to Prevent Blindness given to the UW-Madison Department of Ophthalmology and Visual Sciences P30 EY016665. This work was also supported by the William and Phyllis Huffman Research Professorship at UW-Madison (CMM).

Institutional Review Board Statement

Not applicable.

Informed Consent Statement

Not applicable.

Data Availability Statement

Data sharing not applicable. No new data were created or analyzed in this study.

Conflicts of Interest

The authors declare no conflicts of interest.

Figure Legends

Table 1. Glaucomatous fibrotic and immune system responses in the ONH. The ONH-supporting cell types, such as microglia, astrocytes, and LC cells (left column), are each associated with known fibrotic responses (central column) and immune responses (right column) during glaucoma disease progression.

Figure 1. Known and hypothesized autocrine and paracrine signaling in the glaucomatous ONH. Schematic of immune system, TGFβ2, and neurotrophin (NT) autocrine and paracrine signaling. Purple receptors and arrows represent immune system signaling. Red receptors, molecules, and arrows represent TGFβ2 and DAMP signaling. Yellow receptors, molecules, and arrows represent neurotrophin transport signaling. Solid lines represent the interactions shown in previous studies. The dashed lines represent hypothesized autocrine and paracrine signaling pathways that still need to be explored in the glaucomatous ONH. (1) Known early microglial activation. (2) Known microglia → astrocyte paracrine signaling. (3) Known astrocyte → microglia paracrine signaling. (4) Known TLR4-induced production of DAMPs in astrocytes. (5) Known TLR4-induced DAMP production and autocrine signaling in LC cells. (6) Known DAMP–TLR4 autocrine signaling in LC cells. (7) Hypothesized TLR4-induced DAMP production and autocrine signaling in microglia. (8) Hypothesized TLR4-induced DAMP production and autocrine signaling in astrocytes. (9, 10, 11) Hypothesized DAMP-induced paracrine signaling between LC cells, microglia, and astrocytes. (12) Known loss of NT inhibition of TLR4 signaling in microglia. (13, 14, 15) Hypothesized loss of autocrine NT signaling within microglia, astrocytes, and LC cells. (16, 17, 18) Hypothesized loss of paracrine NT signaling between microglia, astrocytes, and LC cells. Created with BioRender.com.

Table 1. Glaucomatous fibrotic and immune system responses in the ONH.

Glaucomatous Fibrotic and Immune Responses in Major ONH Supporting Cell Types		
Supporting Cell Type	**Glaucomatous Fibrotic Responses**	**Glaucomatous Immune Responses**
Microglia	- Increased TGFβ2 expression [29] - TGFβ2 treatment upregulates CX3CR1 transcription [154], a potent microglial activator [155]	- Innate immune cells of the CNS [82] - Early activation predicates and correlates with RGC degeneration severity [32] - Increased expression of innate and complement system immune activation genes [34, 35] - Inhibition of activation protects RGCs [37]
Astrocytes	- Secrete higher levels of ECM proteins [46] - Primary site of TGFβ2 expression [75] - TGFβ2 treatment significantly increases ECM mRNA and protein expression for FN, COL1, COL4 [66, 69, 76]	- Undergo astrogliosis: rounded bodies, loss of cell processes [46] - Increased levels of MHC-II, highly involved in the adaptive immune response [84] - Upregulate Tenascin-C, a potent proinflammatory DAMP through TLR4 activation [109, 133, 135]
LC Cells	- Secrete higher levels ECM [49, 54] - TGFβ2 treatment significantly increases ECM transcription and expression for FN, COL1, COL4 [56, 57, 66, 69] - Glaucoma-like insults (mechanical strain, hypoxia) increase ECM expression [51, 57]	- TGFβ2-induced ECM production is dependent on functioning TLR4 signaling, a potent activator of the innate immune response [56] - DAMP-induced (FN+EDA) ECM production dependent on TLR4 signaling [56]

Figure 1. Known and hypothesized autocrine and paracrine signaling in the glaucomatous ONH

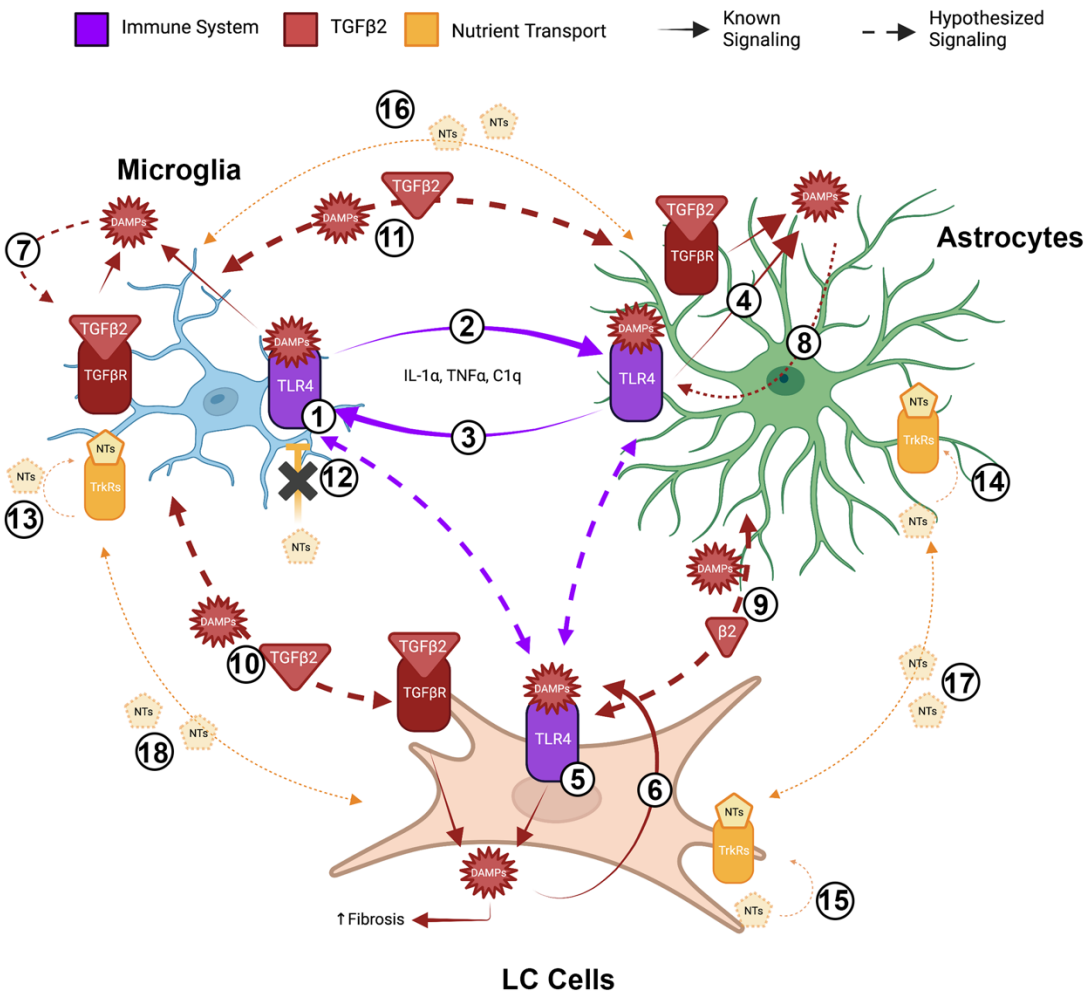

Chapter 2: TLR4 Signaling Modulates Extracellular Matrix Production in the Lamina Cribrosa

Adapted From: **Emma K. Geiduschek**, Milne PD, Mzyk P, Mavlyutov TA, McDowell CM. TLR4 signaling modulates extracellular matrix production in the lamina cribrosa. *Frontiers in Ophthalmology* 2022;2.

Abstract

The optic nerve head (ONH) is a place of vulnerability during glaucoma progression due to increased intraocular pressure damaging the retinal ganglion cell axons. The molecular signaling pathways involved in generating glaucomatous ONH damage has not been fully elucidated. There is a great deal of evidence that pro-fibrotic TGFβ2 signaling is involved in modulating the ECM environment within the lamina cribrosa (LC) region of the ONH. Here we investigated the role of signaling crosstalk between the TGFβ2 pathway and the toll-like receptor 4 (TLR4) pathway within the LC. ECM deposition was examined between healthy and glaucomatous human ONH sections, finding increases in fibronectin and fibronectin extra domain A (FN-EDA) an isoform of fibronectin known to be a damage associated molecular pattern (DAMP) that can activate TLR4 signaling. In primary human LC cell cultures derived from healthy donor eyes, inhibition of TLR4 signaling blocked TGFβ2 induced FN and FN-EDA expression. Activation of TLR4 by cellular FN (cFN) containing the EDA isoform increased both total FN production and Collagen-1 production in the presence of TGFβ2 in LC cells, and this effect was dependent on TLR4 signaling. These studies identify TGFβ2-TLR4 signaling crosstalk in LC cells of the ONH as a novel pathway regulating ECM and DAMP production.

Introduction

Cupping of the optic nerve head (ONH), thinning and loss of the retinal nerve fiber layer, and characteristic visual field defects are all clinical features of glaucoma.[156] Elevated intraocular pressure (IOP) is the most important risk factor for both the development and progression of glaucoma.[6] Current glaucoma therapy involves decreasing IOP by suppression of aqueous humor formation, enhancing uveoscleral outflow or, most recently, directly targeting the trabecular

meshwork. However, these therapies are not uniformly effective, and this therapy generally only slows the progression of vision loss over time.[7, 12, 157] This highlights the crucial need for more effecting glaucoma treatments and an increased understanding of the molecular and cellular mechanisms of disease progression.

The ONH contains retinal ganglion cell (RGC) axon bundles and support tissues and cells. The lamina cribrosa (LC) is the main structural component of the ONH. The LC is a mesh-like connective tissue structure through which the RGC axons pass as they exit the eye to form the myelinated extraocular optic nerve. The LC is composed of a series of interconnected lamellar beams made up of elastin, collagens, laminin, and heparin sulfate proteoglycans. The LC provides support for the RGC axons and resident cells. The LC region is populated by three major cell types; glial fibrillary acidic protein (GFAP)-positive ONH astrocytes, microglia, and α-smooth muscle actin (α-SMA) positive LC cells. The resident LC cells are located within the LC beams, and the ONH astrocytes are located both in longitudinal columns along RGC axon bundles and in transverse orientation investing multiple LC beams.[22] Resident microglia are regularly spaced throughout the normal ONH in the walls of blood vessels, within the glial columns, and in the LC.[19] The ONH region progressively remodels during glaucoma, leading to ONH cupping as well as mechanical failure and fibrosis of the LC; however, the cellular and molecular mechanisms responsible for this remodeling are not fully understood.

The ONH remains the most vulnerable point for the RGC axons, where they are most susceptible to elevated IOP, as the RGC axons have to turn 90° to enter the ONH and traverse the LC.[17] This region is particularly susceptible to pressure because at the ONH, the sclera thins to

form the ECM structure that allows RGC axons to exit the eye. Dysregulation of ECM in the LC causes increased fibrosis, elastosis, thickening of the connective tissue septae surrounding the ON fibers, and a thickening of the basement membranes involving altered collagen fibers and disorganized distribution and deposition of elastin, causing mechanical failure which in turn exacerbates ONH and RGC axon damage.[22, 55, 62] Deposition of ECM causes the LC to initially undergo thickening and posterior migration. Eventual shearing and collapse of the LC plates leads to a thin fibrotic connective tissue structure/scaring. ECM remodeling adversely affects the capacity of the LC to support RGC axons and predisposes RGCs to axonal compression, disruption of axoplasmic flow, and apoptosis.

Both the LC cells and ONH astrocytes are responsible for supporting the RGC axons by synthesizing growth factors and ECM.[22, 127, 158, 159] Several cytokines are known to regulate the production and modulation of ECM, including Toll like receptor 4 (TLR4) signaling as previously described in other fibrotic diseases.[93-95] TLR4 was first discovered as the receptor for lipopolysaccharide (LPS),[160] but can also be activated by endogenous ligands, known as DAMPs, damage associated molecular patterns. DAMPs are generated *in situ* as a result of injury, cell damage, ECM remodeling, and oxidative stress.[102, 161] TLR4 is known to be expressed in astrocytes, microglia, and LC cells in the human ONH.[45, 50, 129] TLR4 pathway related genes, downstream ECM genes, and DAMPs such as tenascin-C and heat shock proteins have been identified as differentially expressed in the human ONH and retina in glaucoma.[34, 64, 100] Importantly, *TLR4* gene polymorphisms have been associated with enhanced glaucoma risk in some populations.[97, 99, 162]

The role of TLR4 signaling in modifying the ECM and fibrotic environment has been studied in hepatic and renal fibrosis, scleroderma, as well as in *Tlr4* mutant mice.[93-95] Recently, we identified TLR4 signaling as an important regulator of the ECM in the TM and ocular hypertension.[74] In addition, DAMPs (including tenascin C, FN-EDA, heat shock proteins, and hyaluronan) have been shown to activate TLR4 and augment TGFβ signaling and downstream fibrotic responses,[93, 150, 151] and DAMPs have been identified in the glaucomatous ONH of both mice and humans.[163] In addition, numerous studies have identified elevated aqueous humor levels of TGFβ2 in glaucoma patients.[164-167] We and others have shown that TGFβ2 treatment of trabecular meshwork (TM) cells alters the ECM composition,[74, 168-170] and induces ECM cross-linking.[171-173] In the posterior segment, TGFβ2 is also the predominant TGFβ isoform in the ONH. Astrocytes, LC cells, and activated microglia are known to express and secrete TGFβ2, with increased expression of TGFβ2 documented in the glaucomatous ONH.[29, 64, 68, 69, 75] TGFβ2 treatment of ONH astrocytes and LC cells *in vitro* increases ECM protein synthesis and secretion via canonical Smad signaling.[68, 69] This dysregulation of ECM components could contribute to the ONH fibrotic environment in the LC in glaucoma. Here we demonstrate crosstalk between the TGFβ2 and TLR4 signaling pathways in primary ONH LC cells and show the DAMP, FN-EDA, is increased in the human glaucomatous LC suggesting this DAMP may have important implications in TLR4 activation and signaling in the glaucomatous ONH.

Materials and Methods

Human donor eyes

Deidentified human donor eyes were obtained from the Lions Eye Bank of Wisconsin (Madison, WI) within 24 hours post-mortem. The eyes were obtained and managed in

compliance with the Declaration of Helsinki. The human donor eyes used for IHC experiments ranged from 59 to 80 years old. Within 24 hours post-mortem, eyes were fixed in 4% paraformaldehyde for 24 hours at 4°C, rinsed with 1X PBS, then cryoprotected in 30% sucrose in PBS for another 48 hours at 4°C. The eyes were embedded into optimum cutting temperature embedding medium (Sakura Finetek 4583, Sakura Finetek USA, Inc., Torrance, CA) in 25mm x 20mm x 5mm Tissue-Tek cryomolds (Sakura Finetek 4557) and frozen on a prechilled metal block. Cryosections at 10μm intervals were cut from the frozen eyecups before being stored at -80°C until immunostaining. Glaucoma diagnosis is based on the patient medial history report. Primary human ONH LC cell strains were isolated from normal (non-glaucomatous) donor eyes (ages 59-74) from the Lions Eye Bank of Wisconsin or received as a kind gift from Dr. Abe Clark at the University of North Texas Health Science Center and characterized as previously described.[127, 158, 174] All donor tissues were obtained and managed according to the guidelines in the Declaration of Helsinki for research involving human tissue. Cells were cultured and maintained in Ham's F-10 growth media containing 10% FBS L-glutamine (0.292 mg/mL), and penicillin (100units/mL)/streptomycin (0.1mg/mL) in a humid chamber at 37°C in 5% CO_2. The medium was replaced every 2-3 days.

Immunohistochemistry

Standard procedures for IHC were utilized as previously described.[96] The OCT was removed via two washes in ddH_2O for 2 minutes each before sections were dried by subsequent washing in 70% ethanol for 2 minutes, 100% ethanol for 2 minutes, and then left to dry at RT for 10 minutes. Sections were then rinsed with 1X PBS for 5 minutes before being incubated in 0.1% Triton X (Sigma-Aldrich REFX100) at RT for 15 minutes to permeabilize cell membranes. Slides were then blocked in

Superblock Blocking Buffer in PBS (REF37580, Thermo Fisher Scientific) for 60 minutes at RT before incubated at 4°C overnight with FN (Sigma-Aldrich Corp., F3648) at 1:250, and FN-EDA (Abcam, ab6328) at 1:100 dilution. Primary antibody was washed off with four rinses in 1X PBS for 5 minutes each before slides were incubated in the appropriate secondary antibody for 2 hours at RT; Alexa Fluor 488 donkey anti-rabbit IgG (A21206, Invitrogen – Thermo Fisher Scientific) at 1:200 dilution and Alexa Fluor 594 donkey anti-mouse IgG (A21203, Invitrogen – Thermo Fisher Scientific) at 1:200 dilution. Slides were washed 5 times in 1X PBS for 5 minutes each and mounted with Prolong Diamond mounting medium containing DAPI (Invitrogen-Molecular Probes). Image acquisition was performed using a Zeiss Axio Imager Z2 microscope.

TLR4 Inhibition and Activation

Primary human ONH LC cells were grown to confluency and pretreated with the selective TLR4 inhibitor, TAK-242 (InvivoGen, San Diego, CA, USA) at 15μM for 2 hours. TAK-242 is a cyclohexene derivative that specifically inhibits TLR4 signaling by binding to the intracellular domain of TLR4 and blocking downstream signaling. Cells were then treated with TGFβ2 (5ng/mL) and/or TAK-242 (15μM) for 72 hours in serum-free medium. For TLR4 activation studies, hONH LC cultures were grown to confluency and treated with cellular fibronectin (cFN) (10μg/mL) containing the FN-EDA isoform (F2518; Sigma-Aldrich Corp., St. Louis, MO, USA) and/or TGFβ2 (5ng/mL), and/or TAK-242 (15μM) for 72 hours in serum-free medium. Western blot and immunocytochemistry experiments were performed as described below.

Immunocytochemistry

Primary human ONH LC cells were seeded on 12-well plates on coverslips and grown to confluency. After undergoing TLR4 inhibition and activation treatments as previously described for 72 hours, cells were washed with 1X PBS, fixed with 4% paraformaldehyde (PFA), permeabilized with 0.95% Triton X-100 in PBS, and blocked using Superblock Blocking Buffer in PBS (REF37580, Thermo Fisher Scientific) for 60 minutes at room temperature. Cells were labeled overnight at 4°C with rabbit anti-Fibronectin (F3648, Sigma-Aldrich) at a 1:100 dilution, or rabbit anti-collagen-1 (NB600-408, Novus Biologicals) at a 1:100 dilution in Superblock Blocking Buffer in PBS. Treatment without the primary antibody was used as a negative control. Coverslips were then incubated at room temperature 2 hours using Alexa Fluor 488 donkey anti-rabbit IgG (REFA21206, Invitrogen – Thermo Fisher Scientific) at a 1:200 dilution. Coverslips were mounted to slides with Prolong Diamond mounting medium containing DAPI (Invitrogen-Molecular Probes). Image acquisition was performed using a Zeiss Axio Imager Z2 microscope.

Western Blot Analysis

Primary human ONH LC cells were treated as previously described above for 48 or 72 hours. Cell lysates were extracted using RIPA buffer with protease and phosphatase inhibitors added. (Pierce RIPA Buffer, REF89901, Thermo Fisher Scientific; cOmplete Mini, EDTA-Free protease inhibitor cocktail, REF11836170001, Sigma-Aldrich; PhosSTOP REF04906837001 Sigma-Aldrich), The Pierce™ BCA Protein Assay Kit (Thermo Fisher Scientific REF23225) was used to estimate protein concentrations of each sample. Each loading sample contained 10µg of protein and the appropriate amount of 4X Protein Loading Buffer (Li-Core REF928-40004). Samples were boiled for 10 minutes, then separated using a 4-12% Bolt™ Bis-Tris Plus mini gel

(Invitrogen, NW04120BOX). Proteins from electrophoresed gels were transferred to polyvinylidene (PVDF) membranes (Bio-Rad Immun-Blot, REF1620177) for one hour at a constant 20V using the Mini Gel Tank wet transfer system (Invitrogen, REFA25977). Membranes were left to dry for 45 minutes before using Revert™ 700 Total Protein Stain (Li-Core REF926-11021) to confirm equal loading for samples and for normalization purposes. After destaining of total protein stain, membranes were blocked for one hour at room temperature with Intercept Blocking Buffer (Li-Cor, REF927-60001). Membranes were immunolabeled overnight at 4°C with primary antibodies: GAPDH (1:5000, Cell Signal REF97166S), Fibronectin (1:1000, Sigma -Aldrich F3648), and/or FN-EDA (1:500, Abcam, ab6328), diluted in Intercept Blocking Buffer. Blots were washed three times for 5 minutes each with 1X TBS-T and then incubated for 1 hour with the appropriate secondary antibodies at a 1:20,000 dilution in Intercept Blocking Buffer (Li-Core Goat anti-rabbit IRDye 800CW; Li-Core Goat anti-rabbit IRDye 680RD; Li-Core Goat anti-mouse IRDye 800CW). Membranes were then imaged on a Licor OdysseyCLx system. Each experiment was repeated 2-3 times in each individual hONH LC strain, and a total of 2-3 independent hONH strains were tested. Band intensity for proteins of interest and total protein were measured using Image Studio Lite (LI-COR Biosciences, Lincoln, NE, USA). Each target protein densitometry value was normalized against either its corresponding GAPDH or total protein value as indicated, and the fold change was calculated to control. Fold changes are represented as the mean +/- SEM. Statistical significance was determined by a 1-way ANOVA and subsequent Tukey's post hoc analysis comparing all treatments.

Results

FN and the DAMP FN-EDA are increased in the LC region of the glaucomatous human ONH

Increased fibrosis of the human ONH during glaucoma disease progression has been well established. The lamina cribrosa forms sieve-like layers of ECM which allow RGC axons to exit. The ECM is primarily made of collagens, elastin, and laminin,[175] all of which have been shown to be increased in the glaucomatous ONH.[49, 59] In addition, it is known that fibronectin is present in the LC region [176]. Here, we show an increase of fibronectin protein expression in the LC region of human glaucomatous donor eyes (Fig. 1O, R, U) compared to normal non-glaucoma control donor eyes (Fig. 1F, I, L). We also demonstrate an increase in the FN-EDA isoform, a known DAMP and activator of TLR4, in the LC region of human glaucomatous donor eyes (Fig. 1P, S, V) compared to normal non-glaucoma control donor eyes (Fig. 1G, J, M). These data suggest that FN and the FN-EDA isoform may have important implications in the development of glaucomatous ONH damage.

Dissection and isolation of the human ONH generates monocultures of LC cells

In order to test the function and role of DAMPs such as FN-EDA in LC cells, primary LC cells were isolated and cultured from human donor eyes. Following previously established protocols,[174] the ONH was dissected and the ONH explant placed into culture to propagate LC cells (Figure 2A). The isolation and characterization of the monocultures of LC cells was performed as previously described by Lopez et al.[174] Here representative images (Fig. 2E-G) and western blots (Fig. 2D) show isolated LC cells are negative for GFAP and positive for αSMA,

previously determined indicators of LC cells.[174] In total we characterized 4 independent LC cell strains from different donors with no history of ocular disease.

Inhibition of TLR4 signaling blocks TGFβ2-induced increases of ECM production in primary human ONH LC Cells

It is well established that TGFβ2 signaling increases in glaucoma and is known to affect the ONH during disease progression. Here, we show that inhibition of TLR4 by the selective inhibitor, TAK-242, blocks TGFβ2 dependent increases of total FN and the DAMP FN-EDA protein expression. Pretreatment of TAK-242 (15μM) for 2 hours prior to TGFβ2 exposure (5ng/mL) has been shown to significantly decrease TGFβ2 (5ng/mL)-induced FN and collagen-1 protein and mRNA expression in the trabecular meshwork,[74] therefore a 15μM concentration was used in these experiments. Primary hONH LC cells were treated with TGFβ2 (5ng/mL) and/or TAK-242 (15μM) for 72 hours. As previously reported, TGFβ2 induces FN expression in LC cells.[68, 69] However, TLR4 signaling inhibition significantly decreases FN (Fig. 3A) and FN-EDA (Fig. 3B) protein expression. Both FN and FN-EDA protein levels returned to control levels, with no significant differences between control and TAK-242 + TGFβ2 treated cells (n = 3 primary hONH LC cell strains, each repeated in 2-3 independent experiments). These data suggests that TLR4 signaling is necessary for TGFβ2 induced fibrosis in LC cells.

Cellular FN-EDA is an isoform of FN and has previously been shown to be a ligand for TLR4 receptor activation.[102, 115] Previous literature has shown that cFN-EDA is significantly increased in the glaucomatous human TM compared to normal eyes,[125] and shown to increase ECM protein expression in human TM cell cultures at a comparable level to TGFβ2.[74] Here we

show that cFN activation of TLR4 is sufficient to induce ECM protein expression increases in the ONH LC cells (Fig. 4). We tested the necessity and sufficiency of TLR4 activation on ECM protein production in ONH LC cells using immunocytochemistry. Human ONH LC cells were grown to confluency on coverslips and treated with TGFβ2 (5ng/mL), TAK-242 (15μM), and/or cFN (10μg/mL). As expected, TGFβ2 increased FN (Fig. 4B) and COL1 (Fig. 4J) protein expression compared to control. This increase was dependent on TLR4 signaling, as the addition of the selective TLR4 inhibitor TAK-242 blocked the increase of both FN (Fig. 4D) and COL1 (Fig. 4L). Addition of cFN was sufficient to increase total FN (Fig. 4E) and COL1 (Fig. 4M) protein deposition, and this increase was blocked by inhibition of TLR4 with the select inhibitor TAK-242 (Fig. 4G, H, O, P). Each experiment was repeated in 2 independent hONH LC cell strains. These data suggests a TGFβ2 – TLR4 signaling crosstalk in the ONH.

Discussion

In primary open angle glaucoma (POAG) the extracellular matrix (ECM) of the LC is disturbed and remodeled resulting in mechanical failure and fibrosis. Cupping of the ONH and changes to the ECM of the LC are associated with disorganized and increased deposition of collagen and elastin fibers.[7, 55, 62] Early histological analysis of the glaucomatous ONH in humans and animal models demonstrated increases in collagen IV, elastin and tenascin.[55, 63, 64, 177] In advanced glaucoma, histological analysis revealed a collapse of the LC plates and the formation of a fibrotic network of connective tissue. Both the LC cells and ONH astrocytes are responsible for supporting the RGC axons by synthesizing growth factors and ECM. Dysregulation of the ECM production and remodeling leads to glaucomatous changes in the ONH and RGC axon damage.

The pathogenic and molecular pathways responsible for the structural changes of the LC in POAG are not completely understood. However, it is well established that aqueous humor levels of TGFβ2 are elevated in POAG patients,[164-167] and there is an increase in the levels of TGFβ2 in the ONH.[64, 75] ONH astrocytes, LC cells, and activated microglia express and secrete TGFβ2.[29, 68, 69] Treatment of ONH astrocytes and LC cells with exogenous TGFβ2 increases ECM protein synthesis and secretion as well as phosphorylation of canonical Smad2/3 signaling proteins in both cell types.[68, 69] Exogenous TGFβ2 also increases co-localization of pSmad2/3 with Co-Smad4 in the nucleus of ONH astrocytes and LC cells.[68, 69] Knockdown of connective tissue growth factor (CTGF), a downstream signaling factor of TGFβ2, blocks the induction of ECM proteins by TGFβ2 in ONH astrocytes.[76] The dysregulation of these ECM components could contribute to the fibrotic environment and basement membrane thickening in the LC of the ONH in glaucoma. In summary, these data suggest that TGFβ2 regulates the expression of ECM proteins in the ONH and the effects of TGFβ2 signaling are a major component in the development of glaucomatous ONH damage. Here we show that there is crosstalk between the TGFβ2 and TLR4 signaling pathways in ONH LC cells, and this signaling crosstalk may also extend to ONH astrocytes and microglia cells contributing to glaucomatous ONH damage.

TLR4 signaling is known to affect not only immune responses, but also initiate fibrotic responses in several disease states. In addition, certain alleles of the *TLR4* gene are associated with an increased risk of glaucoma in some populations.[97, 99, 162] Interestingly, an increase in tenascin C, a large ECM glycoprotein and DAMP, has previously been reported to be increased in the glaucomatous ONH.[64, 163] Here, we show an additional DAMP, FN-EDA, to be elevated in

the glaucomatous ONH and modulate TLR4-TGFβ2 signaling crosstalk in LC cells. TLR4-TGFβ2 signaling crosstalk is likely regulated by the TGFβ pseudoreceptor BMP and activin membrane-bound inhibitor (BAMBI). TLR4 activation downregulates Bambi expression, which enhances TGFβ signaling leading to increased ECM production.[93, 94] BAMBI downregulation by TLR4 is regulated by a MyD88-NFkB-dependent pathway.[94, 150, 151] BAMBI functions to inhibit TGFβ signaling by cooperating with SMAD7 and impairing SMAD3 activation, while knockdown of *Bambi* expression enhances TGFβ signaling.[73] *Bambi* is known to be expressed in both human ONH astrocytes and LC cells.[153] These data suggest a crosstalk between TLR4 and TGFβ signaling pathways in LC cells (Fig. 5). Activation of TLR4 downregulates BAMBI leading to unopposed TGFβ signaling and fibrogenesis. Since the fibrotic response leads to the accumulation of endogenous TLR4 ligands such as FN-EDA and tenascin C, a feed-forward loop could develop leading to a further progression of the fibrotic response. Future studies will elucidate the exact molecular mechanism of TLR4 and TGFβ signaling crosstalk in the ONH.

The structure of the collagenous lamina cribrosa beams are disrupted in glaucoma. Increases of COL4 are seen in the LC region of ONH,[63] and LC primary cell lines isolated from human glaucomatous optic nerve heads have significantly higher COL1 and COL5 mRNA expression than healthy control lines.[54] COL1 protein expression also increases in other fibrotic diseases,[178] and collagen VI staining also increases in other tissue types during stress.[179] Concurrently, there is a marked loosening of the collagen matrix and significant loss of collagen fibers in the LC region of the ONH in POAG human tissue.[177] Both COLVIII and COLXIII mRNA are downregulated when comparing LC cell mRNA synthesis from healthy versus glaucomatous derived primary cell cultures.[54] This all suggests a disruption of collagen fibrils

and density leading towards disease progression and pathogenic ECM modifications. Our results recapitulate previous literature in that TGFβ2 treatment increases COL1 deposition,[50] and we further show that this increase is TLR4 dependent. In addition, we demonstrate that FN-EDA treatment is also sufficient in increasing COL1 expression in a TLR4-dependent manner. Future studies will look at other individual collagen subtype changes in glaucoma progression in the LC.

In conclusion, we show novel findings highlighting increased FN and the DAMP FN-EDA expression in the LC region of the glaucomatous human ONH. TGFβ2-TLR4 crosstalk in hONH LC cells is involved in the production and regulation of the ECM. Both TGFβ2 and cFN containing the EDA isoform can increase ECM protein expression in LC cells, as well as increase the production of the DAMP FN-EDA in the LC cells, and inhibition of TLR4 blocks these effects. These results provide insights into a novel pathway that could be driving glaucoma disease progression and eventual loss of vision. Understanding these cellular signaling mechanisms behind ONH damage offers new targets for developing further treatment therapies.

Conflict of Interest

The authors declare that the research was conducted in the absence of any commercial or financial relationships that could be construed as a potential conflict of interest.

Author Contribution

CMM developed all ideas and experimental designs, analyzed data, and wrote the manuscript. EKG performed all histological, cellular, and molecular experiments, analyzed data,

and wrote the manuscript. PDM assisted with cell culture maintenance and molecular experiments. PM isolated ONH tissue for culture. TAM dissected and embedded human donor eyes for histology. All authors read and approved the final manuscript.

Funding

This work was supported in part by National Institute of Health R01EY02652 (CMM), William and Phyllis Huffman Research Professorship (CMM), and the McPherson Eye Research Institute Grant Summit Program (CMM). This work was also supported in part by an Unrestricted Grant from Research to Prevent Blindness to the UW-Madison Department of Ophthalmology and Visual Sciences, the Core Grant for Vision Research from the NIH to the University of Wisconsin-Madison (P30 EY016665), and a T32 EY027721 to the Department of Ophthalmology and Visual Sciences University of Wisconsin-Madison (PM).

Acknowledgements

The authors would like to thank Dr. Abe Clark and Dr. Tara Tovar-Vidales for providing several LC cells strains for our studies.

Figure Legends

Figure 1. FN and FN-EDA expression in the LC region of normal and glaucomatous human ONH. (A) A cross-section of a hONH with (B-D) inserts of representative imaging locations of the (B) prelaminar, (C) LC, and (D) retrolaminar sections of the hONH. Immunohistochemistry images of the LC region of (E-M) healthy or (N-V) glaucomatous hONHs from donor eyes. Images show an increase in FN (O, R, U) and FN-EDA (P, S, V) expression in the LC region of glaucomatous (n=3) compared to healthy (n=3) eyes (F, I, L, and G, J, M respectively). *Scale bar* represents 200 μm (A) 20μm (B-M). (FN=green; FN-EDA=red; DAPI=blue.)

Figure 2. Isolation and characterization of LC cells from hONH explants. (A-C) Progressive removal of the RPE, peripapillary sclera, and ON from the ONH in initial isolation. The ONH explant was then cultured to isolate the LC section as previously described.[33] (D) Representative western immunoblot for GFAP and αSMA. ONH LC cells were positive for αSMA and negative for GFAP. (E-G) Immunocytochemistry staining of hONH LC cells were positive for αSMA (F) and negative for GFAP (G). *Scale bar* represents 100μm.

Figure 3. Inhibition of TLR4 blocks TGFβ2-induced ECM protein expression. (A, B) Primary hONH LC cells (*n* = 3 strains, each repeated in 2-3 independent experiments) were pretreated with TAK-242 for 2 hours, and subsequently treated with TGFβ2 (5 ng/mL) and/or TAK-242 (15μM) for 72 hours. Western immunoblot for (A) FN and (B) FN-EDA show that inhibition of TLR4 signaling via TAK-242 blocks the fibrotic effects of TGFβ2. Protein expression is normalized to GAPDH signal. (C) Representative immunoblots of FN and

respective GAPDH protein expression, and (D) FN-EDA and respective GAPDH protein expression. Protein expression is imaged on a Licor OdysseyCLx system in infrared, with a secondary antibody of Li-Core Goat anti-rabbit IRDye 680RD for total FN imaged in the red channel and Li-Core Goat anti-mouse IRDye 800CW for FN-EDA imaged in the green channel, and normalized to the same GAPDH for the specific membrane. Representative blots were then pseudo colored to black and white. Statistical significance was determined by 1-way ANOVA and Tukey's post hoc analysis. $*P < 0.05,\ **P < 0.01$.

Figure 4. TLR4 signaling is necessary and sufficient for ECM accumulation in hONH LC cells. Primary hONH LC cells (n = 2 cell strains) were grown to confluency on coverslips and left untreated for control (A) or treated with TGFβ2 (B, D, F, H, J, L, N, P) and/or cFN containing the EDA isoform (E-H, M-P). Cells involved in investigating the role of TLR4 signaling were pretreated with the selective TLR4 inhibitor TAK-242 (C, D, G, H, K, L, O, P) for 2 hours, followed by treatment with TGFβ2 and/or cFN for 72 hours. Immunocytochemistry shows that activation of TLR4 signaling by TGFβ2 and cFN increase staining signaling for FN and COL1 compared to controls. Inhibition of TLR4 signaling blocks the effects of all treatments. *Scale bar* represents 50μm.

Figure 5. Crosstalk of TGFβ2 – TLR4 signaling in LC Cells. TGFβ2 activates the TGFβ receptor complex, phosphorylating Smad2/3. pSmad2/3 forms a complex with Smad 4, which translocates to the nucleus to act as a transcription factor increasing pro-fibrotic and pro-inflammatory gene transcription, including the production of DAMPs. These DAMPs are then able to activate TLR4 signaling, increasing NFκB through the MyD88 dependent pathway. NFκB

translocates to the nucleus acting as a transcription factor, inhibiting the transcription of *Bambi*, which acts as a negative regulator of the TGFβ2 signaling cascade. Thus, these two pathways act in a feedforward loop.

Figure 1. FN and FN-EDA expression in the LC region of normal and glaucomatous human ONH.

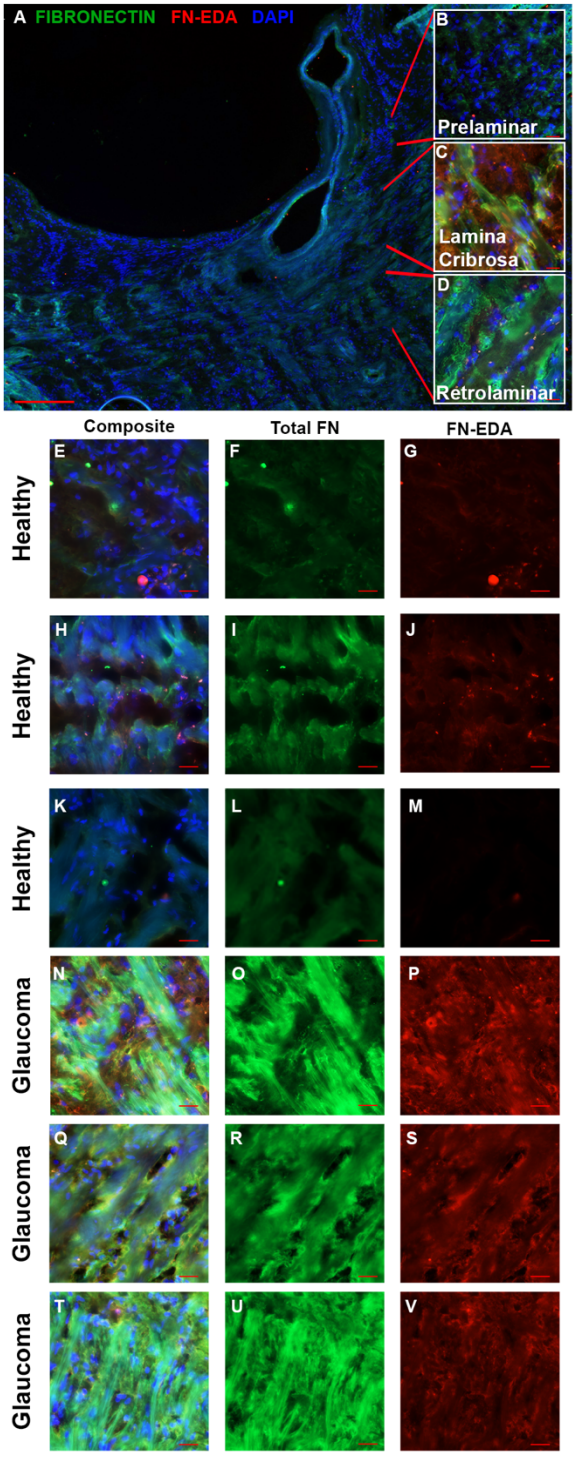

Figure 2. Isolation and characterization of LC cells from hONH explants.

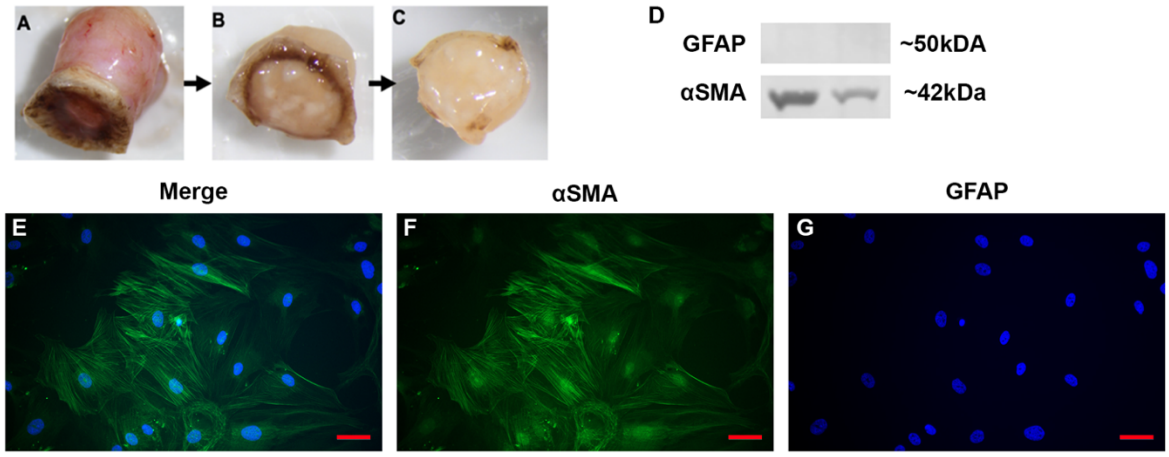

Figure 3. Inhibition of TLR4 blocks TGFβ2-induced ECM protein expression.

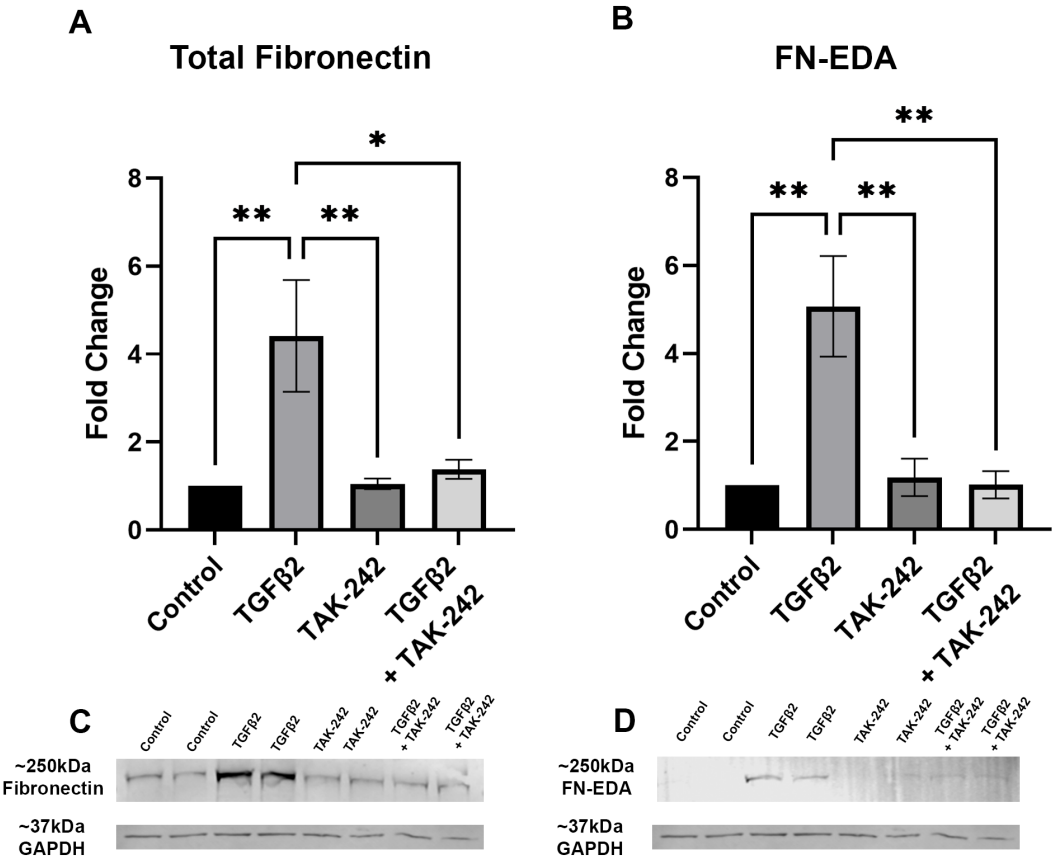

Figure 4. TLR4 signaling is necessary and sufficient for ECM accumulation in hONH LC cells.

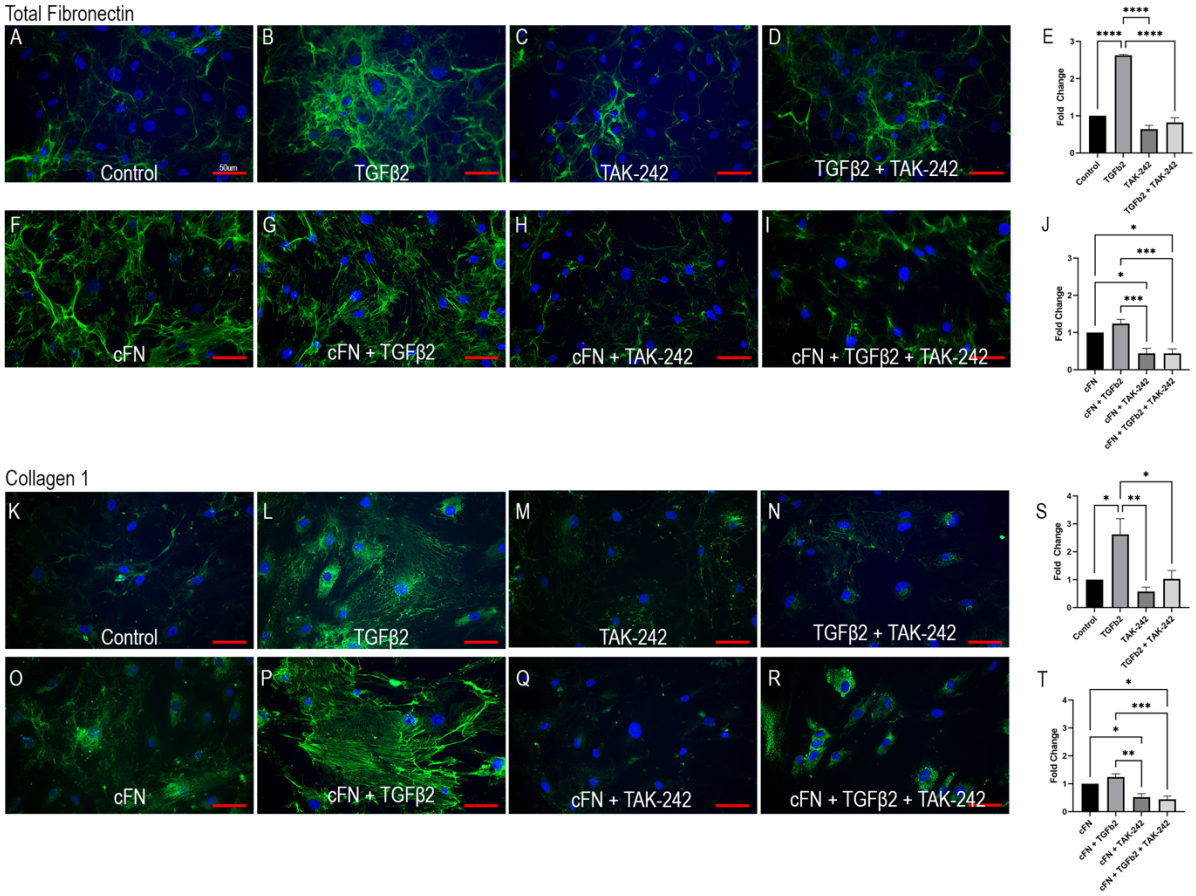

Figure 5. Crosstalk of TGFβ2 – TLR4 signaling in LC Cells.

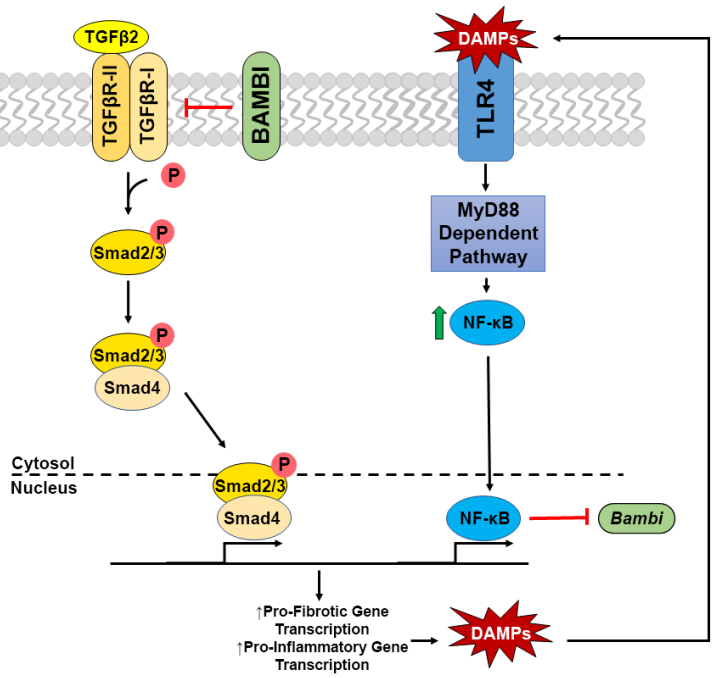

Chapter 3: Pathogenic paracrine signaling between ONH astrocytes and lamina cribrosa cells

Adapted from: **Emma K. Geiduschek**, Kelsey M. Mathers, Colleen M. McDowell. Preprint.

Abstract

It is well known that increased extracellular matrix (ECM) deposition and fibrosis occur at the layer of the lamina cribrosa (LC) in the glaucomatous optic nerve head (ONH). Previous research indicates a role of both transforming growth factor – β2 (TGFβ2) and toll-like receptor 4 (TLR4) signaling in perpetuating this fibrosis within LC cells. Here, we expanded on this work and investigated TGFβ2-TLR4 signaling crosstalk within human ONH astrocytes and between ONH astrocytes and ONH LC cells derived from healthy donor eyes utilizing a co-culturing system. In astrocyte monocultures, TLR4 signaling was necessary for TGFβ2-induced fibronectin (FN) and FN – extra domain A (FN+EDA) protein production. FN+EDA acts as a potent damage associated molecular pattern (DAMP) and is known to activate TLR4 signaling. In the co-culture system, activation of TLR4 in LC cells by cellular FN, which contains the DAMP FN+EDA, was sufficient to increase total FN and tenascin-C protein expression, another TLR4-activating DAMP. Activation of TLR4 in LC cells was also able to significantly increased FN and tenascin-C protein expression in the astrocytes, and subsequently blocking TLR4 in the astrocytes prevented astrocyte production of these ECM proteins. Thus, these data show a novel paracrine signaling between ONH astrocytes and LC cells.

Introduction

The glaucomas, a heterogenous group of ocular neuropathies, are currently the leading cause of blindness, estimated to effect 75 million individuals worldwide.[1, 2] Currently, the only therapeutic involves lowering the interocular pressure (IOP), decreasing aqueous humor production, or targeting the trabecular meshwork (TM). However, these therapies are not

uniformly effective across the patient population, indicating a crucial need for a better understanding of the molecular and cellular signaling resulting in progressive vision loss.[7, 12, 157]

Multiple insults in the ONH, including mechanical stress, hypoxic microenvironments, and loss of nutrient and neurotrophic transport all contribute to the loss of RGCs and eventual vision loss.[15, 16] Damage and disruption to the exiting RGCs occurs primarily in the lamina cribrosa (LC) region of the ONH due to the sharp 90° turn the axons make while exiting the eye to form the optic nerve (ON).[13, 17] The LC is made up of connective tissues and extracellular matrix (ECM) proteins that create a framework to physically support the exiting RGC axons. Additional support cells, such as astrocytes and microglia, are also present in the LC and function to deliver nutrients to the RGC axons. Disruption and increased deposition of ECM proteins in glaucoma leads to the eventual mechanical failure of the LC region.[22, 55, 62] These biomechanics of the LC region have been extensively studied and highly implicated in glaucomatous pathophysiology,[18] with changes in the stiffness and elasticity of the LC region disrupting the interaction between the exiting RGC axons, LC scaffolding, and the supporting cells of the ONH.

The ONH is populated by glial fibrillary acidic (GFAP)-positive astrocytes, α-smooth muscle actin (αSMA) positive LC cells, and Iba1 positive microglia. Astrocytes are the most common glial cell in the human ONH,[22] and facilitate nutrient transport and produce ECM proteins to physically support of the exiting RC axons.[39] LC cells are the primary source of secreted ECM proteins which also physically support the exiting RGC axons.[48] Finally, microglia are the innate immune cells of the central nervous system.[19, 21, 22] All three cell types have been

associated with glaucomatous pathophysiology, but the critical signaling pathways within and between the cell populations is still poorly understood.

The drastic changes in ECM production and increased fibrosis in the glaucomatous LC region of the ONH have been extensively review.[14, 49, 59, 60] Posterior migration of the ONH and remodeling of the LC region occurs due to elevated IOP which exerts significant biomechanical stress and strain on the ONH.[61] Both the astrocytes and LC cells have been shown to increase ECM protein production during glaucoma progression or when exposed to glaucoma-like environments.[22, 56, 68, 158] Immune system activation has been significantly linked to the increase in ECM protein expression in the glaucomatous ONH,[22, 56] including the activation of TLR4 in the glaucomatous ONH,[56] TM,[74] and other fibrotic diseases.[93-95] TLR4 activation, downstream signaling molecules, and *TLR4* gene polymorphisms have all been associated with an increased risk for developing glaucoma and glaucomatous pathophysiology.[56, 74, 97, 99, 162, 180] TLR4, first discovered as the receptor for lipopolysaccharide (LPS) on gram-negative bacteria,[160] can be activated by endogenous damage associated molecular patterns (DAMPs). DAMPs are generated in response to cell injury or death, oxidative stress, or ECM remodeling.[102, 161]

Previous work in our lab has identified TLR4 as a critical modulator of ECM production in the human TM and ONH LC cells, as well as in response to ocular hypertension.[56, 74] Specifically, DAMP activation of TLR4 has been shown to mimic and augment transforming growth factor – β (TGFβ) fibrotic responses.[56, 74, 93, 151] These DAMPs, including fibronectin extra domain A (FN+EDA), tenascin-C, and heat shot proteins have shown increased expression in the glaucomatous ONH in both humans and mouse models.[56, 64, 163] We have previously shown

that FN+EDA increases IOP in a novel mouse model of glaucoma through the TLR4 signaling pathway,[96] and that functional TGFβ2 induced fibrosis requires functional TLR4 signaling.[56, 74] TGFβ2 is the predominate TGFβ isoform in the ONH, and is known to have increased expression in the glaucomatous aqueous humor and ONH.[75, 164-167] We and others have shown that TGFβ2 exposure increased ECM DAMP production in TM cells and human ONH LC cells.[56, 74]

Notably, ONH astrocytes, LC cells, and microglia are known to express both TLR4 and TGFβ receptors, as well as secrete TGFβ2. This indicates a potential mechanism of both autocrine and paracrine signaling within the glaucomatous ONH that can exacerbate ECM production and negative effects on the ONH, leading to eventual RGC loss and blindness in glaucomatous patients. Here we demonstrate integral signaling crosstalk between TLR4 and TGFβ2 signaling in monocultures of human ONH astrocytes, as well as a mechanism for paracrine signaling in co-cultures of human ONH LC cells and astrocytes. These results suggest that DAMP activation of TLR4 via TGFβ2 signaling may have important implications in the glaucomatous ONH.

Methods

Human donor eyes

For the isolation of primary ONH astrocytes and LC cells, healthy human donor eyes were obtained from the Lions Eye Bank of Wisconsin (Madison, WI) within 24hr of death (ages 54 – 80). The eyes were obtained and managed in compliance with the Declaration of Helsinki for research involving human tissues. In addition, primary human LC cells and astrocytes were received as a generous gift from Dr. Abe Clark at the University of North Texas Health Science

Center. Culture strains were characterized as previously described [56, 127, 158, 174]. LC cells were cultured and maintained in Ham's F-10 growth media (Corning, REF# 10-070-CV) containing 10% fetal bovine serum (FBS, Avantor, REF# 97068-085), L-glutamine (0.292 mg/mL, Corning, REF#25-005-CI), and penicillin (100units/mL)/streptomycin (0.1mg/mL). Astrocytes were cultured and maintained in astrocyte medium (ScienCell, REF#: 1801) containing 20% fetal bovine serum (FBS, Avantor, REF# 97068-085) and included supplements penicillin/streptomycin (ScienCell, REF#: 0503) and astrocyte growth supplement (ScienCell, REF#: 1852). Medium for LC cells and astrocytes were replaced every 2-3 days.

TLR4 inhibition and activation in astrocyte monocultures

Primary human ONH astrocyte cells were grown to confluency before being pretreated with the selective TLR4 inhibitor TAK-242 (*In vivo*Gen, San Diego, CA, USA) at 5μM for 2 hours. TAK-242 is a selective TLR4 inhibitor that specifically binds to the intracellular domain of TLR4 to inhibit downstream signaling activation.[181, 182] Cells were subsequently treated with or without exogenous TGFβ2 (5ng/mL) for 72 hours in serum-free medium. Immunocytochemistry and western blot experiments and analysis were performed after as described below.

TLR4 inhibition and activation in astrocyte and LC co-cultures

Primary human ONH astrocytes (2 independent cell strains) were grown to confluency in cell culture inserts (Greiner Bio-One, REF#: 665610) (Fig. 1A). Once confluent, astrocytes in the culture inserts were pretreated with TAK-242 at 5μM astrocytes. After 2 hours, the TAK-242 was removed and replaced with serum-free media for the remainder of the experiment. Subsequently,

LC cells were exposed to cFN+EDA coated 12-well cell culture plates. Wells from these 12-well plates were coated with 180µL cFN containing the FN+EDA isoform (10µg/mL, Sigma-Aldrich Corp., REF#: F2518) and air dried for 2 hours under sterile conditions. Once dried and the TAK-242 pretreatment was complete for the astrocytes in the cell culture inserts, LC cells fro one independent cell strain were seeded onto the cFN coated or uncoated 12-well plate wells in serum free medium. The cell culture inserts were then placed into the seeded cell wells. The use of the cell culture inserts allowed for the free distribution of signaling molecules from each cell type without direct cell-cell contact in four different treatment groups (Fig. 1B). In the control group, astrocytes were grown to confluency and not pretreated with TAK-242, while LC cells were directly seeded onto wells without cFN coating (Fig. 1B). In the cFN group, astrocytes were not pretreated with TAK-242, and LC cells were seeded onto cFN coated wells (Fig. 1B). In the TLR4i group, astrocytes were pretreated with TAK-242 for two hours, the media was washed off and replaced with fresh serum free media and combined with LC cells seeded onto blank wells (Fig. 1B). Finally, in the last group astrocytes were pretreated with TAK-242 for two hours before the media was washed off and replaced with fresh serum free media, and the LC cells were seeded onto cFN coated wells (Fig. 1B). Cells were left for 72 hours before subsequent western blot analysis described below. A total of 5 independent co-culture experiments were performed.

Immunocytochemistry

Primary human ONH astrocytes were seeded onto coverslips in a 12-well plate and grown to confluency. Once confluent, cells were treated with combinations of the TLR4 inhibitor TAK-242 and TGFβ2 as previously described for 72 hours. After 72 hours, coverslips were

washed 3 times with 1X PBS, fixed with 4% paraformaldehyde (PFA), permeabilized with 0.95% Triton X-100 in PBS, and blocked using Superblock Blocking Buffer (Thermo Fischer Scientific, REF# 37580) for 60 minutes at RT. Cells were labeled overnight in 4°C with rabbit anti-fibronectin (Sigma-Aldrich, REF#: F3648, 1:100) or rabbit anti-collagen-I (Novus Biologicals, REF#: NB600-408, 1:100). Treatment without primary antibody was used as a negative control. After the overnight incubation, coverslips were again washed 3 times in 1X PBS before incubation in Alexa Fluor 488 donkey anti-rabbit IgG 2° antibody (Invitrogen – Thermo Fischer Scientific, REF#: A21206, 1:200) for 1 hours. Slides were then washed 3 times with 1X PBS before mounted to slides with Prolong Gold mountain medium containing DAPI (Invitrogen-Molecular Probes). Image acquisition was performed using Zeiss Axio Imager Z2 microscope at 40X. Scale bar represents 20μm.

Western blot analysis

Primary human ONH astrocytes or LC cells were treated with TAK-242, TGFβ2, or cFN as previously described.[56] After 72 hours of exposure to specific treatments, cell lysates were collected using Pierce RIPA lysis buffer (Pierce RIPA Buffer, Thermo Fischer Scientific, REF#: 89901; cOmplete mini, EDTA-Free protease inhibitor cocktail, Thermo Fischer Scientific, REF#: 11836170001; PhosSTOP, Sigma-Aldrich, REF#: 04906837001). Lysate protein concentration was determined by the Pierce BCA Protein Assay Kit (Thermo Fischer Scientific, REF#: 23225). Each loading sample for subsequent western blot analysis contained 7.5μg of protein and the appropriate amount of 4X Protein Loading Buffer (Li-Core, REF#: 928-40004). Samples were then boiled for 10 minutes and separated using a 4-12% Bolt Bis-Tris Plus mini gel (Invitrogen, REF#: NW04120BOX) at 200V for 65 minutes. Proteins from these electrophoresed gels were

transferred to polyvinylidene (PVDF) membranes (Bio-Rad Immun-Blot, REF#: 1620177) using the Mini Gel Tank wet transfer (Invitrogen, REF#: A25977) at a constant 20V for 1 hour. Membranes were then left to dry at RT for 1 hour before using the Revert 700 Total Protein Stain (Li-Core, REF#: 927-60001). After subsequent total protein staining and washing, blots were left at room temperature for 1 hour in Intercept Blocking Buffer (Li-Cor, REF#: 927-60001) and incubated in 1° antibodies overnight at 4°C: Fibronectin (Sigma – Aldrich, REF#: F3648, 1:1000), and/or FN+EDA (IST-9) (Abcam, REF#: ab6328, 1:500), and/or Tenascin (Millipore, REF#: AB19011, 1:500). Membranes were then washed 3 times for 5 minutes in 1X TBS-T before incubation in the appropriate 2° antibodies for 1 hour a room temperature in Intercept Blocking Buffer: 1:20,000 goat anti-rabbit IRDye 680RD (LI-COR, REF#: 926-68071), 1:20,000 goat anti-mouse IRDye 800CW (LI-COR, REF#: 926-32210), or 1:10,000 goat anti-rabbit IRDye 680RD (LI-COR, REF#: 926-68071). Membranes were then washed 3 times in 1X PBS for 5 minutes and then imaged on a Licor OdysseyCLx system. Each experiment was repeated 2-3 times in each individual cell strain, and a total of 3 independent strains were tested. Band intensity for total protein and proteins of interest were measured using Image Studio Lite (LI-COR Biosciences, Lincoln, NE, USA), and each target protein of interest densitometry value was normalized against either its corresponding total protein values. Data is presented as fold change compared to control, represented as the mean +/- SEM.

Results

Characterization of human ONH Astrocytes

The ONHs were dissected form healthy donor eyes, and the explant placed into culture to propagate either LC cells or astrocytes as previously described.[56, 174] Representative

immunocytochemistry images from two independent ONH astrocyte strains show isolated astrocytes are GFAP positive and αSMA negative (Fig. 1). The LC cells have been previously characterized,[56] and the astrocyte cell strains were isolated from different healthy donor eyes with no history of ocular disease.

Inhibition of TLR4 blocks TGFβ2-induced FN and FN+EDA production in primary human ONH astrocytes.

As previously stated, it is well known that TGFβ2-induced fibrosis is known to affect ONH glaucomatous disease progression.[66] TGFβ2 has been shown to induce ECM production in human ONH LC cells.[56, 68, 69] Here, we show that TGFβ2 is sufficient to induce ECM protein expression increases in human ONH astrocytes. Specifically, TGFβ2 exposure caused statistically significant increases in FN (Fig. 2A) and FN+EDA (Fig. 2B) compared to total protein levels (Fig. 2C, D). Concurrent inhibition with the selective TLR4 inhibition, TAK-242, rescues this phenotype and returns protein expression levels back to baseline, with no significant differences between control and TGFβ2 + TAK-242 treatment groups. As expected, FN+EDA levels were negligible in the control treated cells as the levels of FN+EDA are typically minimal in normal healthy cells.[183] Immunocytochemistry analysis of astrocytes recapitulates these results with TGFβ2 and TAK-242 treatments (Fig. 2E-H). TGFβ2 induced significant increases of FN protein expression, and concurrent TLR4 inhibition returned protein levels back to baseline (Fig. 2I).

DAMP FN+EDA-induced fibrosis in human ONH LC cells is sufficient to induce ECM protein expression increases in human ONH astrocytes via paracrine signaling.

Previously, we have shown that DAMP exposure to human LC cells significantly increases ECM production in a TLR4-dependent manner through autocrine signaling.[56] Here we utilize a co-culture system that allows for LC cells alone to be exposed to cFN and astrocytes alone to be exposed to the TLR4 inhibitor TAK-242 before combining insert and plate, allowing for both cell populations to share media without being in direct contact (Fig. 1A). This allows for the harvesting and analysis of LC cell and astrocyte cell populations independently. Western immunoblot analysis represent protein expression changes in either LC cells or astrocytes, never a mixed culture. Here we show that LC cell exposure to cFN, which contains the DAMP FN+EDA, significantly increases total FN protein expression (Fig. 4A) and the DAMP tenascin-C (Fig. 4B).[102] Interestingly, tenascin-C is known to activate TLR4 signaling,[102, 109, 180] implicating it as a crucial signaling molecule progressing glaucomatous damage in the ONH. We also show that astrocytes in co-culture with LC cells exposed to DAMPs have significant FN and tenascin-C protein expression (Fig. 4E, F), and that this increase in protein expression is blocked when the astrocytes are pretreated with the selective TLR4i inhibitor, TAK-242.

Discussion

In primary open angle glaucoma (POAG), the ONH is the primary cite of damage. Changes including increased immune activation, hypoxic microenvironments, ECM remodeling, loss of nutrient transport, and mechanical failure and fibrosis all significantly contribute to glaucomatous pathophysiology and disease progression. There are significant increases of ECM protein deposition, such as fibronectin, collagens, elastin, and the DAMPs tenascin-C and FN+EDA, in the glaucomatous ONH in humans and animal models.[56, 63, 64, 177] Both the astrocytes and LC cells are responsible for producing these ECM molecules to help support the

exiting RGC axons. Pathogenic changes to the ONH leads to eventual RGC death and progressive vision loss seen in glaucoma.

The molecular and cellular signaling pathways within and between the LC cells and astrocytes in the glaucomatous ONH are not fully understood. It is well established that TGFβ2 levels are increased in the AH and ONH of POAG patients,[64, 75, 164-167] though how TGFβ2-induced fibrosis affects and/or activates LC cells and astrocytes in the ONH is also not fully understood. ONH astrocytes and LC cells both express TLR4,[45, 50] TGFβ2,[51, 69, 100] and TGFβ-receptors.[50, 51] This enables a potential for autocrine and paracrine TLR4-TGFβ2 signaling crosstalk within these cell types. Treatment of ONH astrocytes or LC cells with TGFβ2 increases the activation of the canonical Smad2/3 signaling pathway, resulting in increased ECM production.[68, 69, 159] Many ECM proteins are DAMPs, such as FN+EDA and tenascin-c[102], and are able to activate TLR4 signaling.[102] The TLR4-MyD88-dependent pathway leads to the production and translocation of NFκB to the nucleus where it acts as a potent transcription factor for initiating immune system signaling in the cells. One such target is the downregulation of the TGFβ pseudoreceptor BMP and activin membrane bound inhibitor (BAMBI).[93] Thus, TGFβ2-induced DAMP production activates TLR4, which downregulates a TGFβ2 inhibitor, and can initiate a vicious feed forward cycle.[56, 180] Here we show this pathogenic TGFβ2-TLR4 crosstalk in human ONH astrocyte monocultures, as well as in co-culture between ONH LC cells and astrocytes. These data suggest that the response of LC cells to fibrotic changes in the ONH can elicit a further pathogenic response in ONH astrocytes.

DAMP activation of LC cells induced a fibrotic phenotype, significantly increasing protein expression of both FN and tenascin-C, a known DAMP (Fig. 4A, B). The response of the LC cells to cFN+EDA was sufficient to induce a fibrotic phenotype in astrocyte cells, significantly increasing FN and tenascin-C protein levels (Fig. 4E, F). Thus, stimulated LC cells can induce a fibrotic phenotype in astrocytes via paracrine signaling. Tenascin-C protein expression was significantly upregulated in both LC cell and astrocyte populations (Fig. 4B, F). Tenascin-C is an adhesion-modulating ECM protein due to its ability to bind to FN and other ECM proteins, altering ECM-cell signaling.[184-188] In healthy tissue, tenascin-C protein levels are negligible outside of specific stem cell populations and tendons, however tenascin-C levels significantly increase in response to biomechanical strain and/or inflammation in tissues,[189-191] and is known to be significantly upregulated in the human glaucomatous ONH.[64] Importantly, SMAD2/3 signaling has been shown to upregulate tenascin-c transcription, indicating a direct role of TGFβ2 signaling on tenascin-C activation. Future studies are needed to explore the interactions of the DAMP tenascin-C on ECM production *in* vivo in the glaucomatous ONH.

Conclusion

In conclusion, these data begin to identify the complex interplay between the cells of the ONH in glaucoma. We show pathogenic TGFβ2-TLR4 signaling crosstalk in human ONH astrocyte monocultures, and we have identified that DAMP activation of LC cells induces fibrosis in astrocyte cell cultures in a TLR4-dependent manner. These data indicate an important role of paracrine signaling in perpetuating fibrotic damage in the glaucomatous ONH.

Conflict of Interest

The authors declare that the research was conducted in the absence of any commercial or financial relationships that could be construed as a potential conflict of interest.

Acknowledgements

We thank Stacy Curry at the University of North Texas Health Science Center for assistance with optic nerve head dissections and cell cultures.

Author Contribution

CMM developed all ideas and experimental designs, analyzed data, and wrote the manuscript. KM assisted with western blot analyses. EKG performed all cellular experiments, analyzed data, and wrote the manuscript.

Funding

This work was supported in part by National Institute of Health R01EY02652 (CMM), William and Phyllis Huffman Research Professorship (CMM), and the McPherson Eye Research Institute Grant Summit Program (CMM). This work was also supported in part by an Unrestricted Grant from Research to Prevent Blindness to the UW-Madison Department of Ophthalmology and Visual Sciences, the Core Grant for Vision Research from the NIH to the University of Wisconsin-Madison (P30 EY016665).

Chapter 3 Figure Legends

Figure 1. Timeline of co-culture experiments and treatment groups. Primary hONH astrocytes (*n* = 3 independent experiments from 2 cell strains) were grown to confluency on cell culture inserts. Once confluent, astrocytes were pretreated with TAK-242 (5μM) for 2 hours. Concurrently, empty cell culture plates were treated with cFN (μg/mL) and left to dry for 2 hours. After 2 hours, TAK-242 was washed off the astrocyte cell culture inserts and replaced with fresh serum free media, and LC cells (*n* = 3 independent experiments from 1 cell strain) were seeded onto blank or cFN coated wells (A). Cell culture inserts were then inserted into cell-culture plate and left for 72 hours. Co-Culture experiments consisted of four treatments groups with or without TLR4 inhibition in astrocytes only, and with or without cFN coated plates with LC cells (B). Created with BioRender.com.

Figure 2. Isolation and characterization of human ONH astrocytes and LC cells from the LC region of human explants. Human ONH LC cells and astrocytes were isolated and characterized as previously described.[56, 174] Representative ICC staining of GFAP+ (A), αSMA-negative (B) astrocyte cell cultures. 40X magnification, *scale bar* represents 50μm.

Figure 3. Inhibition of TLR4 blocks TGFβ2-induced ECM and DAMP protein expression. Primary hONH astrocytes (*n* = 3 independent experiments from 2 cell strains) were pretreated with TAK-242 (5μM) for 2 hours, and subsequently treated with TGFβ2 (5 ng/mL) and/or TAK-242 (5μM) for 72 hours. Western immunoblot for total FN (A) and FN+EDA (B) show that inhibition of TLR4 via the selective inhibitor TAK-242 blocks the TGFβ2-induced fibrotic and DAMP protein expression. Representative immunoblots of FN and respective total protein stain

(C), and FN+EDA and respective total protein stain (D). Primary hONH astrocytes (*n* = 3 independent experiments from 1 cell strain) were pretreated with TAK-242 (5μM) for 2 hours, and subsequently treated with TGFβ2 (5 ng/mL) and/or TAK-242 (5μM) for 72 hours. ICC for total FN (E) show that inhibition of TLR4 blocks the TGFβ2-induced increases of FN protein expression. Representative ICC images (F-I). Statistical significance was determined by 1-way ANOVA and Tukey's *post hoc* analysis. **P < 0.05, **P < 0.01*.

Figure 4. DAMP-activated LC cells significantly increase astrocyte ECM production in a TLR4-dependent manner Primary hONH LC cells (*n* = 3 independent experiments from 1 cell strain) were plated onto cFN coated wells in a 12-well plate for 72 hours. Western immunoblot for total FN (A) and tenascin-C (B) show that activation of TLR4 by the DAMPs in cFN significantly increase ECM production. Representative immunoblots of FN and respective total protein stain (C), and tenascin-C and respective total protein stain (D). Primary hONH astrocytes (*n* = 2-3 independent experiments from 2 cell strains) were plated onto cell culture inserts and grown to confluency. Once confluent, astrocytes were pretreated with the selective TLR4 inhibitor TAK-242 before being inserted into the plate with LC cells, allowing for shared media without direct contact. Western immunoblot for total FN (E) and tenascin-C (F) show that DAMPs from activated LC cells increase astrocyte ECM production via paracrine signaling. Representative immune blots for FN and respective total protein stain (G), and tenascin-C and respective total protein stain (H). Statistical significance was determined by 1-way ANOVA and Tukey's *post hoc* analysis. **P < 0.05, **P < 0.01, ***P < 0.001, ****P < 0.0001*.

Figure 1. Timeline of co-culture experiments and treatment groups.

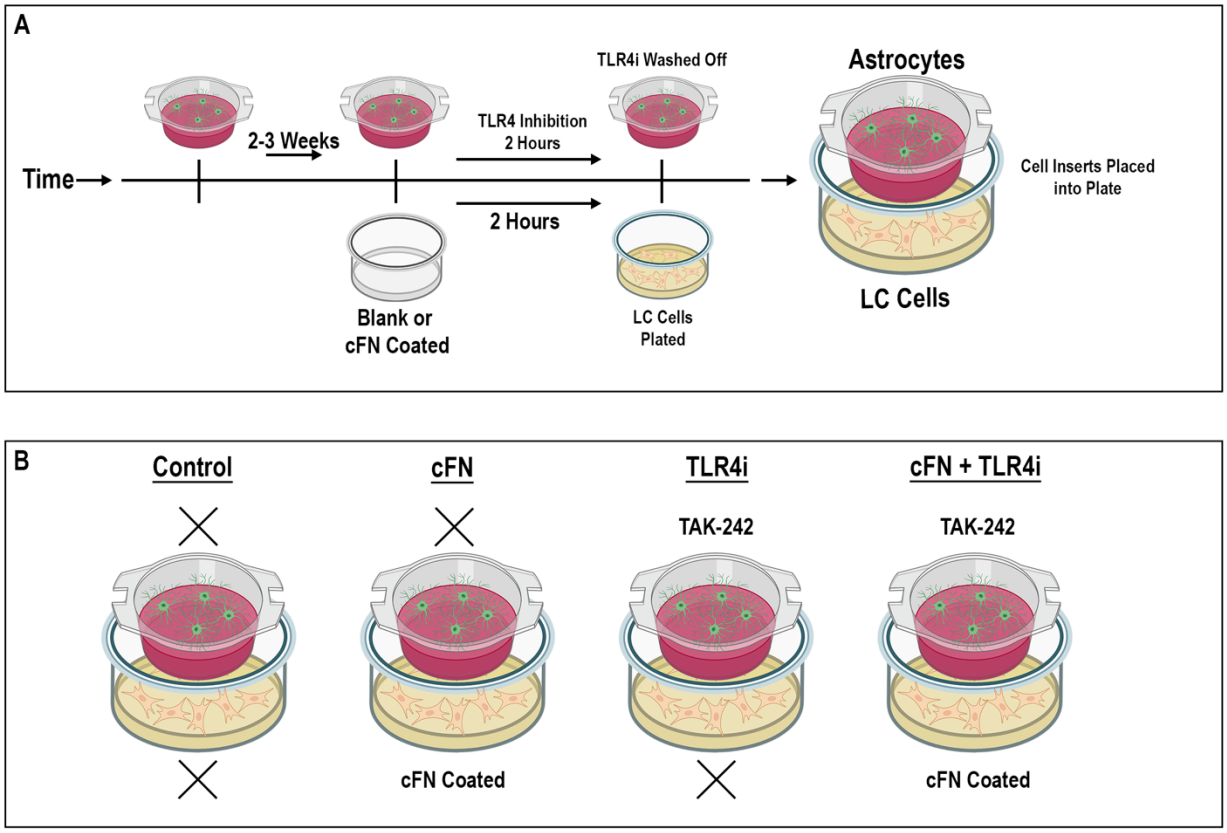

Figure 2. Isolation and characterization of human ONH astrocytes and LC cells from the LC region of human explants.

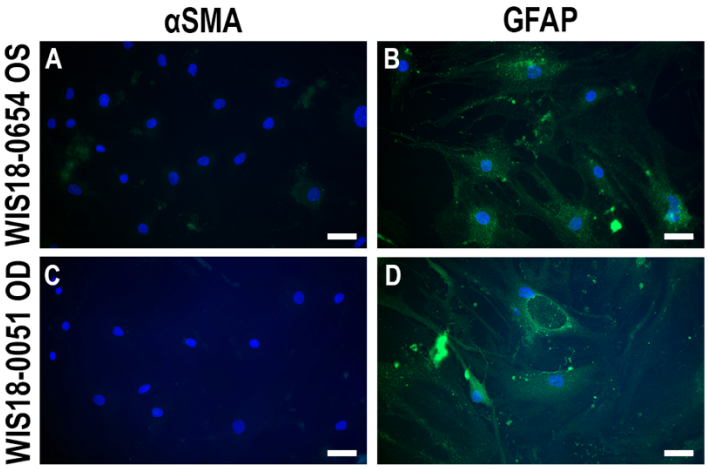

Figure 3. Inhibition of TLR4 blocks TGFβ2-induced ECM and DAMP protein expression.

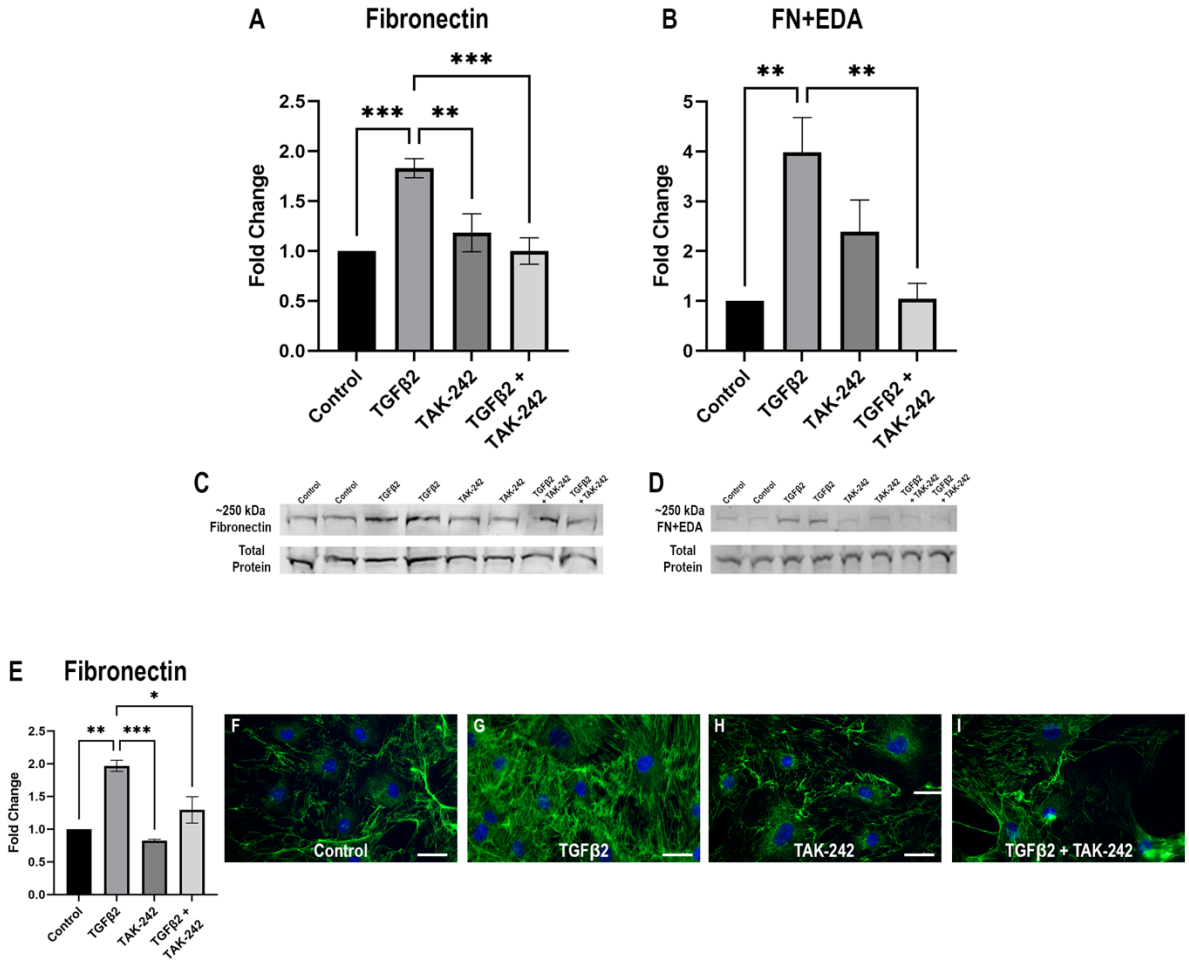

Figure 4. DAMP-activated LC cells significantly increase astrocyte ECM production in a TLR4-dependent manner.

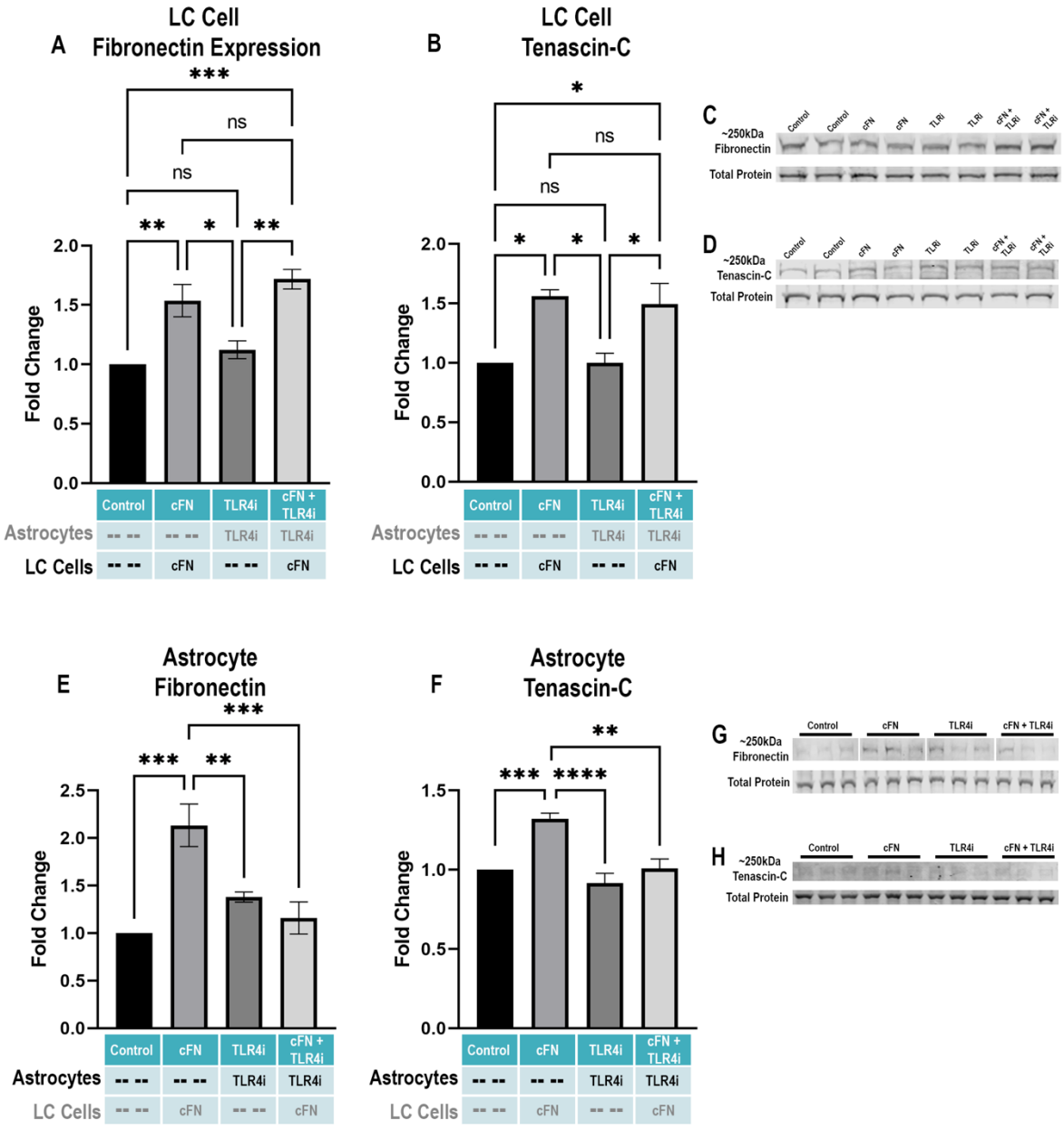

Chapter 4: DAMPs Drive Fibroinflammatory Changes in the Glaucomatous ONH

Adapted from: **Emma K. Geiduschek**, Emma K. Bricco, Colleen M. McDowell. DAMPs Drive Fibroinflammatory Changes in the Glaucomatous ONH. *In review*.

Abstract

Purpose: The ONH is well known to be the initial site of glaucomatous damage. However, the molecular mechanisms initiating this pathology are not fully understood. To further understand the initiating factors in glaucomatous damage we utilized a novel mouse model of glaucoma, B6.EDA$^{+/+}$ mice, that constitutively express FN containing the EDA domain (FN+EDA). FN+EDA is a known DAMP that activates TLR4 and elicits a fibro-inflammatory response.

Methods: Eyes from B6.EDA$^{+/+}$ and C57BL/6J mice were evaluated for RGC death, RNFL thickness, and ON damage at 12 months and 22 months of age. ONH sections were isolated using laser capture microdissection (LCM) for subsequent RNAsequencing and gene set enrichment analysis (GSEA). GSEA results were confirmed using IHC staining.

Results: B6.EDA$^{+/+}$ mice exhibit significantly higher IOP, loss of RGCs, thinning of the RNFL, and progressive levels of ON damage at 12 months and 22 months of age compared to C57BL/6J controls. Protein expression of DAMPs FN+EDA and biglycan were significantly increased in B6.EDA$^{+/+}$ mice compared to C57BL/6J controls. GSEA analysis identified significantly up- and down-regulated gene groupings at both 12 months and 22 months of age, and IHC staining demonstrated significant increases of IFNα, IFNβ, and pSTAT1 expression in B6.EDA$^{+/+}$ mice compared to C57BL/6J controls.

Conclusions: Our study characterizes glaucomatous changes to the retina, ON, and ONH over the course of two years and identifies novel molecular pathways associated with these

pathophysiological changes. These data indicate time specific DAMP production and immune system signaling in a novel mouse model of glaucoma.

Keywords: Glaucoma, FN+EDA, Optic nerve head, Interferons, STAT1

Introduction

Glaucoma is characterized by the loss of retinal ganglion cells (RGCs) and subsequent optic nerve head (ONH) damage resulting in a progressive loss of vision over time.[3-5] The primary site of RGC axonal damage occurs at the layer of the lamina cribrosa (LC) in the ONH, which consists of a fenestrated stack of extracellular matrix (ECM) proteins that provide both physical support for the exiting RGC axons, as well as scaffolding for nutrient transport and vasculature. During disease progression, the ONH undergoes drastic remodeling. Disruption of the ECM in the LC region causes increased fibrosis, thickening of the connective tissue around the ON fibers, elastosis, and thickening of the basement membranes resulting in eventual mechanical failure.[22, 55, 62] This ECM dysregulation adversely affects the capacity of the LC to support the exiting RGC axons.

Previous literature has heavily implicated both pro-fibrotic and pro-inflammatory signaling cascades in the progression and exacerbation of glaucomatous damage. One predominate hypothesis indicates that chronic exposure to mechanical stress and strain from elevated IOP, loss of nutrients, and hypoxic microevironments produce a chronic level of inflammation through the innate immune system.[13, 17, 78, 79, 83, 86] The role of innate immune system activation and subsequent glaucomatous pathology has been extensively reviewed,[16, 78, 80, 192] often focusing on the role of microglia as the resident macrophages of the central nervous system immune responses. In homeostatic environments, microglia constantly monitor their local microenvionments and primarily clear debris and dead cells.[23] Upon activation from damage or in disease states, microglia undergo drastic morphological changes from ramified surveyors to an ameboid shape and migrate to the cite of damage within a matter of minutes.[21, 24-27] Microgliosis

has been implicated in other CNS diseases such as Alzheimer's and Parkinson's disease, as well as glaucoma.[20] Activated microglia induce activation of astrocytes, which subsequently produce pro-inflammatory cytokines and chemokines that are able to initiate innate immune system signaling through toll-like receptors (TLRs).[44, 180]

Notably, toll-like receptor 4 (*Tlr4*) gene polymorphisms have also been associated with an enhanced risk of glaucoma in populations of different racial backgrounds including Japanese and Mexican populations.[97, 99, 162] TLR4 was first discovered as the receptor for lipopolysaccharide (LPS),[160] but it is also activated by endogenous ligands called damage associated molecular patterns (DAMPs). DAMPs are produced *in vivo* from injury, cell damage, oxidative stress, or ECM accumulation.[102, 161] TLR4 is known to be expressed in mouse and human RGC axons, ONH astrocytes, and ONH microglia,[31, 45, 51, 128] indicating it as a global activator of the innate immune system within the ONH. TLR4 pathway related genes, downstream ECM genes, and TLR4-activating DAMPs such as tenascin-C, heat shock proteins, and importantly the EDA isoform of fibronectin (FN+EDA) are differential expression in the human ONH and retina in glaucoma.[34, 56, 64, 100]

FN, a high-molecular weight, multidomain glycoprotein, has previously been shown to be significantly increased in the glaucomatous TM, AH, and LC region of the ONH.[56, 74, 169, 193, 194] There are two types of FN found in vertebrates: cellular FN (cFN) and plasma FN (pFN).[114] Splice variants of cFN contains combinations of the EDA domain, the extra domain – B (EDB), and type III homologies. pFN does not contain the EDA or EDB domains.[114] FN+EDA expression is high during embryonic development, but lowers to near-negligible expression

levels in adult tissue.[116] However, during disease states or inflammatory responses, the expression of FN+EDA is upregulated.[117-120] Importantly, FN+EDA is increased in the glaucomatous human TM and ONH,[56, 125] and acts as a potent activator of TLR4 in TM cells[74, 96] and ONH lamina cribrosa (LC) cells.[56]

Recently, we have shown that TGFβ2 induced ocular hypertension is dependent on both TLR4 and FN+EDA expression.[31, 96] In addition, constitutive expression of FN+EDA is sufficient to induce ocular hypertension and modest glaucomatous damage in the retina and ON.[31, 96] In this model, B6.EDA$^{+/+}$ mice constitutively express FN+EDA. These mice exhibit TLR4-dependent increased IOP starting from 14 weeks of age.[31, 96] At one year of age, these mice have significant reductions in RGCs and increased levels of ON damage.[31] Interestingly, these mice show elevated levels of the microglia marker Iba1 as well as increased *Tlr4* mRNA in microglia compared to age matched controls at 9 months of age, prior to any ONH or ON damage.[31] Here, we test the progressive retinal and ONH damage in this novel mouse model in an aged state, as well as elucidate transcriptome variations responsible for glaucomatous changes.

Methods

Animals

The generation of B6.EDA$^{+/+}$ mice has been previously described,[117] and constitutively express only FN containing the EDA domain. C57BL/6J mice were purchased from the Jackson Laboratories and aged at UW – Madison. All animals were housed in the UW-Madison vivarium,

maintained a normal 12-hr light/dark cycle, and were fed a 4% fat diet (Harkland Tekland, Madison, WI, USA) with food and water available ad libitum.

For quantification of RGC loss and preparation for laser capture microdissection (LCM) of the ONH, mice were euthanized by CO_2 inhalations and eyes were nucleated. One eye was frozen on dry ice in optimal cutting temperature (OCT) compound (Sakura REF#4583) for subsequent LCM and RNA-sequencing. The other eye was prepared for retinal flat mount analysis (see below).

Intraocular Pressure Measurements

IOP was measured with a rebound tonometer as previously described.[31] IOP was measured in isoflurane anesthetized mice with the TonoLab tonometer (Colonial Medical Supply, Franconia, NH). All measurements were made during the same 2hr period of the lights-on phase.

Quantification of Optic Nerve Damage

ON damage was assessed in sections of resin embedded ON's stained with paraphenylenediamine (PPD). Retro-orbital ONs were embedded in plastic and stained with PPD, which stains the myelin sheaths and more darkly stains the axoplasm of sick or dying axons. Each section was ranked for damage by two individuals in a masked manner, and then subsequently evaluated for consensus, as previously described.[195, 196] We and others have previously quantified ON damage using a semi-quantitative ON grading scheme.[157, 195, 197, 198] Here we used a five-point grading scheme.[31, 196]

Quantification of RGC Loss and RNFL Thickness

Loss of RGCs was quantified in RBPMs labeled retinal flat mounts. Dissected retinas were immersed in 4% paraformaldehyde (PFA) in 100nM PBS for 60 minutes at room temperature, then transferred to 30% sucrose in PBS. Retinas remained in 30% sucrose in PBS overnight at 4°C. The retinas were then frozen on dry ice for 10 minutes, then allowed to thaw at benchtop for 15 minutes. The freeze/thaw cycle was repeated two more times, then retinas were washed in 1X PBS three times for 1hr each. After the last wash, PBS was removed and retinas were blocked in 1X PBS containing 2% BSA and 0.1% TritonX-100 overnight. RGCs were labeled using anti-RBPMs antibody (PhosphoSolution - 1830) at 1:100 dilution overnight at 4°C. Primary antibody was washed off with 1X PBS three times for 1hr each. Following the washes, the retinas were incubated with Cy-3 conjugated Donkey anti-rabit (Jackson ImmunoResearch-711-165-152) at 1:200 dilution overnight at 4°C. Slides were then washed in 1X PBS three times for 1hr each and mounted with Vectashield Mounting Medium containing DAPI (Vector Laboratories #H-1200-10) and coverslipped. Retinal images were collected using Zeis Axio Imager Z2 microscope. RBPMs positive cells were counted in 8 central and 8 peripheral regions of the retina, modified from previously described methods.[31] Two quadrants (280µm x 180µm) located 0.7mm (central region) and 1.4mm (peripheral region) away from the ONH in each cardinal direction were selected. Cells were counted in a masked manner. The RGC count was obtained for each retina by averaging the 16 fields and determining the average RGC count per square millimeter.

Thinning of the retinal nerve fiber layer (RNFL) was quantified in cresyl violet stained cross sections. Sections were imaged by light microscopy and RNFL thickness was quantified using ImageJ.

Immunohistochemistry

IHC procedures were utilized as previously described.[96] The OCT compound was removed through two washes in 1X PBS for 2 minutes each before the tissue was dried via subsequent washing in 70% ethanol for 2 minutes, then 100% ethanol for 2 minutes, and left to dry at RT for 10 minutes. Slides were washed in 1X PBS for 5 minutes, then incubated in 0.1% Triton-X (Sigma-Aldrich REFX100) at RT for 15 minutes to permeabilize the cell membranes. Slides were subsequently blocked for 1 hour at RT in Superblock Blocking Buffer in PBS (REF37580, Thermo Fisher Scientific) before being incubated at 4°C overnight in primary antibody: mouse-anti-fibronectin (IST-9, binds the EDA domain) (Abcam REF#: ab6328, 1:100), rabbit-anti-biglycan (Invitrogen, REF#: PA5-76821, 1:100), rabbit-anti-interferon-α (Invitrogen, REF#: PA5-119640, 1:100), mouse-anti-interferon-γ (Invitrogen, REF#: PA1-24782, 1:100), and/or rabbit-anti-phospho-STAT1 (Tyr701) (Invitrogen REF#: 44-376G, 1:100). Slides were then washed in 1X PBS for 5 minutes 3 times at RT before being incubated at RT for 1hr in 2° antibody: Cy3 conjugated donkey-anti-rabbit (Jackson ImmunoResearch, REF#: 711-165-152, 1:200) and/or Cy5-conjugated donkey-anti-mouse (Jackson ImmunoResearch, REF#: 715175150, 1:200). Slides were again washed in 1X PBS for 5 minutes 3 times at RT and mounted with Prolong Gold mounting media containing DAPI (Invitrogen-Molecular Probes). Image acquisition was preformed using Zeiss Axio Imager Z2 microscope at 20X. Scale bar represents 50μm.

Laser Capture Microdissection

1.0 mm Polyethylene naphthalate (PEN) MembraneSlides (1.0 mm, Carl Zeiss Microimaging GmbH, German) were prepared for LCM. To ensure that PEN MembraneSlides are RNase-free and to additionally sterilize the membrane slides, membrane slides were incubated at 180 °C for 4 hours as recommended by Zeiss. 10µm thick frozen sections were mounted on previously treated PEN MembraneSlides with 8 sections per slide and stored at –80°C.

To visualize and map the ONH within each section, the sections were stained with cresyl violet as previously described.[199] Slides were stained and processed one slide at a time to prevent RNA degradation that starts to occur once sections are removed from -80°C storage. Each slide was placed in cold 75% EtOH for 30s immediately after removal from -80°C storage. Slides were then dipped in nuclease-free water for 10-15s before ~300µl of 1.5% cresyl violet in 75% EtOH was pipetted on for 45s at room temperature. The tissue was then dehydrated in subsequent washes of 75%, 95%, and 100% EtOH in nuclease-free water for 30s each. Slides were air dried in a fume hood for 5 minutes before immediately moving to laser capture.

Laser capture microdissection (LCM) was performed with the Zeiss PALM Combi System. LCM cutting speed, microbeam laser energy level, and focus distance were optimized using control tissue of mouse ONH sectioned at 10µm to optimize settings prior to experimental start. Automatic imaging was set at the time before cut, after cut and after UV laser dissection.

ONH segments from all sections from a single eye were collected in a 200µl opaque AdhesiveCap (Carl Zeiss Microimaging GmbH, German) within one hour after staining. Within each section, the ONH region was defined as starting from the inner nuclear layer just below the retinal nerve fiber layer to just above the mylenation zone, determined by the morphological changes in the cresyl violet staining representing the mylenation zone. Immediately after collection, 10 µl lysis buffer (Qiagen RNeasy micro kit, REF#: 74034) was added into the upside-down adhesive cap containing each ONH section. After incubation at room temperature for 10 min, the cap was gently but tightly closed and ONHs with lysis buffer were spun down. Collected samples were immediately processed through RNA extraction with Qiagen RNeasy micro kit (Qiagen RNeasy micro kit, REF#: 74034).

RNA Sequencing, Read Alignment, GSEA Analysis

RNA libraries were generated from total RNA isolated from the ONH. Total RNA was verified for purity and integrity using the NanoDropOne Spectrophotometer and Agilent 2100 Bioanalyzer, respectively. Ultra-low RNA input libraries were generated using the Takara "SMART-Seq v4 Low Input RNA Kit for Sequencing" (Takara, Mountain View, CA, USA) for cDNA synthesis and the Illumina NexteraXT DNA Library Preparation (Illumina, San Diego, CA, USA) kit for cDNA dual indexing. Full length cDNA fragments are generated from 1-10ng total RNA by the Takara SMART technology. cDNA fragments are fragmented and dual indexed in a single step by taking advantage of the Nextera kit's simultaneous transposon and tagmentation step. Libraries were standardized to 2nM. Paired-end 2x150bp sequencing was performed using standard SBS chemistry on an Illumina NovaSeq6000 sequencer. Generated raw reads were qualitied controlled, aligned, and mapped to *Mus musculus* using Spliced Transcripts

Alignment to a Reference (STAR),[200] followed by estimation of mapped pair-end reads using RNA-Seq by Expectation Maximization (RSEM).[201]

Gene Set Enrichment Analysis (GSEA) was performed by ranked enrichment analysis with MolSigDB (https://www.gsea-msigdb.org/gsea/msigdb, version v7.5.1). The subsequent ONH RNAseq data set was analyzed using recommendations from the GSEA tutorial for RNAseq data (https://www.gsea-msigdb.org/gsea/doc/GSEAUserGuideFrame.html). Normalized enrichment scores (NES) were used to quantify the magnitude of enrichment.

Results

Previously we characterized B6.EDA$^{+/+}$ as a novel mouse model of ocular hypertension and glaucoma.[31, 96] B6.EDA$^{+/+}$ mice develop elevated IOP by 14 weeks of age[96] as well as significant RGC loss and ON damage by 12 months of age.[96] Here, we evaluated the glaucomatous phenotypes over the course of 22 months of age to further characterize progressive damage. B6.EDA$^{+/+}$ mice have significantly elevated IOP compared to C57BL/6J controls that persists through 22 months of age (Fig. 1A). In addition, B6.EDA$^{+/+}$ mice have significant RGC loss compared to C57BL/6J controls at both 12 and 22 months (Fig. 1B, representative images Fig. 1C-F). To further evaluate glaucomatous damage to the retina, we evaluated RNFL thickness using cresyl violet staining of the ONH region. To standardize the measurement of the RNFL thickness, a line was drawn (Fig. 1G, white line) from the bottom of the outer nuclear layer (Fig. 1H, green line) to the top of the inner nuclear layer (Fig. 1G, red line). This line was extended through the RNFL (Fig. 1G, yellow line), where only the RNFL thickness was measured (Fig. 1G, yellow arrows) using ImageJ. This methodology allowed for consistent and unbiased

measurement of the RNFL thickness in each section. B6.EDA$^{+/+}$ mice at both 12 months and 22 months of age had a significant decrease in RNFL thickness compared to age matched C57BL/6J controls (Fig. 1H).

Importantly, from 12 to 22 months of age the ON damage significantly worsens in B6.EDA$^{+/+}$ mice, indicating disease progression (Fig. 2A, representative images Fig. 2B-E).

Increases of ECM proteins in the ONH have been heavily implicated with glaucomatous pathophysiology.[14, 49, 56, 59, 60, 74] Specifically, increases of the ECM proteins elastin, tenascin-c, Collagens I, IV, V, XI, proteoglycan, and fibronectin (FN) have all been reported in the human glaucomatous ONH.[54-56, 62-65] To elucidate ECM changes in the ONH of B6.EDA$^{+/+}$ mice, immunohistochemical staining of the ONH at 12 months and 18 months of age were employed. The ECM protein and DAMP FN+EDA is significantly increased in the ONH of B6.EDA$^{+/+}$ mice at both 12 months and 18 months of age compared to age matched C57BL/6J controls (Fig. 3A). In addition, the ECM DAMP biglycan is significantly increased at 18 months of age (Fig. 3F) in B6.EDA$^{+/+}$ mice compared to age matched C57BL/6J mice, while unchanged at 12 months of age. These data show progressive modifications to the ECM in the ONH region in B6.EDA$^{+/+}$ mice overtime.

To further elucidate changes in the transcriptome in the glaucomatous ONH of B6.EDA$^{+/+}$ mice, we utilized LCM, a protocol that allows for highly pure tissue isolation,[199] to specifically isolate the ONH from the surrounding tissue (Fig. 4A,B). The entire ONH from a single sagittal cryosection was collected using LCM, with the sections of the entire ONH

collected and pooled for each eye. This allowed for the collection of the entire three-dimensional ONH from each eye and isolation of RNA from a single ONH. Within each section, the ONH region was defined as starting from the inner nuclear layer just below the RNFL to the mylenation zone, determined by the morphological changes in the cresyl violet staining. RNA was isolated from ONH sections for GSEA analysis of the ONH transcriptome. Normalized enrichment scores (NES) and adjusted p-values were used as a standardized metric for determining significance to compare results across gene sets.[202] Five GSEA defined groups were significantly upregulated between B6.EDA$^{+/+}$ mice and C57BL/6J controls at 12 months of age (Fig. 4C), and four GSEA defined groups were upregulated and four downregulated between B6.EDA$^{+/+}$ mice and age matched C57BL/6J controls at 22 months of age (Fig. 4D). Across both time points, over 600 leading edge genes contributed to the significant changes of GSEA groupings (Fig. 4C, D). Tables showing the NES and adjusted p-value of significantly changes GSEA groupings between B6.EDA$^{+/+}$ at 12 months (Fig. 4E) and 22 months (Fig. 4F) compared to age matched C57BL/6J controls.

Consistent with the hypothesized role of the immune system in glaucoma disease progression, we observed significant increases in interferon (IFN) transcription at both 12 months and 22 months in B6.EDA$^{+/+}$ mice compared to age matched C57BL/6J controls. These data support prior work that has implicated both IFNα and IFNγ signaling in glaucomatous pathophysiology in human patients[131, 203-205] and mouse models.[206] To quantify changes in IFNα and IFNγ at the protein level in B6.EDA$^{+/+}$ mice, we utilized immunohistochemical staining of the ONH region in 12 month and 18-month-old B6.EDA$^{+/+}$ and C57BL/6J age-matched controls. At 12 and 18 months of age there were significant increases in IFNα in the ONH of B6.EDA$^{+/+}$

mice compared to C57BL/6J controls (Fig. 5A, representative images Fig. 5B-E). By 18-months of age IFNγ was significantly increased in the ONH of B6.EDA$^{+/+}$ mice compared to C57BL/6J controls (Fig 5F, representative images Fig. 5G-J). These data suggest progressive changes to the glaucomatous ONH as IFNα is known to be an early indicator of immune system activation, while IFNγ has been shown to be activated in later stages of disease, with evidence pointing towards increases through IFNα signaling.[207, 208]

Further analysis of the 607 leading edge genes generated from the GSEA analysis (Supplementary Excel Spreadsheet 1) identified the signal transducer and activator of transcription (STAT), and downstream STAT signaling proteins, as part of the leading edge for each IFN GSEA group. Janus kinase (JAK), and subsequent STAT gene expression has been implicated in glaucoma disease progression in animal models.[135, 209-211] Specifically, STAT1 has been identified as a hub gene in two glaucoma mouse models: mice with *TDRD7* loss-of-function, and DBA/2J mice.[206, 212, 213] To quantify changes in phospho-STAT1 protein expression levels, the activated form of STAT1, we utilized immunohistochemical staining of the ONH region in 12 month and 18 month old B6.EDA$^{+/+}$ and C57BL/6J age-matched controls. At 18 months of age there were significant increases in pSTAT1 protein expression in the ONH of B6.EDA$^{+/+}$ mice compared to C57BL/6J controls (Fig. 6A, representative images 6B-E). These data supports time-dependent and progressive changes to IFN and subsequent STAT signaling in glaucomatous disease progression.

Discussion

In primary open angle glaucoma (POAG) the activation of the immune system has been heavily implicated in disease progression and pathophysiology.[16, 78, 80, 192] However, the pathogenic signaling pathways responsible for these immune and fibrotic changes are not fully understood. Mice are genetically similar to humans with comparable anatomy, making them an ideal model system to study glaucoma phenotypes and ONH pathophysiology.[214, 215] Previously, we have utilized several transgenic mouse lines to show that constitutively active FN+EDA mice (B6.EDA$^{+/+}$) develop ocular hypertension and exhibit glaucomatous damage by one year of age, and these phenotypes are dependent on TLR4 signaling.[31, 96] Here we further investigate the role of DAMPs, activators of TLR4, and downstream fibro-inflammatory signaling in the development and progression of glaucomatous damage. In addition, we explore the transcriptomic changes at 12 and 22 months of age to further elucidate signaling mechanisms responsible for the development of progressive glaucomatous damage.

To further investigate glaucomatous damage in B6.EDA$^{+/+}$ mice, we used a battery of testing parameters that have previously been used to define damage progression including IOP measurements, RGC loss, RNFL thickness, and ON damage scores.[31, 74, 96, 195-198, 216, 217] Here we demonstrate that IOP remains significantly increased through 22 months of age in B6.EDA$^{+/+}$ mice (Fig. 1A), leading to significant RGC loss (Fig. 1B) and decreases in RNFL thickness (Fig. 1H). Interestingly, the loss of RGCs and RNFL thickness does not significantly progress through this time course. However, ON damage did significantly worsen from 12 months to 22 months in the B6.EDA$^{+/+}$ mice (Fig. 2A). This progression of disease severity indicates a continual effect of

ocular hypertension on ON damage and further suggests that the initial site of damage is occurring in the ON, as is known to occur in the pathophysiology of glaucoma.

Previously, we and others identified that DAMP expression is increased in the human glaucomatous ONH compared to healthy individuals.[34, 56, 62, 64] In addition, DAMP activation of TLR4 has been shown to significantly increase fibrosis in human primary trabecular meshwork cells[74] and hONH LC cells.[56] Previously we have shown that TLR4 signaling is necessary for DAMP induced IOP elevation and trabecular meshwork damage as well as fibrotic changes to LC cells in culture, implicating the innate immune system as a mechanism for glaucoma damage.[56, 96] TLR4 signaling has also been implicated in initiating fibrotic responses in several other fibrotic disease states such as scleroderma,[93] liver disease,[150] and kidney disease,[151] highlighting the importance and relevance of this signaling pathway.[93-95] Here we show that the DAMP FN+EDA is significantly elevated at both 12 months and 18 months of age (Fig. 3A), and we also report significantly higher levels of the DAMP biglycan by 18 months of age in B6.EDA$^{+/+}$ mice (Fig. 3F). FN+EDA is known to amplify the TGFβ2-dependent ECM responses in human TM cells as well as human ONH LC cells,[56, 74] suggesting a mechanism by which DAMPs are modulating the ONH region in glaucoma. Along with FN+EDA, biglycan is a known proinflammatory signaling molecule that acts as a DAMP, activating TLR4 signaling.[102, 107] Biglycan primarily supports tissues when exposed to compressional forces,[104] and has been shown to be upregulated in human ONH LC cell cultures after mechanical stress.[51] Interesting, biglycan expression was significantly increased at 18 months of age in the B6.EDA$^{+/+}$ ONH, but not at 12 months, suggesting a time-dependent increase in this DAMP, likely related to prolonged mechanical stress and strain on the ONH. It is important to note that mice do not have LC cells,

and instead the lamina region is formed and occupied by resident astrocytes and microglia. Thus, these data suggest a time-sensitive role of astrocyte and microglia produced DAMPs in progressive glaucomatous pathophysiology. Although biglycan is known to be expressed in human ONH LC cells, it remains to be determined if expression levels are significantly different in the human glaucomatous ONH.[108] These data suggest a continued response to the elevated IOP, implicated by time-specific responses to the production of various ECM and DAMP molecules. These data identify B6.EDA$^{+/+}$ mice as a novel model of open-angle glaucoma with slowly progressive damage to the retina, ONH, and ON.

To further elucidate the complicated signaling pathways underlying the progressive glaucomatous phenotypes, we performed transcriptomic profiling to gain a comprehensive insight to the progressive changes occurring within the ONH. We identified significant upregulation and downregulation of various signaling groupings using GSEA analysis across three different databases: hallmark, reactome, and KEGG (https://www.gsea-msigdb.org/gsea/doc/GSEAUserGuideFrame.html) (Fig. 4C, D). Significant increases of immune system signaling IFNα, β, and γ signaling were highly enriched gene groupings at both 12 months and 22 months of age (Fig. 4C, D). This is consistent with the known role of the immune system in glaucoma disease progression.[16, 78]

Interferons are crucial inflammatory signaling molecules. IFNα and IFNγ levels are known to be significantly increased in the glaucomatous aqueous humor (AH) and serum levels in human patients.[203, 205, 218, 219] Interestingly, the increased serum IFNγ levels negatively correlated with RNFL thickness, indicating a pathological role of IFN signaling in RGC loss.[203]

In human ONH astrocyte cell cultures, stimulation with IFNγ was sufficient to upregulate astrogliosis and immune system markers.[220] Here, we were able to implicate the pathophysiological role of IFN signaling in the glaucomatous ONH specifically. RNA sequencing identified the important signaling pathways that are differentially expressed, while subsequent protein expression analysis indicated a time-specific response to the IFN family, specifically IFNα and IFNγ (Fig. 5A, F). These data suggest a direct role of IFN signaling in the glaucomatous ONH, where the majority of RGC axonal damage occurs.[4, 5]

Further analysis of leading edge genes in the IFN signaling GSEA groups showed that JAK/STAT genes, specifically *Stat1* and *Stat3*, and downstream JAK/STAT genes were included in the leading edge gene sets for all IFN groups at both time points (Supplementary Excel Spreadsheet 1). IFNs initiate rapid pro-inflammatory signaling primarily through the JAK/STAT pathways. STAT1 has previously been identified as a hub gene in two mouse models of glaucoma,[206] with downstream STAT1 proteins upregulated in various mouse models of ON damage.[135, 209, 221] Downstream signaling of STAT1 have also been implicated in increased immune activation in hONH astrocyte cell cultures as well as rodent models of glaucoma.[222-226] We demonstrate that phospho-STAT1 (pSTAT1) protein expression, the activated form of STAT1, is significantly upregulated at 18 months in our glaucoma model, but not at 12 months (Fig. 6A). This suggests for the first time that activation of the JAK/STAT pathway in the glaucomatous optic nerve head is a late onset response to the glaucomatous ONH damage and chronic ocular hypertension, rather than an initiating mechanism of early damage. Future studies are needed to identify signaling mechanisms of the JAK/STAT pathway in relation of IFN signaling.

Conclusion

In summary, these data show the development of slowly progressive glaucomatous damage in a novel mouse model over 2 years. These data also point to a new method of measuring RNFL thickness using histology. To the best of our knowledge, we are the first to demonstrate integral changes of IFN signaling and the JAK/STAT pathway throughout disease progression in the ONH in response to ocular hypertension. Importantly, there are time-specific responses in DAMP production, IFN signaling activation, and pSTAT1 expression in the glaucomatous ONH, indicating novel therapeutic targets to treat and manage glaucoma disease progression.

Acknowledgements

The authors utilized the University of Wisconsin – Madison Biotechnology Center Gene Expression Center (Research Resource Identifier RRID:SCR_017757) for the generation of cDNA libraries from the LCM harvested ONHs and the University of Wisconsin – Madison Biotechnology Center for Bioinformatics Core Facility (Research Resource Identifier RRID:SCR_017799) for the GSEA analysis of the cDNA libraries.

The authors utilized the University of Wisconsin – Madison Core Grant for Vision Research from the NIH (p30 EY016665) for assistance with statistical analysis and ON sectioning as well as the LCM which was funded by NIH S10OD026957 (DOVS). The authors thank Hongyu Noel for her assistance with the LCM and Kelsey Mathers for managing the mouse colonies.

Chapter 4 Figure Legends

Figure 1. B6.EDA$^{+/+}$ mice exhibit glaucoma phenotypes at 12 months and 22 months of age. IOP is significantly elevated in B6.EDA$^{+/+}$ mice at 12 months (*n* = 12-14) and 22 months (*n* = 16-18) compared to age matched C57BL/6J controls (A). Significance determined by Student's t-test at each time point. B6.EDA$^{+/+}$ mice (*n* = 3-7) have ~20% loss of RGCs at both 12 months and 22 months of age compared to C57BL/6J controls as quantified by RBPMs staining of retinal flat mounts (B). Representative images of RBPMs staining at 12 months and 22 months for B6.EDA$^{+/+}$ mice and age matched C57BL/6J controls (C-F). Significance was determined by a Student's t-test at each time point. The location for measurements of RNFL thickness was standardized by drawing a line from the bottom of the inner nuclear layer (G, green line) to the top of the outer nuclear layer (G, red line) and extended to the top of the RNFL (G, yellow line). Measurements were then taken for the RNFL thickness only (G, yellow arrows). B6.EDA$^{+/+}$ mice exhibit significant thinning of the RNFL at both 12 months and 22 months of age compared to age matched C57BL/6J controls (H). RNFL thickness was measured using ImageJ and significance was determined by a Student's t-test at each time point. *$P < 0.05$, **$P < 0.01$, ****$P < 0.0001$.

Figure 2. B6.EDA$^{+/+}$ mice have progressive degradation of the ON from 12 months of age to 22 months of age. B6. EDA$^{+/+}$ mice exhibit a higher percent of optic nerve damage measured through PPD staining at 22 months of age compared to 12 months of age (*n* = 7-13 ONs) (A). At 22 months of age, B6.EDA$^{+/+}$ mice have significantly increased ON damage compared to age matched C57BL/6J controls (*n* = 11-13 ONs) (A). Representative images of ON PPD staining at both 12 months and 22 months of age (B-E). Significance was determined using a Fisher's exact

test and represented as percentage of total ONs (n = 6-13) measured. Damage was quantified as axons with no damage (1), mild damage (2), or medium damage (3) according to previously described methods [195, 196]. Statistical significance was determined by a Fisher's exact test and the subsequent Hommel post-hoc analysis for multiple comparisons. *$P < 0.05$. **$P < 0.01$.

Figure 3. B6.EDA$^{+/+}$ mice have increased DAMP expression in the ONH. FN+EDA expression is significantly increased in the ONH at 12 months and 18 months of age in B6.EDA$^{+/+}$ mice compared to age matched controls (n = 4-9) (A). Representative images of FN+EDA expression in B6.EDA$^{+/+}$ at 12 months and 18 months of age (C,E) compared to age matched controls (B,D). Biglycan expression is significantly increased in the ONH at 18 months in B6.EDA$^{+/+}$ mice compared to age matched controls, (n = 4-6) (F). Representative images of biglycan expression in B6.EDA$^{+/+}$ at 12 months and 18 months of age (H,J) compared to age matched controls (G,I). White lines outline the measured ONH section of images. Dashed boxes represent location of 40X imaging of FN+EDA, as shown in inserts (B'-E'). Scale bars represent 50μm unless otherwise stated. Significance was determined by Student's t-test. *$P < 0.05$, **$P < 0.01$.

Figure 4. Up- and down-regulated gene sets in the ONH of B6.EDA$^{+/+}$ mice. The ONH of 12 (n = 4-5) and 22 month (n = 3-5) old mice were isolated using LCM before undergoing RNA isolation, cDNA library preparation, and subsequent GSEA analysis. The ONH region was defined as starting from the inner nuclear layer just below the retinal nerve fiber layer down to the mylenation zone, determined by the morphological changes in the H&E staining. The ONH was outlined by hand (A) and isolated (B) for subsequent processing. GSEA analysis showed

significant increases in various signaling pathways across three different pathway databases: hallmark, reactome, and KEGG. Numbers within bars represent the number of leading edge genes. At 12 months of age, B6.EDA$^{+/+}$ had significantly increased expressions of genes related to interferon-α, interferon-γ, MTORC1, visual phototransduction, and interferon-α,β signaling from the hallmark and reactome databases (C). No differences were found between B6.EDA$^{+/+}$ and C57BL/6J RNA expression in the KEGG database at 12 months of age. At 22 months of age, B6.EDA$^{+/+}$ had statistically significant increased expression of genes related to interferon-α response, interferon-γ response, interferon-α,β signaling, and interferon signaling (D, red bars). They also had statistically significant decreases in expression of genes related to mitotic spindle signaling, the rho GTPase cycle, MAPK signaling pathway, and leukocyte transendothelial migration (D, blue bars). White numbers represent total number of leading-edge genes (See Supplementary Excel Spreadsheet 1). Table stating the NES and adjusted p-value for upregulated GSEA groups between B6.EDA$^{+/+}$ at 12 months and age matched C57BL/6J controls (F). Table stating the NES and adjusted p-value for upregulated GSEA groups between B6.EDA$^{+/+}$ at 22 months and age matched C57BL/6J controls (G).

Figure 5. B6.EDA$^{+/+}$ mice have increased interferon–α and –γ protein expression in the ONH. IFNα expression is significantly increased in the ONH at 12 months and 18 months of age in B6.EDA$^{+/+}$ mice compared to age matched controls, (n = 5-9) (A). Representative images of IFNα expression in B6.EDA$^{+/+}$ at 12 months and 18 months of age (C,E) compared to age matched controls (B,D). IFNγ expression is significantly increased in the ONH at 18 months but not 12 months of age in B6.EDA$^{+/+}$ mice compared to age matched controls (n = 7-9) (F). Representative images of IFNγ expression in B6.EDA$^{+/+}$ at 12 months and 18 months of age

(H,J) compared to age matched controls (G,I).White lines outline the measured ONH section of images. Significance was determined by Student's t-test. *$P < 0.05$, **$P < 0.01$.

Figure 6. B6.EDA$^{+/+}$ mice have increased protein expression of pSTAT1 in the ONH at 18 months of age. pSTAT1 expression is significantly increased in the ONH at 18 months of age in B6.EDA$^{+/+}$ mice, but not at 12 months compared to age matched controls, (n = 6-9) (A). Representative images of pSTAT1 expression in B6.EDA$^{+/+}$ at 12 months and 18 months of age (C,E) compared to age matched controls (B,D). White lines outline the measured ONH section of images. Significance was determined by Student's t-test. *$P < 0.05$.

Chapter 4 Supplementary Figure Legends

Supplementary Figure 1. Up- and downregulated GSEA gene sets in the B6.EDA$^{+/+}$ ONH at 12 months. GSEA analysis of RNA isolated from the ONH show that B6.EDA$^{+/+}$ mice have significant upregulations of GSEA groups Visual Phototransduction (A) and Interferon Alpha, Beta Signaling (B) from the reactome database compared to age matched C57BL/6J controls. GSEA analysis also showed significant upregulation in RNA isolated from B6.EDA$^{+/+}$ mice of the Interferon Alpha Response (C), Interferon Gamma Response (D), and MTORC1 Signaling € from the hallmark database compared to age matched C57BL/6JK controls.

Supplementary Figure 2. Up- and downregulated GSEA gene sets in the B6.EDA$^{+/+}$ ONH at 22 months. GSEA analysis of RNA isolated from the ONH show that B6.EDA$^{+/+}$ mice have significant upregulations of GSEA groups Interferon Alpha, Beta Signaling (A), Interferon Signaling (B), and significant downregulation of the Rho GTPase Cycle groups (C) from the reactome database compared to age matched C57BL/6J controls. GSEA analysis also showed significant upregulation in RNA isolated from B6.EDA$^{+/+}$ mice of the Interferon Alpha Response (D) and Interferon Gamma Response (E), and downregulation of the Mitotic Spindle (F) groups from the hallmark database compared to age matched C57BL/6J controls. Finally, GSEA analysis showed significant downregulation of the MAPK Signaling Pathway (G) and Leukocyte Transendothelial Migration (H) groups from the KEGG database.

Figure 1. B6.EDA$^{+/+}$ mice exhibit glaucoma phenotypes at 12 months and 22 months of age.

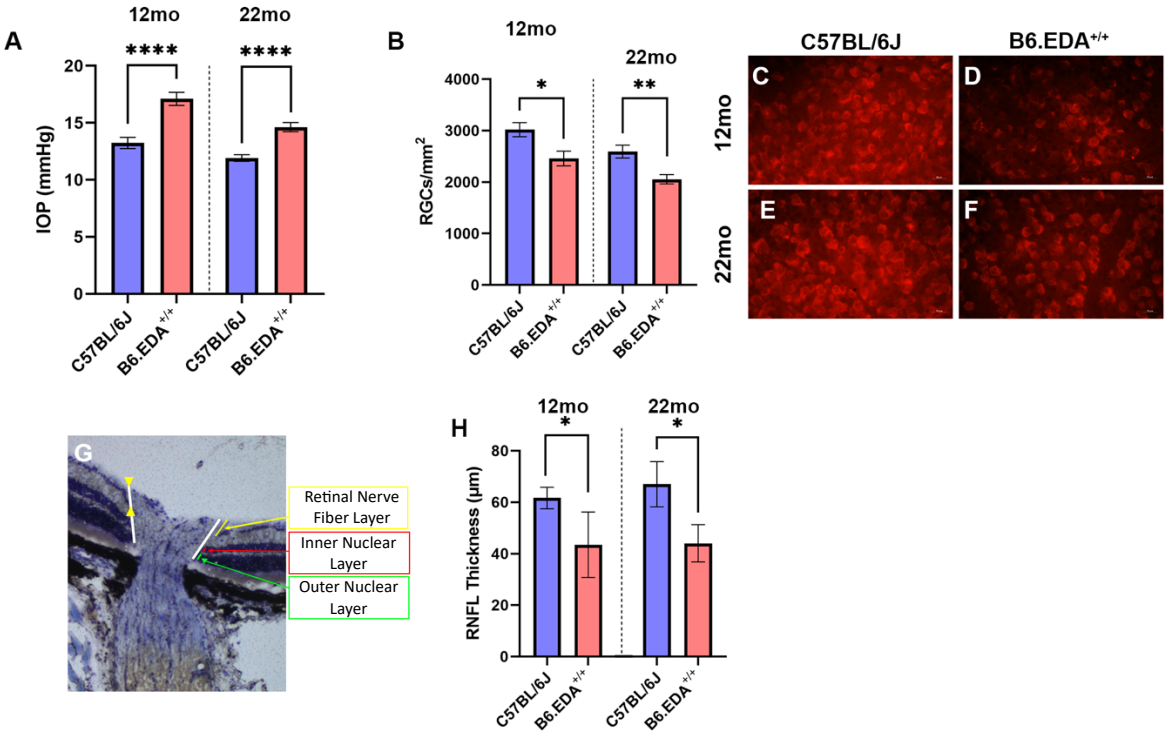

Figure 2. B6.EDA$^{+/+}$ mice have progressive degradation of the ON from 12 months of age to 22 months of age.

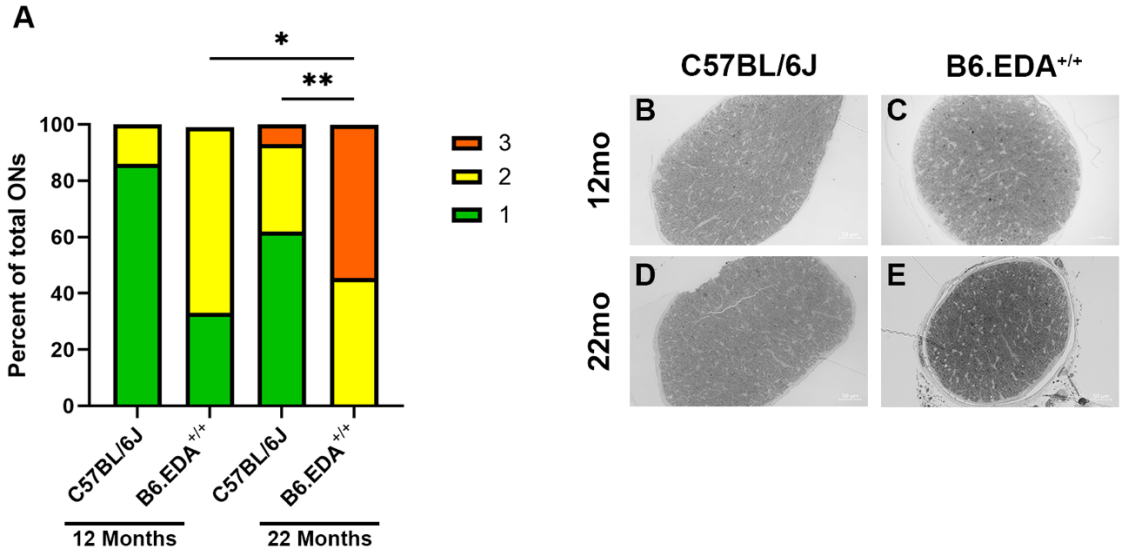

Figure 3. B6.EDA$^{+/+}$ mice have increased DAMP expression in the ONH.

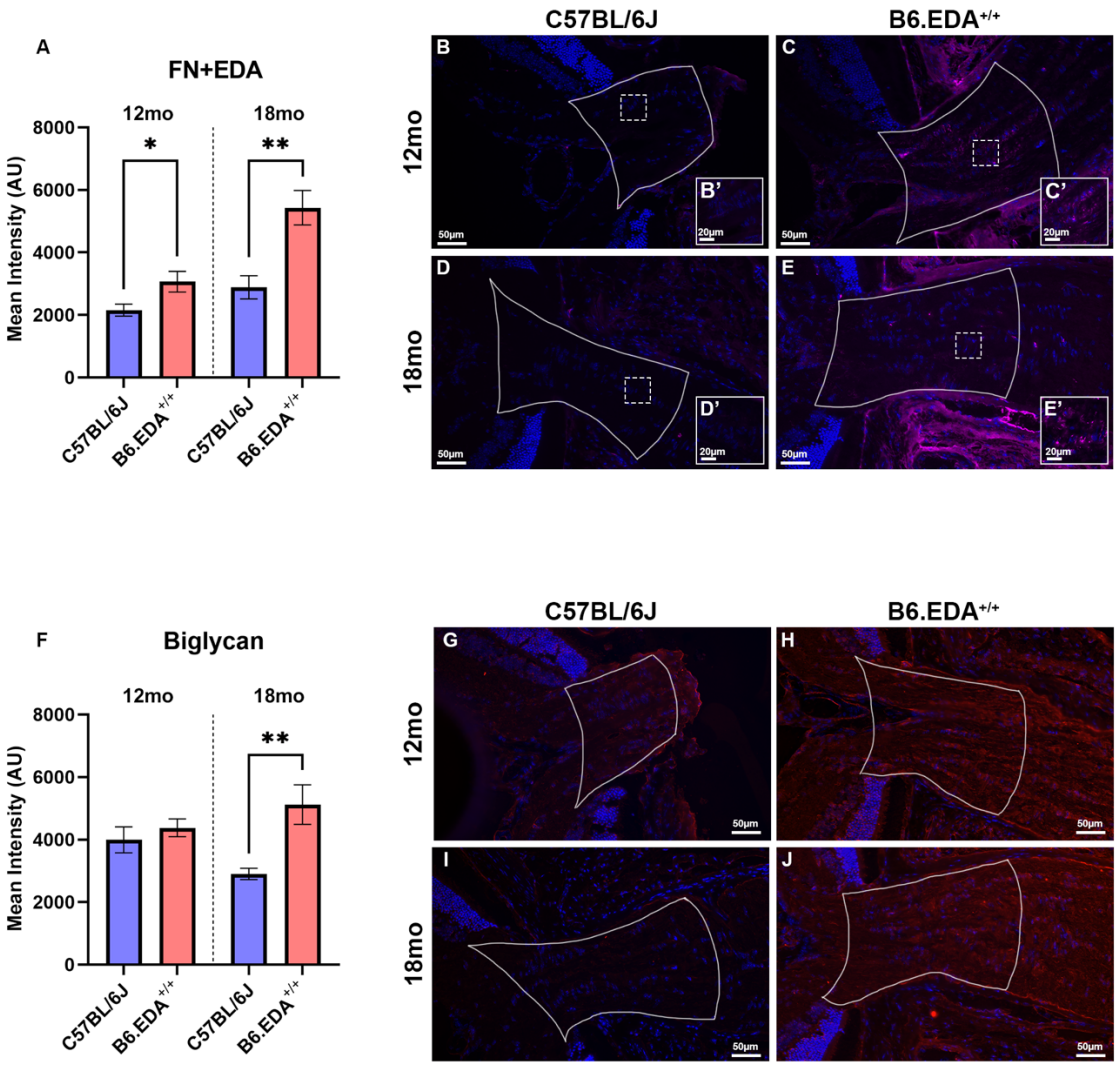

Figure 4. Up- and down-regulated gene sets in the ONH of B6.EDA$^{+/+}$ mice.

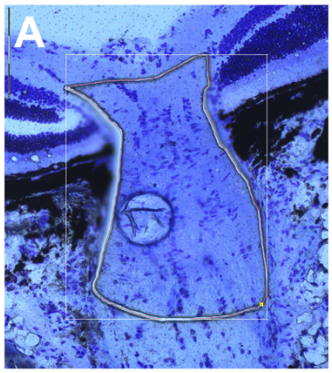

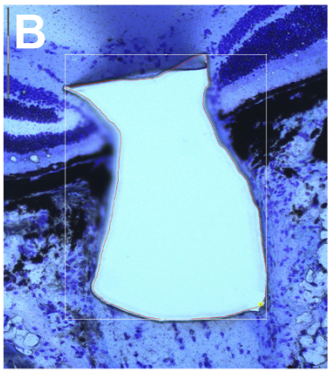

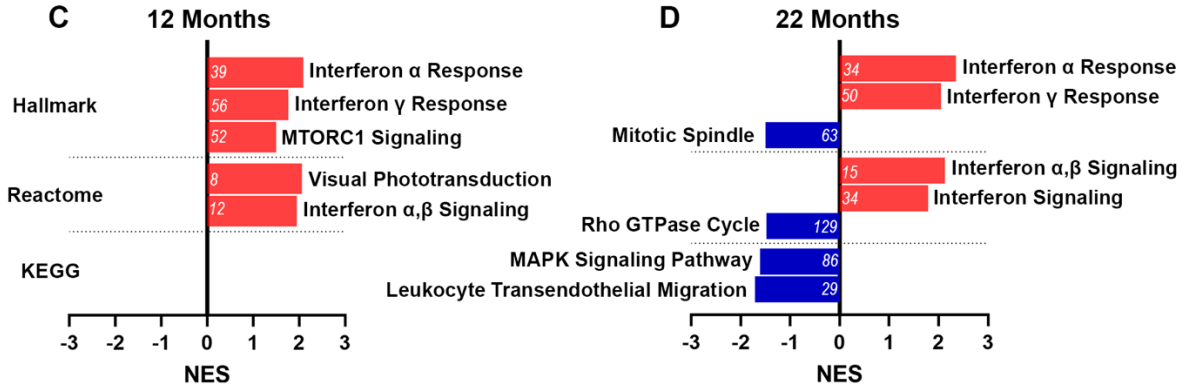

E 12 Months

Database	Pathway	NES	Adjusted p-value
Hallmark	Interferon α Response	2.09	$8.16*10^{-5}$
	Interferon γ Response	1.77	0.0011
	MTORC1 Signaling	1.50	0.0661
Reactome	Visual Phototransduction	2.06	0.0252
	Interferon α,β Signaling	1.95	0.0841

F 22 Months

Database	Pathway	NES	Adjusted p-value
Hallmark	Interferon α Response	2.3520	$3.85*10^{-8}$
	Interferon γ Response	2.0522	$9*10^{-7}$
	Mitotic Spindle	-1.4963	0.0915
Reactome	Interferon α,β Signaling	2.1330	0.0107
	Interferon Signaling	1.7867	0.0113
	Rho GTPase Cycle	-1.4808	0.1535
KEGG	MAPK Signaling	-1.6063	0.0284
	Leukocyte Transendothelial Migration	-1.7064	0.1420

Figure 5. B6.EDA$^{+/+}$ mice have increased interferon–α and –γ protein expression in the ONH.

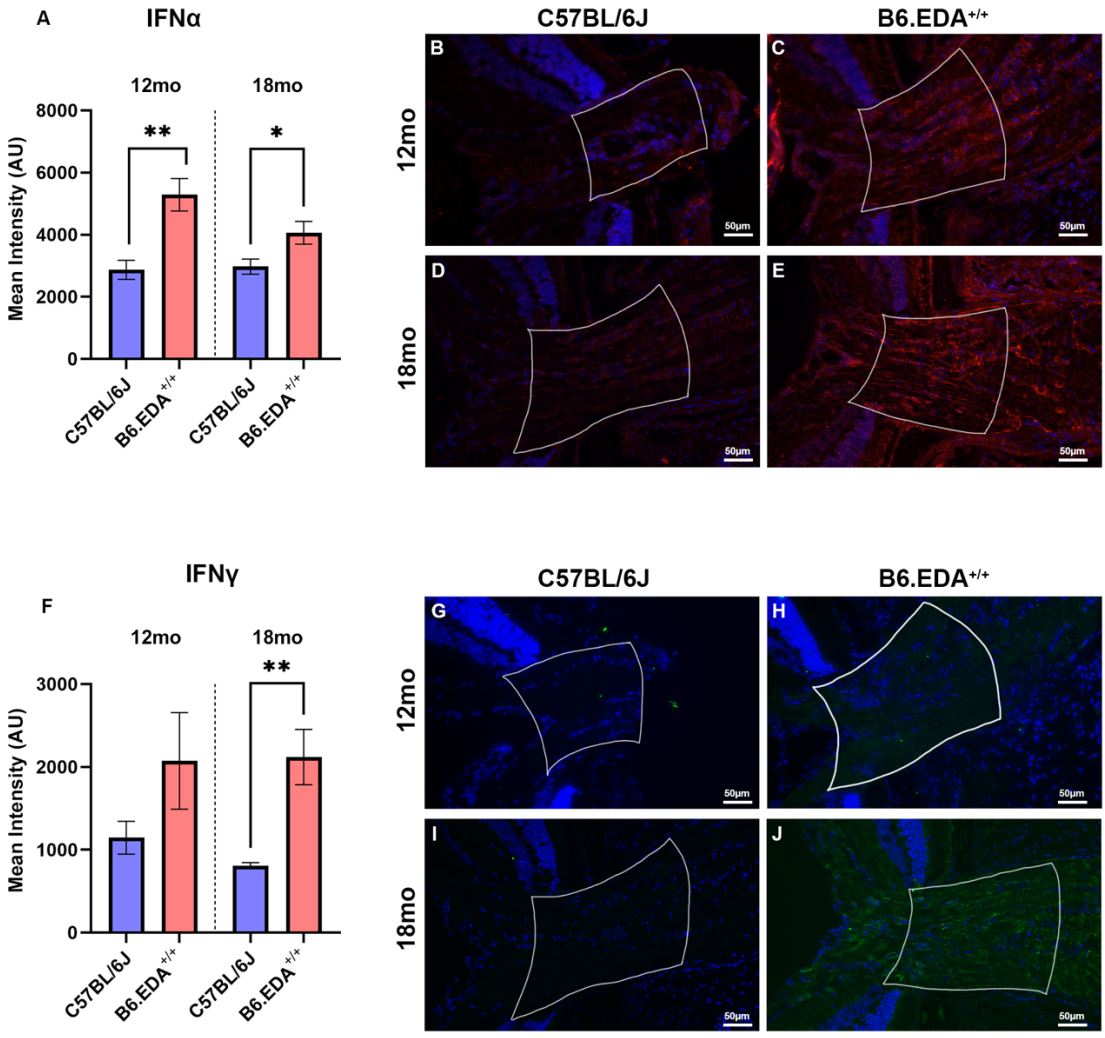

Figure 6. B6.EDA$^{+/+}$ mice have increased protein expression of pSTAT1 in the ONH at 18 months of age.

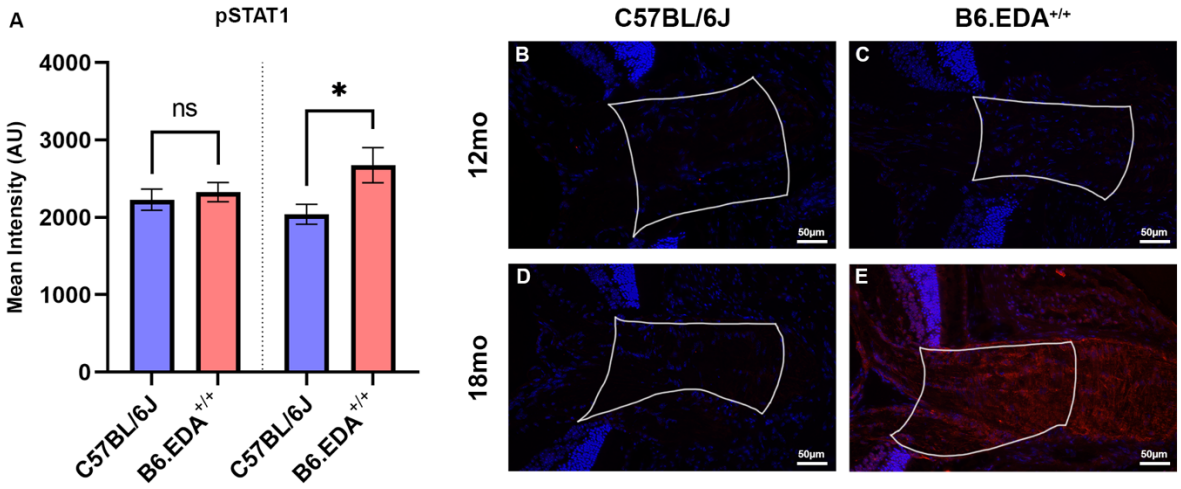

Supplementary Figure 1: Up- and downregulated GSEA gene sets in the B6.EDA$^{+/+}$ ONH at 12 months.

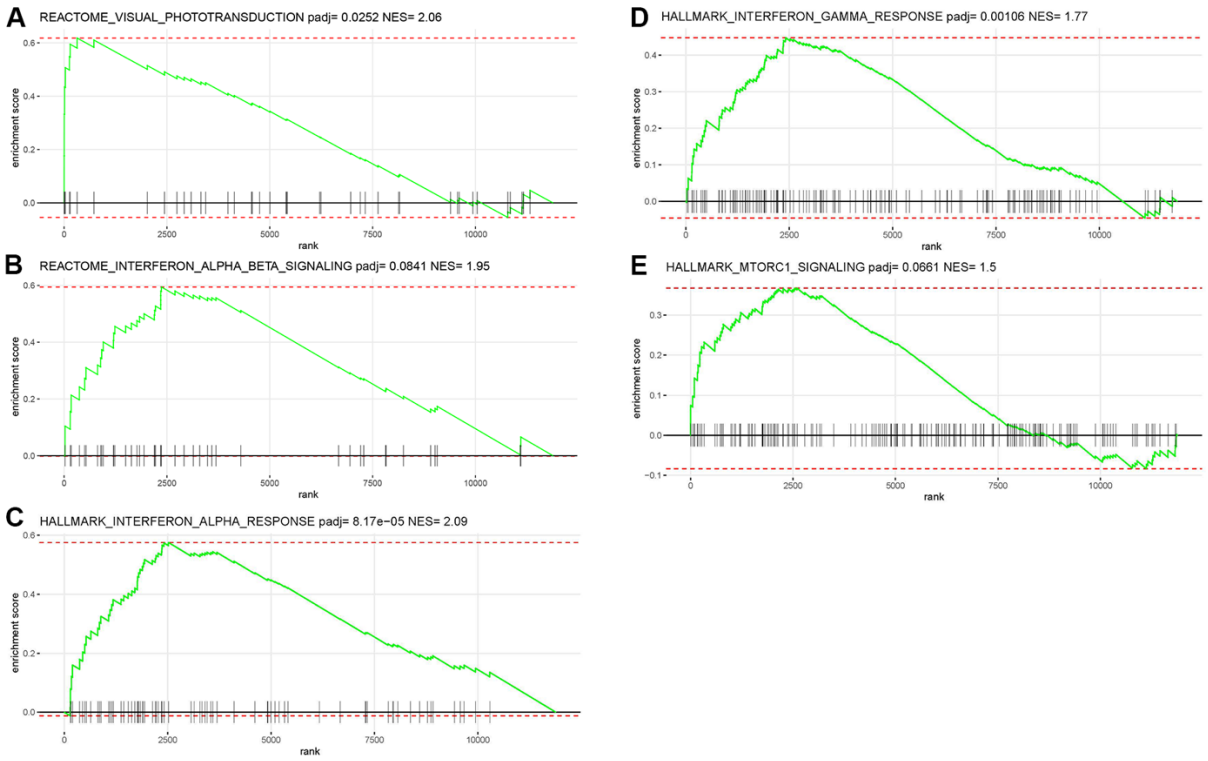

Supplementary Figure 2: Up- and downregulated GSEA gene sets in the B6.EDA$^{+/+}$ ONH at 22 months.

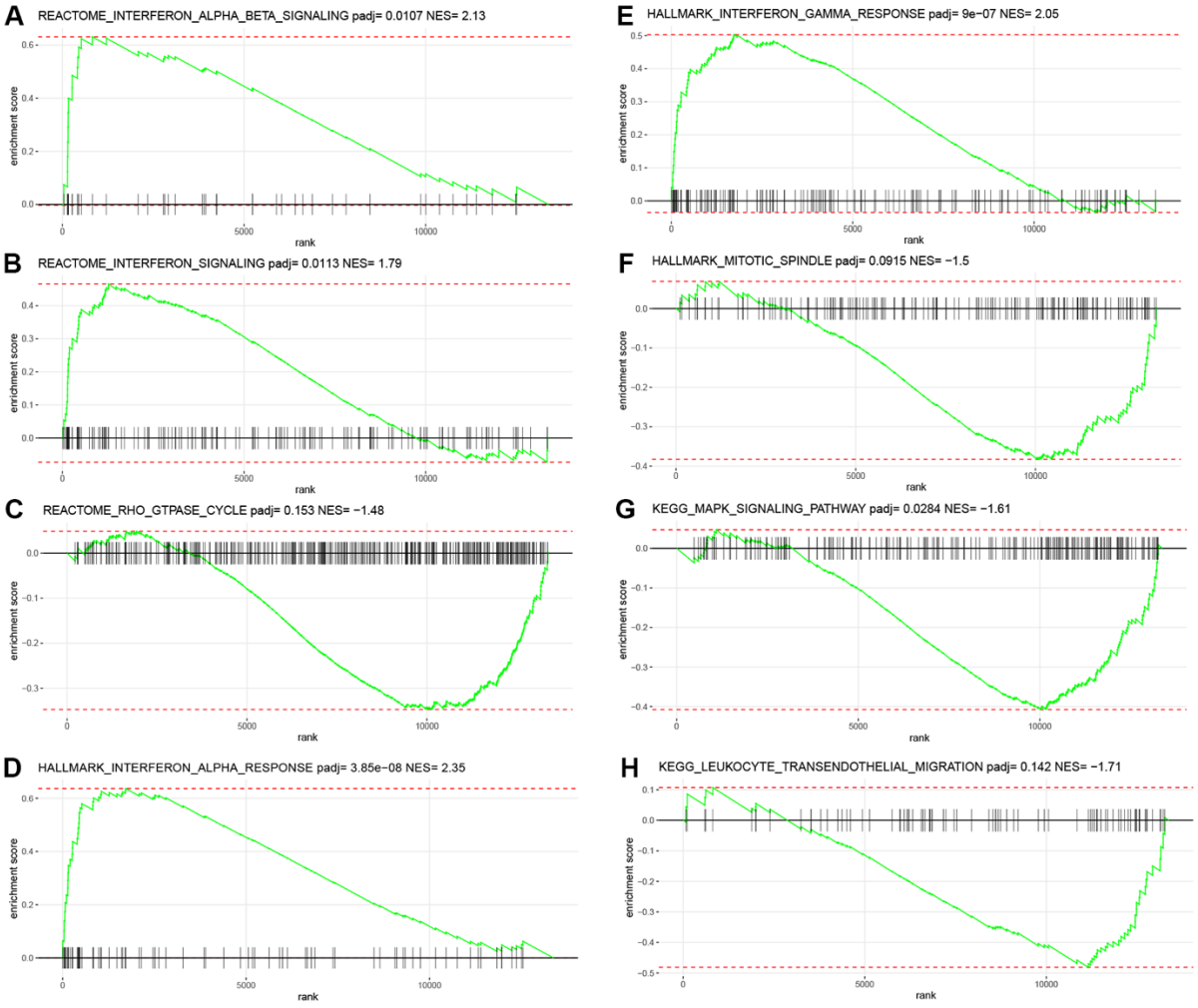

Chapter 5: Conclusions

Chapter 1 Summary:

Glaucoma is the current leading cause of irreversible blindness, affecting over 60 million individuals worldwide and estimated to cost the US over $3 billion per year.[227, 228] Current treatments are only able to target increases of IOP. However, the current therapeutics are not uniformly effective, only slowing the vision loss in patients over time.[7, 12, 157] This highlights the necessity of new therapeutic targets to address the needs of the patient population.

Glaucoma is defined by the loss of RGCs, the thinning of the RNFL, and the cupping and remodeling of the ONH resulting in a gradual progression of vision loss.[13, 14] Elevated IOP slowly causes significant biomechanical stress and strain on the ONH, resulting in a posterior migration of the LC layer, and significantly increased fibrosis.[22] A predominate hypothesis within the field indicates that TGFβ2-induced fibrosis instigates and exacerbates the increased ECM production and fibrosis in glaucoma.[66] Previous chapters have heavily reviewed the production and role of TGFβ2 in the glaucomatous eye. Certain ECM proteins produced by TGFβ2 activation have the ability to act as DAMPs, key signals for tissue injury or damage.[102] Endogenous DAMP expression is significantly increased in the glaucomatous ONH,[34, 56, 64] and act as key activators of the innate immune system.[102, 103]

Significant work has shown that the prolonged exposure to mechanical stress from increased IOP, the subsequent loss of nutrient transportation to the ONH, and hypoxic microenvironments help transition innate immune system activation from protective to neurotoxic.[79] TLR4 signaling and activation have been heavily implicated in the pathophysiology of immune system activation in glaucoma.[78, 87] Importantly, *Tlr4* gene polymorphisms are associated with POAG in multiple patient populations of differing racial backgrounds.[97-99] TLR4 signaling augments fibrosis and the production and regulation of ECM proteins in other fibrotic diseases,[93-95] and in human TM cell cultures and mouse models of glaucoma.[31, 74, 96] These data indicate TLR4 and downstream signaling molecules are crucial instigators of glaucomatous pathophysiology.

TLR4 activation significantly increases NFκB signaling, which is able to act as a transcription factor to initiate the innate immune system signaling. TLR4 activation is known to downregulate the TGFβ pseudoreceptor BAMBI via NFκB signaling.[93, 94, 150, 151] When present, BAMBI inhibits TGFβ2 signaling by amplifying the TGFβ inhibitor Smad7 and sequestering TGFβ receptors.[73] Thus, TLR4 activation amplifies TGFβ2 signaling, which in turn produces more DAMPs to activate TLR4, creating a vicious feed-forward cycle.

There are three supporting cell types within the ONH: astrocytes, microglia, and LC cells. All three cell types have been implicated in glaucoma disease progression and eventual loss of RGCs.[19, 29, 44, 45, 47, 51, 56, 57, 130, 180] Importantly, all three cell types are known to express TGFβ2, TGFβ receptors, TLR4, and BAMBI,[180] indicating that any cell type could initiate the TGFβ2 – TLR4 signaling crosstalk. Previous work in our lab has shown that these cells have known and

hypothesized autocrine and paracrine signaling when exposed to glaucoma-like environments and stimuli (Chapter 1 Fig. 1).[56, 180]

This dissertation helps to elucidate the cell signaling mechanisms exacerbating the immune and fibrotic responses in the glaucomatous ONH. Here we have shown significant evidence for TGFβ2 – TLR4 signaling crosstalk in human ONH cell cultures and the ONH of a mouse model of glaucoma. These data indicate that targeting this crosstalk represents a novel mechanism for pharmaceutical interventions.

Chapter 2 Summary:

In chapter 1, we reviewed what we have dubbed as the Fibro-Inflammatory Hypothesis. The critical role of both TLR4-immune system activation and TGFβ-induced fibrosis in the glaucomatous ONH are heavily implicated in ONH remodeling and eventual loss of RGCs. Previously, we have shown the necessity of TLR4 signaling for TGFβ2-induced fibrosis in human primary TM cells, providing strong evidence for this crosstalk within the ONH.[74] Thus, we proposed a novel mechanism of TLR4-TGFβ2 signaling crosstalk in an autocrine and paracrine manner between the supporting LC cells, astrocytes, and microglia in the glaucomatous ONH.

Chapter 2 describes novel findings for TLR4 - TGFβ2 and DAMP signaling in the glaucomatous human ONH and human ONH LC cell cultures. We show that endogenous levels of the DAMP FN+EDA are significantly increased in human glaucomatous ONH sections compared to healthy controls (Chapter 2 Fig. 1). FN+EDA is a potent activator of TLR4,[102] and

augments downstream TGFβ fibrotic signaling in other fibrotic diseases.[93, 150, 151] Previous studies have found that the ECM DAMP tenascin-C is significantly increased in the glaucomatous ONH, here we further these findings through the identification of a significant increase of a second type of ECM DAMP, further implicating these DAMPs as pathological in the ONH.

To test the role and function of these DAMPs in specific ONH cell cultures, primary LC cells were isolated and cultured from healthy human donor eyes. With these experiments, we were able to improve upon and optimize a previously established protocol.[174] It is well-established that TGFβ2 signaling is increased in glaucoma and known to affect the ONH during disease progression, thus, we exposed cell cultures to exogenous TGFβ2 to mimic a glaucomatous environment. We show that inhibition of TLR4, by the selective TLR4 inhibitor TAK-242, blocks the TGFβ2-induced production of FN (Chapter 2 Fig. 3), FN+EDA (Chapter 2 Fig. 3), and COL1 (Chapter 2 Fig. 4). These data indicated the *necessity* of TLR4 signaling for TGFβ2-induced fibrosis in human ONH LC cells. Simultaneously, we show that DAMP activation of TLR4 by FN+EDA is *sufficient* to induce fibrosis. LC cells exposed to FN+EDA, with or without TGFβ2, had significantly more FN and COL1 protein expression, and concurrent inhibition of TLR4 returned these values to baseline.

This study provides novel insight to the signaling crosstalk between TGFβ2 and TLR4 signaling in the ONH specifically. The ONH is the primary site of damage in glaucoma progression due to the RGCs making a 90° turn to form the ON, it is critical to further our understanding of the cellular signaling mechanisms to develop novel therapy targets.

Chapter 3 Summary:

In Chapter 2, we demonstrate that TLR4 signaling is necessary and sufficient to produce TGFβ2-induced fibrosis in monocultures of human ONH LC cells. However, these cells do not act in isolation during disease progression in the human ONH, suggesting that cell-cell signaling in a paracrine manner between the LC cells, astrocytes, and microglia located in the ONH warrants further study. Understanding the molecular and cellular mechanisms of communication within and between these three cell types is crucial for further elucidating disease mechanisms and discovering potential new therapeutic targets.

Mirroring experiments done in Chapter 2 on human ONH LC cells, human ONH astrocytes were similarly isolated and tested for TGFβ2 – TLR4 crosstalk. TGFβ2 exposure significantly increased ECM protein production, as well as expression of the DAMP FN+EDA (Chapter 3 Fig. 3). Concurrent treatment with the selective TLR4 inhibitor TAK-242 returned these levels to baseline. These data indicate that TLR4 is *necessary* for TGFβ2 – induced fibrosis not only in LC cells, but also in human ONH astrocyte. Thus, identifying this autocrine signaling crosstalk as a pharmaceutical target for two key cell supporting cell types in glaucomatous pathophysiology.

The investigation of LC cell and astrocyte monocultures provides key insights into the extent of TGFβ2 – induced fibrosis that is individually produced, but these cells are not working and responding in isolation. Thus, it is crucial to determine if LC cells and astrocytes are communicating in a paracrine manner. To explore this interaction, we utilized a co-culture

system where LC cells were seeded onto 12-well plates and astrocytes were seeded onto cell culture inserts (Chapter 3 Fig. 1). This allows for the sharing of media between the two cell cultures, and thus any signaling molecules, without direct contact. This also allows for the individual collection of astrocytes and LC cells rather than a conglomerate of the two cell types. We activated only the LC cells by coating the bottom of the 12-well plate with cFN, which contains the DAMP FN+EDA. Astrocytes on cell culture inserts were pretreated with the selective TLR4 inhibitor TAK-242 prior to combining the plate and cell culture inserts (Chapter 3: Fig. 1). As hypothesized, the LC cells exposed to cFN, which contains the DAMP FN+EDA, had significant increases in the ECM proteins FN and tenascin-C (Chapter 3: Fig. 4A, B). We also showed that astrocytes in co-culture with LC cells exposed to DAMPs have significant FN and tenascin-C protein expression (Fig. 4E, F), and that this increase in protein expression is blocked when the astrocytes are pretreated with the selective TLR4i inhibitor, TAK-242. These data show that TLR4 signaling is *necessary* for paracrine signaling between human ONH astrocytes and LC cells. This suggests that the TGFβ2 – TLR4 signaling crosstalk creates a feedforward cycle in both an autocrine and paracrine manner, which continues to exacerbate the fibrotic and immune system signaling that is detrimental to the survival of the exiting RGCs.

Chapter 4 Summary:

Chapters 2 and 3 demonstrate that TLR4 activation is both necessary and sufficient for TGFβ2 – induced fibrosis. However, these studies were performed in an *in vitro* model system. Thus, it is critical to reproduce these findings in an *in vivo* model system to fully understand the time-frame of glaucoma disease progression. Here we utilized a novel mouse model of glaucoma that constitutively expresses FN containing the EDA domain (B6.EDA$^{+/+}$)[31, 96] to test the

progressive retinal and ONH damage as well as elucidate transcriptomic changes at two time points.

Our recent publications show that TGFβ2 – induced ocular hypertension is dependent on both TLR4 and FN+EDA expression.[31, 96] In addition, this previous work demonstrates that constitutive expression of FN+EDA is sufficient to induce ocular hypertension and modest glaucomatous damage in the retina and ON at 1 year of age. In Chapter 4, we showed that B6.EDA$^{+/+}$ mice maintain these glaucoma symptoms through to 22 months of age (Chapter 4 Fig. 1). In addition, B6.EDA$^{+/+}$ mice exhibit a significant increase in IOP, loss of RGCs, and thinning of the RNFL compared to age-matched controls at both 12 months and 22 months of age. The evaluation of the RNFL enabled us to further characterize glaucomatous symptoms in our mouse model that are seen in human patients.[229] Interestingly, we found that the loss of RGCs and thinning of the RNFL do not significantly worsen between 12 months and 22 months of age in the B6.EDA$^{+/+}$ mice compared to age matched controls. However, ON damage did significantly worsen over this time course (Chapter 4 Fig. 2), indicating that continuous ocular hypertensions produces a progressive phenotype and suggesting that the site of damage in this model occurs in the ON.[230]

Previous work in our cell culture models indicated that DAMP production plays a significant role in fibrotic phenotypes and ECM dysregulation in the glaucomatous ONH. It has been previously shown that the significant increase of IOP in B6.EDA$^{+/+}$ mice is dependent on TLR4 signaling, implicating it in the induction of a fibrotic response in this mouse model. Here we identified time-specific responses of the DAMPs FN+EDA and biglycan (Chapter 4 Fig 3).

FN+EDA protein expression is significantly elevated at both 12 and 18 months in the ONH of B6.EDA$^{+/+}$ mice compared to age matched controls. Interestingly, biglycan protein expression is upregulated at 18 months of age but not at 12 months.[230] This indicates a time-specific response in the production of various DAMPs, implying that DAMP activation of the TGFβ2- TLR4 feedforward cycle has a critical window for therapeutic interventions.

To further elucidate changes in the transcriptome in the glaucomatous ONH of B6.EDA$^{+/+}$ mice, we utilized LCM to isolate the ONH specifically from the surrounding tissue.[199] Utilizing GSEA analysis and subsequent ICC for confirmation of transcriptomic changes, we found over 600 genes contributing to the significant up- and down-regulated gene groupings at both 12 months of age and 22 months of age in B6.EDA$^{+/+}$. IFNα, β, and γ groups were significantly upregulated in B6.EDA$^{+/+}$ mice at both 12 months and 22 months of age compared to age-matched controls (Chapter 4 Fig. 4). The IFN signaling system is a potent immune system activator,[231-234] and IFN signaling is implicated in glaucomatous pathophysiology in human patients[203-205] and mouse models.[206]

There are two classes of IFNs: Type 1 consists of IFNα, β, δ, ε, κ, τ, and ω, while Type 2 consists only of IFNγ.[235] Type 1 IFNs bind to Type 1 IFN receptors, and Type 2 IFNs bind to Type 2 IFN receptors. These receptors form a dimer on the cell surface to interact with the JAK/STAT signaling pathway.[235, 236] Type 1 IFN receptors activated by IFNα autophosphorylate specifically tyrosine kinase 2 (TYK2) and JAK2, which subsequently phosphorylate STATs 1, 2, 3, and 5, turning them to an activated form.[235, 237, 238] These activated STATs form homo- or heterodimers that translocate to the nucleus to act as transcription factors, binding to IFN-

stimulating gene (IGS) promoter sequences and initiating transcription.[235, 237-239] Type 2 IFN receptors activated by IFNγ result in the autophosphorylation of JAK1 and JAK2 instead of TYK2 and JAK2. JAK1:JAK2 phosphorylates STAT1 at the Tyr701 position to initiate subsequent signaling.[238, 240, 241]

To confirm the GSEA results, ONH sections from 12 month old and 18 month old B6.EDA$^{+/+}$ mice and age matched controls were stained for IFNα and IFNγ. IFNα and IFNγ levels are known to be significantly increased in the AH and serum of glaucomatous patients compared to healthy controls.[203, 205, 218, 219] Interestingly, the increased serum IFNγ serum levels negatively correlated with RNFL thickness, indicating a pathological role of IFN signaling in RGC loss in humans,[203] as well as the B6.EDA$^{+/+}$ mouse model.[230] Here we discovered time-dependent significant protein expression increases of IFNα and IFNγ in B6.EDA$^{+/+}$ mice compared to age matched controls (Chapter 4 Fig. 5). IFNα protein expression was significantly increased in the B6.EDA$^{+/+}$ OHN at both 12 months and 18 months of age compared to age matched controls, and IFNγ protein expression was increased at the 18 month time point. These data is consistent with known findings showing that IFNγ signaling is positively regulated by IFNα signaling, inducing progressive inflammatory changes to the glaucomatous ONH over time.[207, 208, 234, 242, 243]

Further analysis of the combined 240 leading edge genes from each IFN GSEA group, we identified that STAT, and downstream STAT signaling proteins, were included in the leading edge for each IFN group. STAT1 has previously been identified as a hub gene in glaucomatous human ONH astrocytes,[244] and in two glaucoma mouse models.[206, 212, 213] We determined that

pSTAT1 protein expression is significantly upregulated at 18 months in the B6.EDA$^{+/+}$ mouse model of glaucoma, but not at 12 months (Chapter 4 Fig. 6).

To the best of our knowledge, we are the first to demonstrate integral changes to DAMP, IFN, and STAT1 protein expression in the glaucomatous ONH throughout disease progression. Interestingly, IFNα is able to increase MyD88 protein expression, indicating a potential second feed-forward loop exacerbating TGFβ2-induced fibrosis and TLR4 activation.[243] These responses indicate that targeting these systems will need to account for time-specific disease state changes that can potentially affect efficacy.

Additional Data Analysis and Hypotheses: GSEA Visual Phototransduction: Intrinsically Photosensitive RGCs

GSEA analysis of isolated ONHs from B6.EDA$^{+/+}$ mice at 12 months and 22 months identified over 600 leading edge genes belonging to six GSEA groups upregulated at 12 months of age or eight up- and down-regulated GSEA groups at 22 months of age (Chapter 4: Fig. 4). Surprisingly, one group upregulated at 12 months of age was “Visual Phototransduction.” LCM allows for the collection of highly pure tissue isolation,[199] thus the appearance of “Visual Phototransduction” as an upregulated gene group via the GSEA analysis was unexpected, as we are confident that we did not have any contamination of rods or cones. Further literature review indicated a potential role of intrinsically photosensitive RGCs (ipRGCs, also referred to as pRGCs, mRGCs). ipRGCs express the photosensitive opsin melanopsin, or OPN4,[245-248] an opsin that is not expressed in rods and cones but instead in RGCs and horizontal cells.[249, 250] ipRGCs contribute to a plethora of non-image forming light responses including control of the pupillary

light response,[245, 251] sleep induction/circadian rhythm maintenance,[252-254] alertness,[255, 256] and mood/anxiety/behavior responses.[256-258] The human internal circadian clock isn't exactly 24 hours, thus the brain and body have to "re-set" daily based on light and visual cues that come from the ipRGCs.[248] Interestingly, blind patients report a history of insomnia, potentially due to the loss of circadian cues from the dead ipRGCs, and glaucoma comorbidities include sleep disruption and sleep apnea.[259]

It has been previously shown that chronic disruption of circadian rhythm, like that seen in night-shift workers, is associated with a higher association of cancer diagnosis,[260] Alzheimer's disease Parkinson's disease,[261] and the inflammatory disease multiple sclerosis (MS).[262] Interestingly, TLR4 has been repeatedly implicated in MS pathology, linking inflammation to circadian disruption.[263] Pro-inflammatory cytokine levels have also been shown to cycle with circadian rhythms,[261] and that manipulation of critical circadian rhythm genes is sufficient to induce astrogliosis across the brain and spinal cord.[264-267] This information, along with the data presented here, indicates that a loss of non-image forming signaling from ipRGCs may induce a pro-inflammatory response in the glaucomatous ONH.

ipRGCs have been studied in relation to glaucoma and glaucomatous ON damage. In human retinal flat mounts, there is no significant loss of ipRGCs between healthy donors and donors with a mild glaucoma diagnosis at time of death.[268] This is consistant with previous literature which shows that ipRGCs are more resilient to nerve injury compared to the general RGC population.[216, 269] However, there is a significant loss of ipRGCs in the human retina from donors diagnosed with severe glaucoma compared to healthy donor eyes,[268] indicating changes

in ipRGC population resiliency with disease progression. These trends are consistant with our GSEA data in which the "Visual Phototransduction" group is upregulated in the ONH of B6.EDA$^{+/+}$ mice at 12 months, but not at 22 months (Chapter 4 Fig. 4). We postulate that this is due to an eventual loss of the ipRGC population, thus inhibiting them from influencing RNAsequencing data at a scale large enough to come to significance in the small number of replicates we were able to analyze. Future experiments are still needed to determine which genes may be responsible for the ipRGC resiliency, though looking at the leading-edge genes from the RNAsequencing data (Chapter 4 Supplementary Excel Spreadsheet 1) can provide initial directions.[230]

Potential Novel Therapeutic Targets

The data presented on human ONH astrocyte and LC cell cultures identified a novel mechanism for TGFβ2-TLR4 signaling crosstalk in an autocrine and paracrine manner within the glaucomatous ONH. Thus, two obvious targets for intervention are TGFβ2 and TLR4 themselves. Significant research has studied various drug targets and drug delivery systems, including targeting fibrotic and immune responses.[270, 271] Previously, the TGFβ2-targeting pharmaceutical Lerdelimumab was used in an attempt to reduce post-surgery fibrosis after glaucoma drainage surgery. Unfortunately, the use of Lerdelimumab was halted when found to be unhelpful for preventing fibrosis after surgery.[272] However, it is important to note that Lerdelimumab was only used for acute fibrosis, and no studies have looked at long term administration in human patients. Thus, repurposing Lerdelimumab may be a viable strategy in developing new glaucoma treatments. Outside of Lerdelimumab, targeting TGFβ signaling has been heavily studied in the context of peripheral fibrotic diseases and cancer.[273-276] However,

preclinical models of global inhibition or knock-out in mouse models resulted in a plethora of negative symptoms including developmental deformities of the heart, lungs, eyes, bones, and non-viable offspring.[277] In human patients, TGFβ2-inhibiting pharmaceuticals must be directly injected into various cancerous tumors to avoid off-target toxicity.[274, 278] These data indicate that direct delivery of TGFβ2 inhibitors to the TM or ONH is necessary to reduce adverse side effects.

Interestingly, two FDA approved TLR4 inhibitors already exist: Naloxone and Thalidomide. Preclinical research has shown that either drug significantly inhibits TLR4 signaling in osteoarthritic cells *in vitro*.[279] In addition to these two drugs, almost 40 compounds out of 2000 known drugs have the potential to bind TLR4 based off of morphological dimension analysis.[280] The ability to "piggy-back" off of pharmaceuticals that are already approved by the FDA indicates that TLR4 inhibition is a strong contender for a novel pharmaceutical target for glaucoma treatment. This prediction also corroborates the data previously shown and presented here, that TLR4 signaling is necessary for TGFβ2-induced fibrosis in the human TM, ONH astrocytes, and ONH LC cells.[56, 74] It is also known that ocular hypertension in the B6.EDA$^{+/+}$ glaucoma mouse model also requires TLR4 signaling.[96]

Unfortunately, it is well documented that compliance for glaucoma eyedrop treatments is low, especially in aging populations.[281] The glaucoma patient population also has limited acceptance of treatment delivery alternatives to eye-drops.[282] Thus, easy, long-acting drug delivery mechanisms are necessary to broadly treat glaucoma patients and maximize compliance. Current literature has looked at the use of delivery systems such as hydrogels, contact lenses,

ocular inserts, and other methods.[271, 283, 284] However during drug development, care should be taken when analyzing the increased risks of complications with anything involving implants, incorrect use by patients, or potential patient contamination.

Future Directions and Experimental Limitations

Subsequent experiments based off the data presented in this dissertation can focus on three main aspects: 1) continued exploration of ECM DAMP expression in the human glaucomatous ONH; 2) Interactions between human ONH LC cells or astrocytes with microglia *in vitro*; and 3) pharmacological interference to reduce glaucomatous phenotypes in B6.EDA$^{+/+}$ mouse model.

As previously stated, the ECM DAMP biglycan is a proteoglycan that primarily supports tissue when exposed to compressional forces.[104] It is known that biglycan is upregulated in culture human LC cells after mechanical stress,[51] and initiates a proinflammatory phenotype through TLR4 signaling.[107] Here we have shown that biglycan protein expression is significantly increased in the ONH of B6.EDA$^{+/+}$ mice at 18 months but not 12 months compared to age matched controls (Chapter 4. Fig. 3), indicating a role in glaucomatous pathology at later, more severe time points.[230] Unfortunately, it remains to be determined if expression levels differ between healthy and glaucomatous ONH in human patients. Thus, future studies could explore protein expression levels in the glaucomatous ONH compared to the healthy ONH, as well as expression patterns compared to astrocyte, LC cell, and/or microglia cell markers.

The data presented in Chapters 1 and 2 identify signaling crosstalk between TGFβ2 and TLR4 that exacerbates the fibrotic and immune system activation via autocrine and paracrine signaling. A key experiment would complete the trifecta by investigating microglial cell cultures in monoculture and co-culture experiments. Unfortunately, no protocol to isolate ONH microglia currently exists, and subsequent attempts in the McDowell lab have come across issues with survivability and experimental volume for microglia monocultures. To receive enough microglia for one experiment, an entire ONH explant would need to be used solely for the growth of the microglia. While protocols exist to isolate retinal microglia, care should be taken when considering the most optimal use of donated human tissue.[285] Retinal microglia are difficult to culture, and once removed from the retinal culture-conglomerate, the microglia can only be used once. These microglia will not survive alone in cell culture for longer than one passage, thus creating and maintaining a cell line is near impossible.

While isolation from the human retina or other CNS tissues offers a promising alternative, it is well known that microglial populations are not homogenous across the entire CNS.[286, 287] Microglial subtypes include populations that only interact with the axon initial segment, are only found near motor neurons in the PNS, are involved in early life neurogenesis, primarily interact with vasculature, and other defining characteristics.[286] Subtype differentiation also depends on response to insult, morphology, and gene expression profiles.[286, 287] Microglial heterogeneity exists even within the retina itself, with variations in layer location, microgliosis marker expression, and small molecule expression.[288] To surpass this hurdle, many researchers have utilized immortalized microglial cell lines.[289, 290] Advantages for the use of immortalized microglia primarily rest in their ability to grow as a monoculture to a high enough cell count for

repeated experiments and have been shown to be viable up to passage 35.[289] Unfortunately, immortalized microglia have been shown to express variable levels of immune system proteins in control or stimulated conditions.[290] Thus, these cell lines represent an advantageous initial experimental model to study TGFβ2-TLR4 paracrine signaling in the ONH LC, but conclusions drawn should address transcriptional differences between primary and immortalized cell cultures.

Translating *in vitro* findings from future experiments to *in vivo* paradigms allows for a more complete understanding of disease progression and time-sensitive responses. Multiple models of glaucoma, optic nerve damage, or glaucoma-like phenotypes exist to further the understanding of how this disease progresses and if there are any neuroprotective mechanisms. Specifically, mouse models represent an ideal model system to study glaucoma phenotypes and ONH pathophysiology due to their genetic similarity and comparable anatomy to the human eye.[214, 215] Mouse models are also able to accurately mimic the human cyclical IOP patterns during a 24hr day.[291] Many genetic models of glaucoma or ocular hypertension exist, including two models previously mentioned in Chapter 4 that show STAT1 as a glaucoma hub-gene; DBA/2J and TDRD7 KO mice.[291, 292]

DBA/2J mice have mutations in two melanosome proteins, Tryp1 and Gpnmb, and develop a pigment dispersing iris disease which eventually leads to significantly increased IOP and RGC loss.[198, 291, 293, 294] IOP increased start around 6 months of age and continue to ~16 months of age, with the majority of ON damage seen at 12 months of age.[198] This mouse model has contributed greatly to the field of glaucoma research, with studies discovering insights into the role of apoptotic signaling,[295, 296] mechanisms for RGC apoptosis,[198] and testing therapeutic

interventions to mitigate glaucomatous damage.[296, 297] Unfortunately, there are serious practical challenges with the use of the DBA/2J mouse model for longitudinal studies. Primarily, there are significant levels of variability of glaucomatous phenotypes between mice despite being genetically identical, thus requiring large sample sizes to generate significant differences between treatment groups and controls.[298] The DBA/2J model works well for studying late onset, severe glaucomatous phenotypes, but these pitfalls indicate a need for early-stage glaucoma modeling systems.

Tdrd7 is a component of RNA granules and is highly conserved across evolution. Expression patters are significantly increased during the development of the vertebrate ocular lens.[212] Tdrd7 was initially studied due to its essential role in the correct remodeling of chromatoid bodies during spermatogenesis.[212, 299] However, it was also shown that TDRD7$^{-/-}$ mice develop congenital cataracts [300, 301] and significantly increased IOP by six months of age, as well as severe RNFL thinning and ON damage by 20 months.[212] Very recently, Xie and collaborators showed that STAT1 is a hub gene for glaucomatous damage in TDRD7$^{-/-}$ mice, indicating a role for proinflammatory signaling in this model of glaucoma as well.[206] These data presented in this dissertation continue to imply the importance of the innate immune system activation through the JAK/STAT pathways as seen in other glaucoma models.

This dissertation characterizes the B6.EDA$^{+/+}$ mouse model of mild-to-moderate glaucomatous symptoms up to 22 months of age.[230] If used in conjunction with the DBA/2J or TDRD7$^{-/-}$ models, this represents an opportunity for further longitudinal studies from mild-to-severe symptoms, as well as the opportunity to combine genetic manipulations in either model

system. Such experiments could include blocking TLR4 or DAMP production in either model system to assess severity of glaucoma phenotypes.

Previously we discussed the resiliency of ipRGCs, and the significantly upregulated GSEA group of "Visual Phototransduction" in the ONH of B6.EDA$^{+/+}$ mice at 12 months (Chapter 4: Fig. 4). Since ipRGCs exclusively express the photosensitive opsin melanopsin,[245-248] magnetic beads labeled for melanopsin allow for the specific isolation of these RGCs. Previous studies have utilized magnetic labeled bead separation of retinal cell types to isolate highly pure populations of cells using surface signaling receptors.[302, 303] In the eye, magnetic microbeads have been used to isolate human retinal microglia,[304] the mouse trabecular meshwork,[305] rat retinal endothelial cells,[306] and mouse rod photoreceptor precursors.[307] Subsequent RNAsequencing or targeted protein or mRNA expression analysis could identify time-specific changes that contribute to the resiliency of ipRGCs or susceptibility of normal RGCs in the B6.EDA$^{+/+}$ model of glaucoma.

Contribution to the Field

The data presented in this dissertation has, for the first time, identified a causative role for TGFβ2 – TLR4 signaling crosstalk and subsequent DAMP production in glaucomatous pathophysiology in the ONH and subsequent loss of RGCs.

While we have hypothesized a potential role of both autocrine and paracrine signaling between all three supporting cell types in the ONH, here we only present data showing autocrine and paracrine signaling in LC cells and astrocytes. However, the role of microglia in the immune

and fibrotic responses has been extensively reviewed in Chapter 1. Specifically, it is known that microglia can express TGFβ2,[29] TGFβ2 receptors,[129] TLR4,[128] and BAMBI.[129] These expression pattens heavily implicate that microglia can undergo paracrine signaling to both LC and astrocyte cell populations.

To continue to explore the role of TLR4 signaling in an *in vivo* model, we identified novel characterizations of glaucoma in the B6.EDA$^{+/+}$ mouse model.[230] B6.EDA$^{+/+}$ continuous ocular hypertension is known to be TLR4 dependent, and present significant IOP increases and RGC loss at both 12 months and 22 months.[31, 96, 230] Further investigating human glaucomatous symptoms in the B6.EDA$^{+/+}$ model, we discovered significant thinning of the RNFL at both 12 and 22 months of age, identifying a novel symptom in this model.[230] In addition, we present significant transcriptomic changes at 12 months and 22 months to further elucidate signaling mechanisms responsible for the development of progressive glaucomatous damage. RNAsequencing analysis identified 13 novel up- and down-regulated signaling groups, consisting of 607 leading edge genes total. Specifically, genes related to IFN signaling were significantly upregulated at both ages, further implicating a role of TLR4 signaling and immune system activation.[230] IFNα and IFNγ protein expression was significantly upregulated in the B6.EDA$^{+/+}$ mouse ONH, and the IFN downstream signaling molecule pSTAT1 was significantly upregulated at 18 months of age. These data indicate crucial timing windows for anti-inflammatory therapeutic interventions to prevent glaucomatous damage.

The primary focus of this dissertations is on crosstalk between fibrotic and immune system signaling, thus it is important to note the ability of astrocytes, microglia, and LC cells to

produce and/or respond to IFN and STAT signaling cascades. It is known that microglia and astrocytes express IFNα,[308, 309] IFNγ,[309, 310] Type 1 IFN receptors,[236, 311] Type 2 IFN receptors,[311, 312] and STAT1.[311, 313, 314] However, to the best of our knowledge, there is no literature exploring whether LC cells express Type 1 or Type 2 IFN receptors, STAT1, or secrete IFNs themselves. Previous literature has looked at protein expression changes and the effect of IFN exposure in other fibroblast cell types to examine the rate of proliferation and ECM production. IFNα exposure significantly affects dermal fibroblast survivability and ECM production, indicating Type 1 IFN expression.[315] Synovial fibroblasts, which are heavily involved in rheumatoid arthritis pathology,[316] have significant immune responses upon exposure to IFNγ, indicating expression of Type 2 IFN receptors.[317] Finally, intestinal fibroblasts and dermal fibroblasts have both been shown to express STAT1.[318, 319] Thus, while we cannot draw conclusions about the specific expression of IFNs, IFN receptors, nor STAT1 by LC cells, we can hypothesize the potential for paracrine IFN signaling between the ONH microglia, astrocytes, and LC cells.

Final Conclusions

Glaucoma is one of the leading causes of irreversible blindness, with patient numbers estimated to increase with the aging population. Unfortunately, managing IOP is the only modifiable risk factor, and even with lowered IOP, many patients still exhibit progressive loss of vision. This indicates a crucial need for a more cohesive understanding of the molecular and cellular signaling pathways underlying disease progression with the ultimate goal of identifying novel pharmaceutical targets. Chronic fibrotic and immune system activation have been heavily implicated in glaucoma pathophysiology, including TGFβ2-induced fibrosis and TLR4-induced innate immune system activation. Recent research has indicated that there is crosstalk between

these two prominent signaling pathways, creating a vicious feedforward cycle that exacerbates both fibrotic and immune signaling through DAMP production.

This dissertation identifies crucial increases in DAMP expression, novel autocrine and paracrine signaling with the ONH, and time-specific DAMP and IFN responses in a novel mouse model of glaucoma. Fundamentally, this work identifies novel signaling pathways resulting in fibrotic or immune responses. Broadly, this work contributes to our understanding of disease progression and postulates on new therapeutic targets.

References

1. Tham YC, Li X, Wong TY, Quigley HA, Aung T, Cheng CY. Global prevalence of glaucoma and projections of glaucoma burden through 2040: a systematic review and meta-analysis. *Ophthalmology* 2014;121:2081-2090.

2. Flaxman SR, Bourne RRA, Resnikoff S, et al. Global causes of blindness and distance vision impairment 1990-2020: a systematic review and meta-analysis. *Lancet Glob Health* 2017;5:e1221-e1234.

3. Aboobakar IF, Wiggs JL. The genetics of glaucoma: Disease associations, personalised risk assessment and therapeutic opportunities-A review. *Clin Exp Ophthalmol* 2022;50:143-162.

4. Weinreb RN, Aung T, Medeiros FA. The Pathophysiology and Treatment of Glaucoma. *Jama* 2014;311.

5. Weinreb RN, Leung CK, Crowston JG, et al. Primary open-angle glaucoma. *Nat Rev Dis Primers* 2016;2:16067.

6. McMonnies CW. Glaucoma history and risk factors. *J Optom* 2017;10:71-78.

7. Investigators TA. The Advanced Glaucoma Intervention Study (AGIS): 7. The relationship between control of intraocular pressure and visual field deterioration.The AGIS Investigators. *Am J Ophthalmol* 2000;130:429-440.

8. Musch DC, Gillespie BW, Lichter PR, Niziol LM, Janz NK, Investigators CS. Visual field progression in the Collaborative Initial Glaucoma Treatment Study the impact of treatment and other baseline factors. *Ophthalmology* 2009;116:200-207.

9. Kass MA, Heuer DK, Higginbotham EJ, et al. The Ocular Hypertension Treatment Study: a randomized trial determines that topical ocular hypotensive medication delays or prevents the onset of primary open-angle glaucoma. *Arch Ophthalmol* 2002;120:701-713; discussion 829-730.

10. Tamm ER. The trabecular meshwork outflow pathways: structural and functional aspects. *Exp Eye Res* 2009;88:648-655.

11. Johnson M. 'What controls aqueous humour outflow resistance?'. *Exp Eye Res* 2006;82:545-557.

12. Leske MC, Heijl A, Hussein M, et al. Factors for glaucoma progression and the effect of treatment: the early manifest glaucoma trial. *Arch Ophthalmol* 2003;121:48-56.

13. Quigley HA, Addicks EM, Green WR, Maumenee AE. Optic nerve damage in human glaucoma. II. The site of injury and susceptibility to damage. *Arch Ophthalmol* 1981;99:635-649.

14. Jonas JB, Aung T, Bourne RR, Bron AM, Ritch R, Panda-Jonas S. Glaucoma. *Lancet* 2017;390:2183-2193.

15. Burgoyne CF, Downs JC, Bellezza AJ, Suh JK, Hart RT. The optic nerve head as a biomechanical structure: a new paradigm for understanding the role of IOP-related stress and strain in the pathophysiology of glaucomatous optic nerve head damage. *Prog Retin Eye Res* 2005;24:39-73.

16. Vohra R, Tsai JC, Kolko M. The role of inflammation in the pathogenesis of glaucoma. *Surv Ophthalmol* 2013;58:311-320.

17. Morgan JE. Circulation and axonal transport in the optic nerve. *Eye (Lond)* 2004;18:1089-1095.

18. Safa BN, Wong CA, Ha J, Ethier CR. Glaucoma and biomechanics. *Curr Opin Ophthalmol* 2022;33:80-90.

19. Neufeld AH. Microglia in the optic nerve head and the region of parapapillary chorioretinal atrophy in glaucoma. *Arch Ophthalmol* 1999;117:1050-1056.

20. Prinz M, Jung S, Priller J. Microglia Biology: One Century of Evolving Concepts. *Cell* 2019;179:292-311.

21. Nimmerjahn A, Kirchhoff F, Helmchen F. Resting microglial cells are highly dynamic surveillants of brain parenchyma in vivo. *Science* 2005;308:1314-1318.

22. Hernandez MR. The optic nerve head in glaucoma: role of astrocytes in tissue remodeling. *Prog Retin Eye Res* 2000;19:297-321.

23. Sierra A, Encinas JM, Deudero JJ, et al. Microglia shape adult hippocampal neurogenesis through apoptosis-coupled phagocytosis. *Cell Stem Cell* 2010;7:483-495.

24. Cuenca N, Fernandez-Sanchez L, Campello L, et al. Cellular responses following retinal injuries and therapeutic approaches for neurodegenerative diseases. *Prog Retin Eye Res* 2014;43:17-75.

25. Hanisch UK, Kettenmann H. Microglia: active sensor and versatile effector cells in the normal and pathologic brain. *Nat Neurosci* 2007;10:1387-1394.

26. Raivich G, Bohatschek M, Kloss CU, Werner A, Jones LL, Kreutzberg GW. Neuroglial activation repertoire in the injured brain: graded response, molecular mechanisms and cues to physiological function. *Brain Res Brain Res Rev* 1999;30:77-105.

27. Davalos D, Grutzendler J, Yang G, et al. ATP mediates rapid microglial response to local brain injury in vivo. *Nat Neurosci* 2005;8:752-758.

28. Campagno KE, Lu W, Jassim AH, et al. Rapid morphologic changes to microglial cells and upregulation of mixed microglial activation state markers induced by P2X7 receptor stimulation and increased intraocular pressure. *J Neuroinflammation* 2021;18:217.

29. Yuan L, Neufeld AH. Activated microglia in the human glaucomatous optic nerve head. *J Neurosci Res* 2001;64:523-532.

30. Inman DM, Horner PJ. Reactive nonproliferative gliosis predominates in a chronic mouse model of glaucoma. *Glia* 2007;55:942-953.

31. Mavlyutov TA, Myrah JJ, Chauhan AK, Liu Y, McDowell CM. Fibronectin extra domain A (FN-EDA) causes glaucomatous trabecular meshwork, retina, and optic nerve damage in mice. *Cell Biosci* 2022;12:72.

32. Bosco A, Romero CO, Breen KT, et al. Neurodegeneration severity can be predicted from early microglia alterations monitored in vivo in a mouse model of chronic glaucoma. *Dis Model Mech* 2015;8:443-455.

33. Ramirez AI, de Hoz R, Fernandez-Albarral JA, et al. Time course of bilateral microglial activation in a mouse model of laser-induced glaucoma. *Sci Rep* 2020;10:4890.

34. Luo C, Yang X, Kain AD, Powell DW, Kuehn MH, Tezel G. Glaucomatous tissue stress and the regulation of immune response through glial Toll-like receptor signaling. *Invest Ophthalmol Vis Sci* 2010;51:5697-5707.

35. Johnson EC, Jia L, Cepurna WO, Doser TA, Morrison JC. Global changes in optic nerve head gene expression after exposure to elevated intraocular pressure in a rat glaucoma model. *Invest Ophthalmol Vis Sci* 2007;48:3161-3177.

36. Shimazawa M, Yamashima T, Agarwal N, Hara H. Neuroprotective effects of minocycline against in vitro and in vivo retinal ganglion cell damage. *Brain Res* 2005;1053:185-194.

37. Bosco A, Inman DM, Steele MR, et al. Reduced retina microglial activation and improved optic nerve integrity with minocycline treatment in the DBA/2J mouse model of glaucoma. *Invest Ophthalmol Vis Sci* 2008;49:1437-1446.

38. Levkovitch-Verbin H, Kalev-Landoy M, Habot-Wilner Z, Melamed S. Minocycline delays death of retinal ganglion cells in experimental glaucoma and after optic nerve transection. *Arch Ophthalmol* 2006;124:520-526.

39. Cooper ML, Pasini S, Lambert WS, et al. Redistribution of metabolic resources through astrocyte networks mitigates neurodegenerative stress. *Proc Natl Acad Sci U S A* 2020;117:18810-18821.

40. Ye H, Hernandez MR. Heterogeneity of astrocytes in human optic nerve head. *J Comp Neurol* 1995;362:441-452.

41. Tang Y, Chen Y, Chen D. The heterogeneity of astrocytes in glaucoma. *Front Neuroanat* 2022;16:995369.

42. Sun D, Qu J, Jakobs TC. Reversible reactivity by optic nerve astrocytes. *Glia* 2013;61:1218-1235.

43. Sun D, Moore S, Jakobs TC. Optic nerve astrocyte reactivity protects function in experimental glaucoma and other nerve injuries. *J Exp Med* 2017;214:1411-1430.

44. Liddelow SA, Guttenplan KA, Clarke LE, et al. Neurotoxic reactive astrocytes are induced by activated microglia. *Nature* 2017;541:481-487.

45. Tarassishin L, Suh HS, Lee SC. LPS and IL-1 differentially activate mouse and human astrocytes: role of CD14. *Glia* 2014;62:999-1013.

46. Varela HJ, Hernandez MR. Astrocyte responses in human optic nerve head with primary open-angle glaucoma. *J Glaucoma* 1997;6:303-313.

47. Hernandez MR, Ye H, Roy S. Collagen type IV gene expression in human optic nerve heads with primary open angle glaucoma. *Exp Eye Res* 1994;59:41-51.

48. Strickland RG, Garner MA, Gross AK, Girkin CA. Remodeling of the Lamina Cribrosa: Mechanisms and Potential Therapeutic Approaches for Glaucoma. *Int J Mol Sci* 2022;23.

49. Wallace DM, O'Brien CJ. The role of lamina cribrosa cells in optic nerve head fibrosis in glaucoma. *Exp Eye Res* 2016;142:102-109.

50. Kirwan RP, Leonard MO, Murphy M, Clark AF, O'Brien CJ. Transforming growth factor-beta-regulated gene transcription and protein expression in human GFAP-negative lamina cribrosa cells. *Glia* 2005;52:309-324.

51. Kirwan RP, Fenerty CH, Crean J, Wordinger RJ, Clark AF, O'Brien CJ. Influence of cyclical mechanical strain on extracellular matrix gene expression in human lamina cribrosa cells in vitro. *Mol Vis* 2005;11:798-810.

52. Cordeiro MF, Chang L, Lim KS, et al. Modulating conjunctival wound healing. *Eye (Lond)* 2000;14 (Pt 3B):536-547.

53. Picht G, Welge-Luessen U, Grehn F, Lutjen-Drecoll E. Transforming growth factor beta 2 levels in the aqueous humor in different types of glaucoma and the relation to filtering bleb development. *Graefes Arch Clin Exp Ophthalmol* 2001;239:199-207.

54. Kirwan RP, Wordinger RJ, Clark AF, O'Brien CJ. Differential global and extra-cellular matrix focused gene expression patterns between normal and glaucomatous human lamina cribrosa cells. *Mol Vis* 2009;15:76-88.

55. Hernandez MR, Andrzejewska WM, Neufeld AH. Changes in the extracellular matrix of the human optic nerve head in primary open-angle glaucoma. *Am J Ophthalmol* 1990;109:180-188.

56. Geiduschek EK, Milne PD, Mzyk P, Mavlyutov TA, McDowell CM. TLR4 signaling modulates extracellular matrix production in the lamina cribrosa. *Frontiers in Ophthalmology* 2022;2.

57. Kirwan RP, Felice L, Clark AF, O'Brien CJ, Leonard MO. Hypoxia regulated gene transcription in human optic nerve lamina cribrosa cells in culture. *Invest Ophthalmol Vis Sci* 2012;53:2243-2255.

58. Yan X, Tezel G, Wax MB, Edward DP. Matrix metalloproteinases and tumor necrosis factor alpha in glaucomatous optic nerve head. *Arch Ophthalmol* 2000;118:666-673.

59. Schneider M, Fuchshofer R. The role of astrocytes in optic nerve head fibrosis in glaucoma. *Exp Eye Res* 2016;142:49-55.

60. Hopkins AA, Murphy R, Irnaten M, Wallace DM, Quill B, O'Brien C. The role of lamina cribrosa tissue stiffness and fibrosis as fundamental biomechanical drivers of pathological glaucoma cupping. *Am J Physiol Cell Physiol* 2020;319:C611-C623.

61. Jun JI, Lau LF. Resolution of organ fibrosis. *J Clin Invest* 2018;128:97-107.

62. Pena JD, Netland PA, Vidal I, Dorr DA, Rasky A, Hernandez MR. Elastosis of the lamina cribrosa in glaucomatous optic neuropathy. *Exp Eye Res* 1998;67:517-524.

63. Hernandez MR, Pena JD. The optic nerve head in glaucomatous optic neuropathy. *Arch Ophthalmol* 1997;115:389-395.

64. Pena JD, Varela HJ, Ricard CS, Hernandez MR. Enhanced tenascin expression associated with reactive astrocytes in human optic nerve heads with primary open angle glaucoma. *Exp Eye Res* 1999;68:29-40.

65. Fukuchi T, Sawaguchi S, Yue BY, Iwata K, Hara H, Kaiya T. Sulfated proteoglycans in the lamina cribrosa of normal monkey eyes and monkey eyes with laser-induced glaucoma. *Exp Eye Res* 1994;58:231-243.

66. Fuchshofer R, Tamm ER. The role of TGF-beta in the pathogenesis of primary open-angle glaucoma. *Cell Tissue Res* 2012;347:279-290.

67. Heldin CH, Moustakas A. Signaling Receptors for TGF-beta Family Members. *Cold Spring Harb Perspect Biol* 2016;8.

68. Zode GS, Clark AF, Wordinger RJ. Bone morphogenetic protein 4 inhibits TGF-beta2 stimulation of extracellular matrix proteins in optic nerve head cells: role of gremlin in ECM modulation. *Glia* 2009;57:755-766.

69. Zode GS, Sethi A, Brun-Zinkernagel AM, Chang IF, Clark AF, Wordinger RJ. Transforming growth factor-beta2 increases extracellular matrix proteins in optic nerve head cells via activation of the Smad signaling pathway. *Mol Vis* 2011;17:1745-1758.

70. Nakao A, Afrakhte M, Moren A, et al. Identification of Smad7, a TGFbeta-inducible antagonist of TGF-beta signalling. *Nature* 1997;389:631-635.

71. Hayashi H, Abdollah S, Qiu Y, et al. The MAD-related protein Smad7 associates with the TGFbeta receptor and functions as an antagonist of TGFbeta signaling. *Cell* 1997;89:1165-1173.

72. Wrana JL, Attisano L. The Smad pathway. *Cytokine Growth Factor Rev* 2000;11:5-13.

73. Yan X, Lin Z, Chen F, et al. Human BAMBI cooperates with Smad7 to inhibit transforming growth factor-beta signaling. *J Biol Chem* 2009;284:30097-30104.

74. Hernandez H, Medina-Ortiz WE, Luan T, Clark AF, McDowell CM. Crosstalk Between Transforming Growth Factor Beta-2 and Toll-Like Receptor 4 in the Trabecular Meshwork. *Invest Ophthalmol Vis Sci* 2017;58:1811-1823.

75. Pena JD, Taylor AW, Ricard CS, Vidal I, Hernandez MR. Transforming growth factor beta isoforms in human optic nerve heads. *Br J Ophthalmol* 1999;83:209-218.

76. Fuchshofer R, Birke M, Welge-Lussen U, Kook D, Lutjen-Drecoll E. Transforming growth factor-beta 2 modulated extracellular matrix component expression in cultured human optic nerve head astrocytes. *Invest Ophthalmol Vis Sci* 2005;46:568-578.

77. Neumann C, Yu A, Welge-Lussen U, Lutjen-Drecoll E, Birke M. The effect of TGF-beta2 on elastin, type VI collagen, and components of the proteolytic degradation system in human optic nerve astrocytes. *Invest Ophthalmol Vis Sci* 2008;49:1464-1472.

78. Baudouin C, Kolko M, Melik-Parsadaniantz S, Messmer EM. Inflammation in Glaucoma: From the back to the front of the eye, and beyond. *Prog Retin Eye Res* 2021;83:100916.

79. Tezel G. The immune response in glaucoma: a perspective on the roles of oxidative stress. *Exp Eye Res* 2011;93:178-186.

80. Rieck J. The pathogenesis of glaucoma in the interplay with the immune system. *Invest Ophthalmol Vis Sci* 2013;54:2393-2409.

81. Shinozaki Y, Kashiwagi K, Koizumi S. Astrocyte Immune Functions and Glaucoma. *Int J Mol Sci* 2023;24.

82. Wei X, Cho KS, Thee EF, Jager MJ, Chen DF. Neuroinflammation and microglia in glaucoma: time for a paradigm shift. *J Neurosci Res* 2019;97:70-76.

83. Ramirez AI, de Hoz R, Salobrar-Garcia E, et al. The Role of Microglia in Retinal Neurodegeneration: Alzheimer's Disease, Parkinson, and Glaucoma. *Front Aging Neurosci* 2017;9:214.

84. Yang J, Yang P, Tezel G, Patil RV, Hernandez MR, Wax MB. Induction of HLA-DR expression in human lamina cribrosa astrocytes by cytokines and simulated ischemia. *Invest Ophthalmol Vis Sci* 2001;42:365-371.

85. Subhramanyam CS, Wang C, Hu Q, Dheen ST. Microglia-mediated neuroinflammation in neurodegenerative diseases. *Semin Cell Dev Biol* 2019;94:112-120.

86. Bosco A, Crish SD, Steele MR, et al. Early reduction of microglia activation by irradiation in a model of chronic glaucoma. *PLoS One* 2012;7:e43602.

87. Tezel G. Molecular regulation of neuroinflammation in glaucoma: Current knowledge and the ongoing search for new treatment targets. *Prog Retin Eye Res* 2022;87:100998.

88. Xu WQ, Wang YS. The role of Toll-like receptors in retinal ischemic diseases. *Int J Ophthalmol* 2016;9:1343-1351.

89. Mulfaul K, Rhatigan M, Doyle S. Toll-Like Receptors and Age-Related Macular Degeneration. *Adv Exp Med Biol* 2018;1074:19-28.

90. Miller FC, Coburn PS, Huzzatul MM, LaGrow AL, Livingston E, Callegan MC. Targets of immunomodulation in bacterial endophthalmitis. *Prog Retin Eye Res* 2019;73:100763.

91. Poltorak A, He X, Smirnova I, et al. Defective LPS signaling in C3H/HeJ and C57BL/10ScCr mice: mutations in Tlr4 gene. *Science* 1998;282:2085-2088.

92. Alexander C, Rietschel ET. Bacterial lipopolysaccharides and innate immunity. *J Endotoxin Res* 2001;7:167-202.

93. Bhattacharyya S, Kelley K, Melichian DS, et al. Toll-like receptor 4 signaling augments transforming growth factor-beta responses: a novel mechanism for maintaining and amplifying fibrosis in scleroderma. *Am J Pathol* 2013;182:192-205.

94. Seki E, De Minicis S, Osterreicher CH, et al. TLR4 enhances TGF-beta signaling and hepatic fibrosis. *Nat Med* 2007;13:1324-1332.

95. Pulskens WP, Rampanelli E, Teske GJ, et al. TLR4 promotes fibrosis but attenuates tubular damage in progressive renal injury. *J Am Soc Nephrol* 2010;21:1299-1308.

96. Roberts AL, Mavlyutov TA, Perlmutter TE, et al. Fibronectin extra domain A (FN-EDA) elevates intraocular pressure through Toll-like receptor 4 signaling. *Sci Rep* 2020;10:9815.

97. Shibuya E, Meguro A, Ota M, et al. Association of Toll-like receptor 4 gene polymorphisms with normal tension glaucoma. *Invest Ophthalmol Vis Sci* 2008;49:4453-4457.

98. Chen LJ, Tam PO, Leung DY, et al. SNP rs1533428 at 2p16.3 as a marker for late-onset primary open-angle glaucoma. *Mol Vis* 2012;18:1629-1639.

99. Takano Y, Shi D, Shimizu A, et al. Association of Toll-like receptor 4 gene polymorphisms in Japanese subjects with primary open-angle, normal-tension, and exfoliation glaucoma. *Am J Ophthalmol* 2012;154:825-832 e821.

100. Hernandez MR, Agapova OA, Yang P, Salvador-Silva M, Ricard CS, Aoi S. Differential gene expression in astrocytes from human normal and glaucomatous optic nerve head analyzed by cDNA microarray. *Glia* 2002;38:45-64.

101. Lee KM, Seong SY. Partial role of TLR4 as a receptor responding to damage-associated molecular pattern. *Immunol Lett* 2009;125:31-39.

102. Piccinini AM, Midwood KS. DAMPening inflammation by modulating TLR signalling. *Mediators Inflamm* 2010;2010.

103. Ohashi K, Burkart V, Flohe S, Kolb H. Cutting edge: heat shock protein 60 is a putative endogenous ligand of the toll-like receptor-4 complex. *J Immunol* 2000;164:558-561.

104. Yanagishita M. Function of proteoglycans in the extracellular matrix. *Acta Pathol Jpn* 1993;43:283-293.

105. Schaefer L. Small leucine-rich proteoglycans in kidney disease. *J Am Soc Nephrol* 2011;22:1200-1207.

106. Nastase MV, Young MF, Schaefer L. Biglycan: a multivalent proteoglycan providing structure and signals. *J Histochem Cytochem* 2012;60:963-975.

107. Schaefer L, Babelova A, Kiss E, et al. The matrix component biglycan is proinflammatory and signals through Toll-like receptors 4 and 2 in macrophages. *J Clin Invest* 2005;115:2223-2233.

108. Fukuchi T, Ueda J, Abe H, Sawaguchi S. Cell adhesion glycoproteins in the human lamina cribrosa. *Jpn J Ophthalmol* 2001;45:363-367.

109. Midwood K, Sacre S, Piccinini AM, et al. Tenascin-C is an endogenous activator of Toll-like receptor 4 that is essential for maintaining inflammation in arthritic joint disease. *Nat Med* 2009;15:774-780.

110. Keller KE, Vranka JA, Haddadin RI, et al. The effects of tenascin C knockdown on trabecular meshwork outflow resistance. *Invest Ophthalmol Vis Sci* 2013;54:5613-5623.

111. Reinehr S, Reinhard J, Wiemann S, et al. Early remodelling of the extracellular matrix proteins tenascin-C and phosphacan in retina and optic nerve of an experimental autoimmune glaucoma model. *J Cell Mol Med* 2016;20:2122-2137.

112. Wiemann S, Reinhard J, Reinehr S, Cibir Z, Joachim SC, Faissner A. Loss of the Extracellular Matrix Molecule Tenascin-C Leads to Absence of Reactive Gliosis and Promotes Anti-inflammatory Cytokine Expression in an Autoimmune Glaucoma Mouse Model. *Front Immunol* 2020;11:566279.

113. Saika S, Yamanaka O, Okada Y, Sumioka T. Modulation of Smad signaling by non-TGFbeta components in myofibroblast generation during wound healing in corneal stroma. *Exp Eye Res* 2016;142:40-48.

114. White ES, Baralle FE, Muro AF. New insights into form and function of fibronectin splice variants. *J Pathol* 2008;216:1-14.

115. Okamura Y, Watari M, Jerud ES, et al. The extra domain A of fibronectin activates Toll-like receptor 4. *J Biol Chem* 2001;276:10229-10233.

116. ffrench-Constant C. Alternative splicing of fibronectin--many different proteins but few different functions. *Exp Cell Res* 1995;221:261-271.

117. Muro AF, Chauhan AK, Gajovic S, et al. Regulated splicing of the fibronectin EDA exon is essential for proper skin wound healing and normal lifespan. *J Cell Biol* 2003;162:149-160.

118. Ffrench-Constant C, Van de Water L, Dvorak HF, Hynes RO. Reappearance of an embryonic pattern of fibronectin splicing during wound healing in the adult rat. *J Cell Biol* 1989;109:903-914.

119. Hino K, Shiozawa S, Kuroki Y, et al. EDA-containing fibronectin is synthesized from rheumatoid synovial fibroblast-like cells. *Arthritis Rheum* 1995;38:678-683.

120. Kuhn C, 3rd, Boldt J, King TE, Jr., Crouch E, Vartio T, McDonald JA. An immunohistochemical study of architectural remodeling and connective tissue synthesis in pulmonary fibrosis. *Am Rev Respir Dis* 1989;140:1693-1703.

121. van Keulen JK, de Kleijn DP, Nijhuis MM, et al. Levels of extra domain A containing fibronectin in human atherosclerotic plaques are associated with a stable plaque phenotype. *Atherosclerosis* 2007;195:e83-91.

122. Ting KM, Rothaupt D, McCormick TS, et al. Overexpression of the oncofetal Fn variant containing the EDA splice-in segment in the dermal-epidermal junction of psoriatic uninvolved skin. *J Invest Dermatol* 2000;114:706-711.

123. Scott DL, Delamere JP, Walton KW. The distribution of fibronectin in the pannus in rheumatoid arthritis. *Br J Exp Pathol* 1981;62:362-368.

124. Brown M, O'Reilly S. Innate immunity and Toll-like receptor signaling in the pathogenesis of scleroderma: advances and opportunities for therapy. *Curr Opin Rheumatol* 2018;30:600-605.

125. Medina-Ortiz WE, Belmares R, Neubauer S, Wordinger RJ, Clark AF. Cellular fibronectin expression in human trabecular meshwork and induction by transforming growth factor-beta2. *Invest Ophthalmol Vis Sci* 2013;54:6779-6788.

126. Lambert W, Agarwal R, Howe W, Clark AF, Wordinger RJ. Neurotrophin and neurotrophin receptor expression by cells of the human lamina cribrosa. *Invest Ophthalmol Vis Sci* 2001;42:2315-2323.

127. Lambert WS, Clark AF, Wordinger RJ. Neurotrophin and Trk expression by cells of the human lamina cribrosa following oxygen-glucose deprivation. *BMC Neurosci* 2004;5:51.

128. Kumar V. Toll-like receptors in the pathogenesis of neuroinflammation. *J Neuroimmunol* 2019;332:16-30.

129. Affram KO, Mitchell K, Symes AJ. Microglial Activation Results in Inhibition of TGF-beta-Regulated Gene Expression. *J Mol Neurosci* 2017;63:308-319.

130. Guttenplan KA, Stafford BK, El-Danaf RN, et al. Neurotoxic Reactive Astrocytes Drive Neuronal Death after Retinal Injury. *Cell Rep* 2020;31:107776.

131. Benitez-Del-Castillo J, Cantu-Dibildox J, Sanz-Gonzalez SM, Zanon-Moreno V, Pinazo-Duran MD. Cytokine expression in tears of patients with glaucoma or dry eye disease: A prospective, observational cohort study. *Eur J Ophthalmol* 2019;29:437-443.

132. Ten Berge JC, Fazil Z, van den Born I, et al. Intraocular cytokine profile and autoimmune reactions in retinitis pigmentosa, age-related macular degeneration, glaucoma and cataract. *Acta Ophthalmol* 2019;97:185-192.

133. Soto I, Howell GR. The complex role of neuroinflammation in glaucoma. *Cold Spring Harb Perspect Med* 2014;4.

134. Howell GR, Macalinao DG, Sousa GL, et al. Molecular clustering identifies complement and endothelin induction as early events in a mouse model of glaucoma. *J Clin Invest* 2011;121:1429-1444.

135. Johnson EC, Doser TA, Cepurna WO, et al. Cell proliferation and interleukin-6-type cytokine signaling are implicated by gene expression responses in early optic nerve head injury in rat glaucoma. *Invest Ophthalmol Vis Sci* 2011;52:504-518.

136. Hu Y, Mai W, Chen L, et al. mTOR-mediated metabolic reprogramming shapes distinct microglia functions in response to lipopolysaccharide and ATP. *Glia* 2020;68:1031-1045.

137. Haage V, Elmadany N, Roll L, et al. Tenascin C regulates multiple microglial functions involving TLR4 signaling and HDAC1. *Brain Behav Immun* 2019;81:470-483.

138. Vega JA, Garcia-Suarez O, Hannestad J, Perez-Perez M, Germana A. Neurotrophins and the immune system. *J Anat* 2003;203:1-19.

139. Dengler-Crish CM, Smith MA, Inman DM, Wilson GN, Young JW, Crish SD. Anterograde transport blockade precedes deficits in retrograde transport in the visual projection of the DBA/2J mouse model of glaucoma. *Front Neurosci* 2014;8:290.

140. Chitranshi N, Dheer Y, Abbasi M, You Y, Graham SL, Gupta V. Glaucoma Pathogenesis and Neurotrophins: Focus on the Molecular and Genetic Basis for Therapeutic Prospects. *Curr Neuropharmacol* 2018;16:1018-1035.

141. Patterson SL. Immune dysregulation and cognitive vulnerability in the aging brain: Interactions of microglia, IL-1beta, BDNF and synaptic plasticity. *Neuropharmacology* 2015;96:11-18.

142. Condorelli DF, Salin T, Dell' Albani P, et al. Neurotrophins and their trk receptors in cultured cells of the glial lineage and in white matter of the central nervous system. *J Mol Neurosci* 1995;6:237-248.

143. Sobrado-Calvo P, Vidal-Sanz M, Villegas-Perez MP. Rat retinal microglial cells under normal conditions, after optic nerve section, and after optic nerve section and intravitreal injection of trophic factors or macrophage inhibitory factor. *J Comp Neurol* 2007;501:866-878.

144. Nakajima K, Tohyama Y, Maeda S, Kohsaka S, Kurihara T. Neuronal regulation by which microglia enhance the production of neurotrophic factors for GABAergic, catecholaminergic, and cholinergic neurons. *Neurochem Int* 2007;50:807-820.

145. Quigley HA, McKinnon SJ, Zack DJ, et al. Retrograde axonal transport of BDNF in retinal ganglion cells is blocked by acute IOP elevation in rats. *Invest Ophthalmol Vis Sci* 2000;41:3460-3466.

146. Johnson EC, Deppmeier LM, Wentzien SK, Hsu I, Morrison JC. Chronology of optic nerve head and retinal responses to elevated intraocular pressure. *Invest Ophthalmol Vis Sci* 2000;41:431-442.

147. Wu SY, Pan BS, Tsai SF, et al. BDNF reverses aging-related microglial activation. *J Neuroinflammation* 2020;17:210.

148. Cramer T, Gill R, Thirouin ZS, et al. Cross-talk between GABAergic postsynapse and microglia regulate synapse loss after brain ischemia. *Sci Adv* 2022;8:eabj0112.

149. Krieglstein K, Strelau J, Schober A, Sullivan A, Unsicker K. TGF-beta and the regulation of neuron survival and death. *J Physiol Paris* 2002;96:25-30.

150. Guo J, Friedman SL. Toll-like receptor 4 signaling in liver injury and hepatic fibrogenesis. *Fibrogenesis Tissue Repair* 2010;3:21.

151. Yang L, Seki E. Toll-like receptors in liver fibrosis: cellular crosstalk and mechanisms. *Front Physiol* 2012;3:138.

152. Hernandez H, Millar JC, Curry SM, Clark AF, McDowell CM. BMP and Activin Membrane Bound Inhibitor Regulates the Extracellular Matrix in the Trabecular Meshwork. *Invest Ophthalmol Vis Sci* 2018;59:2154-2166.

153. Wordinger RJ, Agarwal R, Talati M, Fuller J, Lambert W, Clark AF. Expression of bone morphogenetic proteins (BMP), BMP receptors, and BMP associated proteins in human trabecular meshwork and optic nerve head cells and tissues. *Mol Vis* 2002;8:241-250.

154. Zhang SZ, Wang QQ, Yang QQ, et al. NG2 glia regulate brain innate immunity via TGF-beta2/TGFBR2 axis. *BMC Med* 2019;17:204.

155. Pawelec P, Ziemka-Nalecz M, Sypecka J, Zalewska T. The Impact of the CX3CL1/CX3CR1 Axis in Neurological Disorders. *Cells* 2020;9.

156. Quigley HA. Open-angle glaucoma. *N Engl J Med* 1993;328:1097-1106.

157. Anderson DR, Normal Tension Glaucoma S. Collaborative normal tension glaucoma study. *Curr Opin Ophthalmol* 2003;14:86-90.

158. Hernandez MR, Igoe F, Neufeld AH. Cell culture of the human lamina cribrosa. *Invest Ophthalmol Vis Sci* 1988;29:78-89.

159. Zode GS, Clark AF, Wordinger RJ. Activation of the BMP canonical signaling pathway in human optic nerve head tissue and isolated optic nerve head astrocytes and lamina cribrosa cells. *Invest Ophthalmol Vis Sci* 2007;48:5058-5067.

160. Kawai T, Akira S. The role of pattern-recognition receptors in innate immunity: update on Toll-like receptors. *Nat Immunol* 2010;11:373-384.

161. Miyake K. Innate immune sensing of pathogens and danger signals by cell surface Toll-like receptors. *Semin Immunol* 2007;19:3-10.

162. Navarro-Partida J, Alvarado Castillo B, Martinez-Rizo AB, Rosales-Diaz R, Velazquez-Fernandez JB, Santos A. Association of single-nucleotide polymorphisms in non-coding regions of the TLR4 gene with primary open angle glaucoma in a Mexican population. *Ophthalmic Genet* 2017;38:325-329.

163. Reinhard J, Roll L, Faissner A. Tenascins in Retinal and Optic Nerve Neurodegeneration. *Front Integr Neurosci* 2017;11:30.

164. Inatani M, Tanihara H, Katsuta H, Honjo M, Kido N, Honda Y. Transforming growth factor-beta 2 levels in aqueous humor of glaucomatous eyes. *Graefes Arch Clin Exp Ophthalmol* 2001;239:109-113.

165. Ochiai Y, Ochiai H. Higher concentration of transforming growth factor-beta in aqueous humor of glaucomatous eyes and diabetic eyes. *Jpn J Ophthalmol* 2002;46:249-253.

166. Ozcan AA, Ozdemir N, Canataroglu A. The aqueous levels of TGF-beta2 in patients with glaucoma. *Int Ophthalmol* 2004;25:19-22.

167. Tripathi RC, Li J, Chan WF, Tripathi BJ. Aqueous humor in glaucomatous eyes contains an increased level of TGF-beta 2. *Exp Eye Res* 1994;59:723-727.

168. Fleenor DL, Shepard AR, Hellberg PE, Jacobson N, Pang IH, Clark AF. TGFbeta2-induced changes in human trabecular meshwork: implications for intraocular pressure. *Investigative ophthalmology & visual science* 2006;47:226-234.

169. Wordinger RJ, Fleenor DL, Hellberg PE, et al. Effects of TGF-beta2, BMP-4, and gremlin in the trabecular meshwork: implications for glaucoma. *Invest Ophthalmol Vis Sci* 2007;48:1191-1200.

170. Fuchshofer R, Yu AH, Welge-Lussen U, Tamm ER. Bone morphogenetic protein-7 is an antagonist of transforming growth factor-beta2 in human trabecular meshwork cells. *Investigative ophthalmology & visual science* 2007;48:715-726.

171. Tovar-Vidales T, Clark AF, Wordinger RJ. Transforming growth factor-beta2 utilizes the canonical Smad-signaling pathway to regulate tissue transglutaminase expression in human trabecular meshwork cells. *Experimental eye research* 2011;93:442-451.

172. Sethi A, Jain A, Zode GS, Wordinger RJ, Clark AF. Role of TGFbeta/Smad signaling in gremlin induction of human trabecular meshwork extracellular matrix proteins. *Invest Ophthalmol Vis Sci* 2011;52:5251-5259.

173. Welge-Lussen U, May CA, Eichhorn M, Bloemendal H, Lutjen-Drecoll E. AlphaB-crystallin in the trabecular meshwork is inducible by transforming growth factor-beta. *Investigative ophthalmology & visual science* 1999;40:2235-2241.

174. Lopez NN, Clark AF, Tovar-Vidales T. Isolation and characterization of human optic nerve head astrocytes and lamina cribrosa cells. *Exp Eye Res* 2020;197:108103.

175. Morrison JC, Jerdan JA, Dorman ME, Quigley HA. Structural proteins of the neonatal and adult lamina cribrosa. *Arch Ophthalmol* 1989;107:1220-1224.

176. Goldbaum MH, Jeng SY, Logemann R, Weinreb RN. The extracellular matrix of the human optic nerve. *Arch Ophthalmol* 1989;107:1225-1231.

177. Hernandez MR. Ultrastructural immunocytochemical analysis of elastin in the human lamina cribrosa. Changes in elastic fibers in primary open-angle glaucoma. *Invest Ophthalmol Vis Sci* 1992;33:2891-2903.

178. Corpechot C, Barbu V, Wendum D, et al. Hypoxia-induced VEGF and collagen I expressions are associated with angiogenesis and fibrogenesis in experimental cirrhosis. *Hepatology* 2002;35:1010-1021.

179. Roggendorf W, Opitz H, Schuppan D. Altered expression of collagen type VI in brain vessels of patients with chronic hypertension. A comparison with the distribution of collagen IV and procollagen III. *Acta Neuropathol* 1988;77:55-60.

180. Geiduschek EK, McDowell CM. The Fibro-Inflammatory Response in the Glaucomatous Optic Nerve Head. *Int J Mol Sci* 2023;24.

181. Ii M, Matsunaga N, Hazeki K, et al. A novel cyclohexene derivative, ethyl (6R)-6-[N-(2-Chloro-4-fluorophenyl)sulfamoyl]cyclohex-1-ene-1-carboxylate (TAK-242), selectively inhibits toll-like receptor 4-mediated cytokine production through suppression of intracellular signaling. *Mol Pharmacol* 2006;69:1288-1295.

182. Matsunaga N, Tsuchimori N, Matsumoto T, Ii M. TAK-242 (resatorvid), a small-molecule inhibitor of Toll-like receptor (TLR) 4 signaling, binds selectively to TLR4 and interferes with interactions between TLR4 and its adaptor molecules. *Mol Pharmacol* 2011;79:34-41.

183. Serini G, Bochaton-Piallat ML, Ropraz P, et al. The fibronectin domain ED-A is crucial for myofibroblastic phenotype induction by transforming growth factor-beta1. *J Cell Biol* 1998;142:873-881.

184. Midwood KS, Chiquet M, Tucker RP, Orend G. Tenascin-C at a glance. *J Cell Sci* 2016;129:4321-4327.

185. Chiquet-Ehrismann R, Mackie EJ, Pearson CA, Sakakura T. Tenascin: an extracellular matrix protein involved in tissue interactions during fetal development and oncogenesis. *Cell* 1986;47:131-139.

186. Huang W, Chiquet-Ehrismann R, Moyano JV, Garcia-Pardo A, Orend G. Interference of tenascin-C with syndecan-4 binding to fibronectin blocks cell adhesion and stimulates tumor cell proliferation. *Cancer Res* 2001;61:8586-8594.

187. Midwood KS, Valenick LV, Hsia HC, Schwarzbauer JE. Coregulation of fibronectin signaling and matrix contraction by tenascin-C and syndecan-4. *Mol Biol Cell* 2004;15:5670-5677.

188. Miroshnikova YA, Mouw JK, Barnes JM, et al. Tissue mechanics promote IDH1-dependent HIF1alpha-tenascin C feedback to regulate glioblastoma aggression. *Nat Cell Biol* 2016;18:1336-1345.

189. Chiquet-Ehrismann R, Orend G, Chiquet M, Tucker RP, Midwood KS. Tenascins in stem cell niches. *Matrix Biol* 2014;37:112-123.

190. Midwood KS, Hussenet T, Langlois B, Orend G. Advances in tenascin-C biology. *Cell Mol Life Sci* 2011;68:3175-3199.

191. Fluck M, Tunc-Civelek V, Chiquet M. Rapid and reciprocal regulation of tenascin-C and tenascin-Y expression by loading of skeletal muscle. *J Cell Sci* 2000;113 (Pt 20):3583-3591.

192. Rolle T, Ponzetto A, Malinverni L. The Role of Neuroinflammation in Glaucoma: An Update on Molecular Mechanisms and New Therapeutic Options. *Front Neurol* 2020;11:612422.

193. Acott TS, Kelley MJ. Extracellular matrix in the trabecular meshwork. *Exp Eye Res* 2008;86:543-561.

194. Faralli JA, Filla MS, Peters DM. Role of Fibronectin in Primary Open Angle Glaucoma. *Cells* 2019;8.

195. McDowell CM, Luan T, Zhang Z, et al. Mutant human myocilin induces strain specific differences in ocular hypertension and optic nerve damage in mice. *Exp Eye Res* 2012;100:65-72.

196. Pang IH, Clark AF. Rodent models for glaucoma retinopathy and optic neuropathy. *J Glaucoma* 2007;16:483-505.

197. Chauhan BC, Levatte TL, Garnier KL, et al. Semiquantitative optic nerve grading scheme for determining axonal loss in experimental optic neuropathy. *Invest Ophthalmol Vis Sci* 2006;47:634-640.

198. Libby RT, Anderson MG, Pang IH, et al. Inherited glaucoma in DBA/2J mice: pertinent disease features for studying the neurodegeneration. *Vis Neurosci* 2005;22:637-648.

199. Sutherland C, Wang Y, Brown RV, et al. Laser Capture Microdissection of Highly Pure Trabecular Meshwork from Mouse Eyes for Gene Expression Analysis. *J Vis Exp* 2018.

200. Dobin A, Davis CA, Schlesinger F, et al. STAR: ultrafast universal RNA-seq aligner. *Bioinformatics* 2013;29:15-21.

201. Li B, Dewey CN. RSEM: accurate transcript quantification from RNA-Seq data with or without a reference genome. *BMC Bioinformatics* 2011;12:323.

202. Subramanian A, Tamayo P, Mootha VK, et al. Gene set enrichment analysis: a knowledge-based approach for interpreting genome-wide expression profiles. *Proc Natl Acad Sci U S A* 2005;102:15545-15550.

203. Saini C, Jiang S, Devlin J, et al. Association between HSP-Specific T-Cell Counts and Retinal Nerve Fiber Layer Thickness in Patients with Primary Open-Angle Glaucoma. *Ophthalmol Sci* 2023;3:100310.

204. Ayaki M. Development of neovascular glaucoma in the course of interferon alfa therapy for hepatitis type C. *Br J Ophthalmol* 1994;78:238.

205. Burgos-Blasco B, Vidal-Villegas B, Saenz-Frances F, et al. Tear and aqueous humour cytokine profile in primary open-angle glaucoma. *Acta Ophthalmol* 2020;98:e768-e772.

206. Xie RL, Nie HY, Xu YX. Identification of hub genes for glaucoma: a study based on bioinformatics analysis and experimental verification. *Int J Ophthalmol* 2023;16:1015-1025.

207. Taylor JL, Grossberg SE. The effects of interferon-alpha on the production and action of other cytokines. *Semin Oncol* 1998;25:23-29.

208. Pinto C, Giordano DM, Maroni L, Marzioni M. Role of inflammation and proinflammatory cytokines in cholangiocyte pathophysiology. *Biochim Biophys Acta Mol Basis Dis* 2018;1864:1270-1278.

209. Lozano DC, Jayaram H, Cepurna WO, et al. Optic Nerve Head Gene Transcription Sequelae to a Single Elevated IOP Exposure Provides Insights Into Known Responses to Chronically Elevated IOP. *Invest Ophthalmol Vis Sci* 2023;64:4.

210. Lozano DC, Choe TE, Cepurna WO, Morrison JC, Johnson EC. Early Optic Nerve Head Glial Proliferation and Jak-Stat Pathway Activation in Chronic Experimental Glaucoma. *Invest Ophthalmol Vis Sci* 2019;60:921-932.

211. Wong M, Huang P, Li W, Li Y, Zhang SS, Zhang C. T-helper1/T-helper2 cytokine imbalance in the iris of patients with glaucoma. *PLoS One* 2015;10:e0122184.

212. Lachke SA, Alkuraya FS, Kneeland SC, et al. Mutations in the RNA granule component TDRD7 cause cataract and glaucoma. *Science* 2011;331:1571-1576.

213. Howell GR, Soto I, Zhu X, et al. Radiation treatment inhibits monocyte entry into the optic nerve head and prevents neuronal damage in a mouse model of glaucoma. *J Clin Invest* 2012;122:1246-1261.

214. Pang IH, Clark AF. Inducible rodent models of glaucoma. *Prog Retin Eye Res* 2020;75:100799.

215. Emes RD, Goodstadt L, Winter EE, Ponting CP. Comparison of the genomes of human and mouse lays the foundation of genome zoology. *Hum Mol Genet* 2003;12:701-709.

216. Daniel S, Clark AF, McDowell CM. Subtype-specific response of retinal ganglion cells to optic nerve crush. *Cell Death Discov* 2018;4:7.

217. Daniel S, Meyer KJ, Clark AF, Anderson MG, McDowell CM. Effect of ocular hypertension on the pattern of retinal ganglion cell subtype loss in a mouse model of early-onset glaucoma. *Exp Eye Res* 2019;185:107703.

218. Chua J, Vania M, Cheung CM, et al. Expression profile of inflammatory cytokines in aqueous from glaucomatous eyes. *Mol Vis* 2012;18:431-438.

219. Yang X, Zeng Q, Goktas E, et al. T-Lymphocyte Subset Distribution and Activity in Patients With Glaucoma. *Invest Ophthalmol Vis Sci* 2019;60:877-888.

220. Liu B, Neufeld AH. Expression of nitric oxide synthase-2 (NOS-2) in reactive astrocytes of the human glaucomatous optic nerve head. *Glia* 2000;30:178-186.

221. Satoh J, Tabunoki H. A Comprehensive Profile of ChIP-Seq-Based STAT1 Target Genes Suggests the Complexity of STAT1-Mediated Gene Regulatory Mechanisms. *Gene Regul Syst Bio* 2013;7:41-56.

222. Andl CD, Mizushima T, Oyama K, Bowser M, Nakagawa H, Rustgi AK. EGFR-induced cell migration is mediated predominantly by the JAK-STAT pathway in primary esophageal keratinocytes. *Am J Physiol Gastrointest Liver Physiol* 2004;287:G1227-1237.

223. Eitsuka T, Tatewaki N, Nishida H, Nakagawa K, Miyazawa T. Synergistic Anticancer Effect of Tocotrienol Combined with Chemotherapeutic Agents or Dietary Components: A Review. *Int J Mol Sci* 2016;17.

224. Liu B, Neufeld AH. Activation of epidermal growth factor receptor causes astrocytes to form cribriform structures. *Glia* 2004;46:153-168.

225. Neufeld AH. Nitric oxide: a potential mediator of retinal ganglion cell damage in glaucoma. *Surv Ophthalmol* 1999;43 Suppl 1:S129-135.

226. Lin CC, Lin WN, Cheng SE, Tung WH, Wang HH, Yang CM. Transactivation of EGFR/PI3K/Akt involved in ATP-induced inflammatory protein expression and cell motility. *J Cell Physiol* 2012;227:1628-1638.

227. Quigley HA, Broman AT. The number of people with glaucoma worldwide in 2010 and 2020. *Br J Ophthalmol* 2006;90:262-267.

228. Varma R, Lee PP, Goldberg I, Kotak S. An assessment of the health and economic burdens of glaucoma. *Am J Ophthalmol* 2011;152:515-522.

229. Soliman MA, Van Den Berg TJ, Ismaeil AA, De Jong LA, De Smet MD. Retinal nerve fiber layer analysis: relationship between optical coherence tomography and red-free photography. *Am J Ophthalmol* 2002;133:187-195.

230. Geiduschek EK, Bricco EK, McDowell CM. DAMPs Drive Fibroinflammatory Changes in the Glaucomatous ONH. *Investigative Ophthalmology and Visual Sciences* 2024;*in review*.

231. Samuel CE. Antiviral actions of interferons. *Clin Microbiol Rev* 2001;14:778-809, table of contents.

232. Katze MG, He Y, Gale M, Jr. Viruses and interferon: a fight for supremacy. *Nat Rev Immunol* 2002;2:675-687.

233. Levy DE, Garcia-Sastre A. The virus battles: IFN induction of the antiviral state and mechanisms of viral evasion. *Cytokine Growth Factor Rev* 2001;12:143-156.

234. Biron CA. Interferons alpha and beta as immune regulators--a new look. *Immunity* 2001;14:661-664.

235. Platanias LC. Mechanisms of type-I- and type-II-interferon-mediated signalling. *Nat Rev Immunol* 2005;5:375-386.

236. Goldmann T, Blank T, Prinz M. Fine-tuning of type I IFN-signaling in microglia--implications for homeostasis, CNS autoimmunity and interferonopathies. *Curr Opin Neurobiol* 2016;36:38-42.

237. Darnell JE, Jr., Kerr IM, Stark GR. Jak-STAT pathways and transcriptional activation in response to IFNs and other extracellular signaling proteins. *Science* 1994;264:1415-1421.

238. Darnell JE, Jr. STATs and gene regulation. *Science* 1997;277:1630-1635.

239. Chen J, Baig E, Fish EN. Diversity and relatedness among the type I interferons. *J Interferon Cytokine Res* 2004;24:687-698.

240. Aaronson DS, Horvath CM. A road map for those who don't know JAK-STAT. *Science* 2002;296:1653-1655.

241. Boehm U, Klamp T, Groot M, Howard JC. Cellular responses to interferon-gamma. *Annu Rev Immunol* 1997;15:749-795.

242. Brinkmann V, Geiger T, Alkan S, Heusser CH. Interferon alpha increases the frequency of interferon gamma-producing human CD4+ T cells. *J Exp Med* 1993;178:1655-1663.

243. Sareneva T, Julkunen I, Matikainen S. IFN-alpha and IL-12 induce IL-18 receptor gene expression in human NK and T cells. *J Immunol* 2000;165:1933-1938.

244. Wong ZY, Nee E, Coles M, Buckley CD. Why does understanding the biology of fibroblasts in immunity really matter? *PLoS Biol* 2023;21.

245. Lucas RJ, Hattar S, Takao M, Berson DM, Foster RG, Yau KW. Diminished pupillary light reflex at high irradiances in melanopsin-knockout mice. *Science* 2003;299:245-247.
246. Ruby NF, Brennan TJ, Xie X, et al. Role of melanopsin in circadian responses to light. *Science* 2002;298:2211-2213.

247. Panda S, Sato TK, Castrucci AM, et al. Melanopsin (Opn4) requirement for normal light-induced circadian phase shifting. *Science* 2002;298:2213-2216.

248. Foster RG, Hughes S, Peirson SN. Circadian Photoentrainment in Mice and Humans. *Biology (Basel)* 2020;9.

249. Soni BG, Foster RG. A novel and ancient vertebrate opsin. *FEBS Lett* 1997;406:279-283.

250. Soni BG, Philp AR, Foster RG, Knox BE. Novel retinal photoreceptors. *Nature* 1998;394:27-28.

251. Lucas RJ, Douglas RH, Foster RG. Characterization of an ocular photopigment capable of driving pupillary constriction in mice. *Nat Neurosci* 2001;4:621-626.

252. Hubbard J, Ruppert E, Gropp CM, Bourgin P. Non-circadian direct effects of light on sleep and alertness: lessons from transgenic mouse models. *Sleep Med Rev* 2013;17:445-452.

253. Altimus CM, Guler AD, Villa KL, McNeill DS, Legates TA, Hattar S. Rods-cones and melanopsin detect light and dark to modulate sleep independent of image formation. *Proc Natl Acad Sci U S A* 2008;105:19998-20003.

254. Tsai JW, Hannibal J, Hagiwara G, et al. Melanopsin as a sleep modulator: circadian gating of the direct effects of light on sleep and altered sleep homeostasis in Opn4(-/-) mice. *PLoS Biol* 2009;7:e1000125.

255. Pilorz V, Tam SK, Hughes S, et al. Melanopsin Regulates Both Sleep-Promoting and Arousal-Promoting Responses to Light. *PLoS Biol* 2016;14:e1002482.

256. Milosavljevic N, Cehajic-Kapetanovic J, Procyk CA, Lucas RJ. Chemogenetic Activation of Melanopsin Retinal Ganglion Cells Induces Signatures of Arousal and/or Anxiety in Mice. *Curr Biol* 2016;26:2358-2363.

257. Fernandez DC, Fogerson PM, Lazzerini Ospri L, et al. Light Affects Mood and Learning through Distinct Retina-Brain Pathways. *Cell* 2018;175:71-84 e18.

258. LeGates TA, Altimus CM, Wang H, et al. Aberrant light directly impairs mood and learning through melanopsin-expressing neurons. *Nature* 2012;491:594-598.

259. Liu S, Lin Y, Liu X. Meta-Analysis of Association of Obstructive Sleep Apnea With Glaucoma. *J Glaucoma* 2016;25:1-7.

260. Sulli G, Lam MTY, Panda S. Interplay between Circadian Clock and Cancer: New Frontiers for Cancer Treatment. *Trends Cancer* 2019;5:475-494.

261. Brecier A, Li VW, Smith CS, Halievski K, Ghasemlou N. Circadian rhythms and glial cells of the central nervous system. *Biol Rev Camb Philos Soc* 2023;98:520-539.

262. Papantoniou K, Massa J, Devore E, et al. Rotating night shift work and risk of multiple sclerosis in the Nurses' Health Studies. *Occup Environ Med* 2019;76:733-738.

263. Asadzadeh Manjili F, Yousefi-Ahmadipour A, Kazemi Arababadi M. The roles played by TLR4 in the pathogenesis of multiple sclerosis; A systematic review article. *Immunol Lett* 2020;220:63-70.

264. Musiek ES. Circadian clock disruption in neurodegenerative diseases: cause and effect? *Front Pharmacol* 2015;6:29.

265. Nakazato R, Kawabe K, Yamada D, et al. Disruption of Bmal1 Impairs Blood-Brain Barrier Integrity via Pericyte Dysfunction. *J Neurosci* 2017;37:10052-10062.

266. Ali AAH, Schwarz-Herzke B, Rollenhagen A, et al. Bmal1-deficiency affects glial synaptic coverage of the hippocampal mossy fiber synapse and the actin cytoskeleton in astrocytes. *Glia* 2020;68:947-962.

267. Lananna BV, Nadarajah CJ, Izumo M, et al. Cell-Autonomous Regulation of Astrocyte Activation by the Circadian Clock Protein BMAL1. *Cell Rep* 2018;25:1-9 e5.

268. Obara EA, Hannibal J, Heegaard S, Fahrenkrug J. Loss of Melanopsin-Expressing Retinal Ganglion Cells in Severely Staged Glaucoma Patients. *Invest Ophthalmol Vis Sci* 2016;57:4661-4667.

269. Nadal-Nicolas FM, Sobrado-Calvo P, Jimenez-Lopez M, Vidal-Sanz M, Agudo-Barriuso M. Long-Term Effect of Optic Nerve Axotomy on the Retinal Ganglion Cell Layer. *Invest Ophthalmol Vis Sci* 2015;56:6095-6112.

270. Balendra SI, Shah PA, Jain M, Grzybowski A, Cordeiro MF. Glaucoma: Hot Topics in Pharmacology. *Curr Pharm Des* 2017;23:596-607.

271. Al-Qaysi ZK, Beadham IG, Schwikkard SL, Bear JC, Al-Kinani AA, Alany RG. Sustained release ocular drug delivery systems for glaucoma therapy. *Expert Opin Drug Deliv* 2023;20:905-919.

272. D. DR. Lerdelimumab. 2003;3:106-108.

273. Shi N, Wang Z, Zhu H, et al. Research progress on drugs targeting the TGF-beta signaling pathway in fibrotic diseases. *Immunol Res* 2022;70:276-288.

274. Akhurst RJ, Hata A. Targeting the TGFbeta signalling pathway in disease. *Nat Rev Drug Discov* 2012;11:790-811.

275. Parola M, Pinzani M. Liver fibrosis: Pathophysiology, pathogenetic targets and clinical issues. *Mol Aspects Med* 2019;65:37-55.

276. Roehlen N, Crouchet E, Baumert TF. Liver Fibrosis: Mechanistic Concepts and Therapeutic Perspectives. *Cells* 2020;9.

277. Sanford LP, Ormsby I, Gittenberger-de Groot AC, et al. TGFbeta2 knockout mice have multiple developmental defects that are non-overlapping with other TGFbeta knockout phenotypes. *Development* 1997;124:2659-2670.

278. Bogdahn U, Hau P, Stockhammer G, et al. Targeted therapy for high-grade glioma with the TGF-beta2 inhibitor trabedersen: results of a randomized and controlled phase IIb study. *Neuro Oncol* 2011;13:132-142.

279. Franco-Trepat E, Guillan-Fresco M, Alonso-Perez A, et al. Repurposing drugs to inhibit innate immune responses associated with TLR4, IL1, and NLRP3 signaling in joint cells. *Biomed Pharmacother* 2022;155:113671.

280. Zali H, Golchin A, Farahani M, Yazdani M, Ranjbar MM, Dabbagh A. FDA Approved Drugs Repurposing of Toll-Like Receptor4 (TLR4) Candidate for Neuropathy. *Iran J Pharm Res* 2019;18:1639-1647.

281. Budenz DL. A clinician's guide to the assessment and management of nonadherence in glaucoma. *Ophthalmology* 2009;116:S43-47.

282. Wang BB, Lin MM, Nguyen T, Turalba AV. Patient attitudes toward novel glaucoma drug delivery approaches. *Digit J Ophthalmol* 2018;24:16-23.

283. Al-Kinani AA, Zidan G, Elsaid N, Seyfoddin A, Alani AWG, Alany RG. Ophthalmic gels: Past, present and future. *Adv Drug Deliv Rev* 2018;126:113-126.

284. Sharma S, Bhatia V. Nanoscale Drug Delivery Systems for Glaucoma: Experimental and In Silico Advances. *Curr Top Med Chem* 2021;21:115-125.

285. Wang L, Qian Y, Che X, Jiang J, Suo J, Wang Z. Isolation and Characterization of Primary Retinal Microglia From the Human Post-mortem Eyes for Future Studies of Ocular Diseases. *Front Cell Neurosci* 2021;15:786020.

286. Stratoulias V, Venero JL, Tremblay ME, Joseph B. Microglial subtypes: diversity within the microglial community. *EMBO J* 2019;38:e101997.

287. Masuda T, Sankowski R, Staszewski O, Prinz M. Microglia Heterogeneity in the Single-Cell Era. *Cell Rep* 2020;30:1271-1281.

288. Zhang C, Lam TT, Tso M. Heterogenous populations of microglia/macrophages in the retina and their activation after retinal ischemia and reperfusion injury. *Experimental Eye Research* 2005;81:700-709.

289. Dello Russo C, Cappoli N, Coletta I, et al. The human microglial HMC3 cell line: where do we stand? A systematic literature review. *J Neuroinflammation* 2018;15:259.

290. Melief J, Sneeboer MA, Litjens M, et al. Characterizing primary human microglia: A comparative study with myeloid subsets and culture models. *Glia* 2016;64:1857-1868.

291. Fernandes KA, Harder JM, Williams PA, et al. Using genetic mouse models to gain insight into glaucoma: Past results and future possibilities. *Exp Eye Res* 2015;141:42-56.

292. Agarwal R, Iezhitsa I. Genetic rodent models of glaucoma in representing disease phenotype and insights into the pathogenesis. *Mol Aspects Med* 2023;94:101228.

293. John SW, Smith RS, Savinova OV, et al. Essential iris atrophy, pigment dispersion, and glaucoma in DBA/2J mice. *Invest Ophthalmol Vis Sci* 1998;39:951-962.

294. Chang B, Smith RS, Hawes NL, et al. Interacting loci cause severe iris atrophy and glaucoma in DBA/2J mice. *Nat Genet* 1999;21:405-409.

295. Libby RT, Li Y, Savinova OV, et al. Susceptibility to neurodegeneration in a glaucoma is modified by Bax gene dosage. *PLoS Genet* 2005;1:17-26.

296. Donahue RJ, Fehrman RL, Gustafson JR, Nickells RW. BCLX(L) gene therapy moderates neuropathology in the DBA/2J mouse model of inherited glaucoma. *Cell Death Dis* 2021;12:781.

297. Anderson MG, Libby RT, Gould DB, Smith RS, John SW. High-dose radiation with bone marrow transfer prevents neurodegeneration in an inherited glaucoma. *Proc Natl Acad Sci U S A* 2005;102:4566-4571.

298. Turner AJ, Vander Wall R, Gupta V, Klistorner A, Graham SL. DBA/2J mouse model for experimental glaucoma: pitfalls and problems. *Clin Exp Ophthalmol* 2017;45:911-922.

299. Tanaka T, Hosokawa M, Vagin VV, et al. Tudor domain containing 7 (Tdrd7) is essential for dynamic ribonucleoprotein (RNP) remodeling of chromatoid bodies during spermatogenesis. *Proc Natl Acad Sci U S A* 2011;108:10579-10584.

300. Anand D, Al Saai S, Shrestha SK, Barnum CE, Chuma S, Lachke SA. Genome-Wide Analysis of Differentially Expressed miRNAs and Their Associated Regulatory Networks in Lenses Deficient for the Congenital Cataract-Linked Tudor Domain Containing Protein TDRD7. *Front Cell Dev Biol* 2021;9:615761.

301. Dash S, Siddam AD, Barnum CE, Janga SC, Lachke SA. RNA-binding proteins in eye development and disease: implication of conserved RNA granule components. *Wiley Interdiscip Rev RNA* 2016;7:527-557.

302. Pezzi HM, Niles DJ, Schehr JL, Beebe DJ, Lang JM. Integration of Magnetic Bead-Based Cell Selection into Complex Isolations. *ACS Omega* 2018;3:3908-3917.

303. Ma Y, Chen T, Iqbal MZ, et al. Applications of magnetic materials separation in biological nanomedicine. *Electrophoresis* 2019;40:2011-2028.

304. Carter DA, Balasubramaniam B, Dick AD. Functional analysis of retinal microglia and their effects on progenitors. *Methods Mol Biol* 2013;935:271-283.

305. Mao W, Liu Y, Wordinger RJ, Clark AF. A magnetic bead-based method for mouse trabecular meshwork cell isolation. *Invest Ophthalmol Vis Sci* 2013;54:3600-3606.

306. Matsubara TA, Murata TA, Wu GS, Barron EA, Rao NA. Isolation and culture of rat retinal microvessel endothelial cells using magnetic beads coated with antibodies to PECAM-1. *Curr Eye Res* 2000;20:1-7.

307. Eberle D, Santos-Ferreira T, Grahl S, Ader M. Subretinal transplantation of MACS purified photoreceptor precursor cells into the adult mouse retina. *J Vis Exp* 2014;e50932.

308. McDonough A, Lee RV, Weinstein JR. Microglial Interferon Signaling and White Matter. *Neurochem Res* 2017;42:2625-2638.

309. Traugott U, Lebon P. Demonstration of alpha, beta, and gamma interferon in active chronic multiple sclerosis lesions. *Ann N Y Acad Sci* 1988;540:309-311.

310. Wang X, Suzuki Y. Microglia produce IFN-gamma independently from T cells during acute toxoplasmosis in the brain. *J Interferon Cytokine Res* 2007;27:599-605.

311. Hidano S, Randall LM, Dawson L, et al. STAT1 Signaling in Astrocytes Is Essential for Control of Infection in the Central Nervous System. *mBio* 2016;7.

312. Kann O, Almouhanna F, Chausse B. Interferon gamma: a master cytokine in microglia-mediated neural network dysfunction and neurodegeneration. *Trends Neurosci* 2022;45:913-927.

313. Roy ER, Chiu G, Li S, et al. Concerted type I interferon signaling in microglia and neural cells promotes memory impairment associated with amyloid beta plaques. *Immunity* 2022;55:879-894 e876.

314. Yan X, Yuan F, Chen X, Dong C. Bioinformatics analysis to identify the differentially expressed genes of glaucoma. *Mol Med Rep* 2015;12:4829-4836.

315. Santak G, Santak M, Forcic D. Native human IFN-alpha is a more potent suppressor of HDF response to profibrotic stimuli than recombinant human IFN-alpha. *J Interferon Cytokine Res* 2007;27:481-490.

316. Ospelt C. Synovial fibroblasts in 2017. *RMD Open* 2017;3:e000471.

317. Lowin T, Anssar TM, Bauml M, Classen T, Schneider M, Pongratz G. Positive and negative cooperativity of TNF and Interferon-gamma in regulating synovial fibroblast function and B cell survival in fibroblast/B cell co-cultures. *Sci Rep* 2020;10:780.

318. Kaler P, Owusu BY, Augenlicht L, Klampfer L. The Role of STAT1 for Crosstalk between Fibroblasts and Colon Cancer Cells. *Front Oncol* 2014;4:88.

319. Medley SC, Rathnakar BH, Georgescu C, Wren JD, Olson LE. Fibroblast-specific Stat1 deletion enhances the myofibroblast phenotype during tissue repair. *Wound Repair Regen* 2020;28:448-459.